Title	エネルギー貯蔵を用いた階層的なマルチコミュニティのエネルギー共有管理システム
Author(s)	
Citation	
Issue Date	2024-09
Type	Thesis or Dissertation
Text version	ETD
URL	http://hdl.handle.net/10119/19395
Rights	
Description	Supervisor: リム 勇仁, 先端科学技術研究科, 博士

Doctoral Dissertation

Hierarchical Multi-Communities Energy Sharing Management System using Energy Storage

Ruengwit KHWANRIT

Supervisor : Yuto LIM

Graduate School of Advanced Science and Technology
Japan Advanced Institute of Science and Technology
[Information Science]
September, 2024

Abstract

Recent advancements in renewable energy (RE) technologies, along with reduced installation costs, have led to their widespread adoption. However, challenges arise due to the intermittent nature of RE influenced by variable weather conditions, impacting its reliability. Irregular human behavior and the widespread adoption of high-demand loads, like electric vehicles (EVs), lead to significant energy demand fluctuations. To address these challenges, the integration of energy storage systems (ESS) emerges as a crucial solution. ESS provides fast response times, managing surplus energy during off-peak periods and discharging stored energy during peaks. Strategic deployment of ESS, combined with energy sharing and demand-side management, enables smart grid communities to balance supply and demand, mitigating fluctuations, and reduce reliance on costly and environmentally harmful peak power plants.

This dissertation aims to explore the integration of various forms of ESS into the hierarchical multiple levels of the electrical grid by proposing a framework called "hierarchical multi-communities energy-sharing management framework (hMESH) to provide efficient energy sharing management through three schemes: energy-sharing management for non-moving energy storage (eNMES), critical hour energy sharing management for partially moving energy storage (ePMES), and inter-community energy sharing management for fully moving energy storage (eFMES).

The first scheme, energy-sharing management for non-moving energy storage (eNMES), focuses on a smart home environment, comprising multiple REs, home appliances, and multiple ESS units. This chapter proposes a novel scheme to address the challenge of minimizing energy loss in ESSs and optimal ESS capacity design. It utilizes distributed power-flow assignment with a load-shifting algorithm, and the optimal energy storage capacity is determined using linear programming techniques.

The second scheme, critical hour energy sharing management for partially moving energy storage (ePMES), focuses on EVs with predictable usage patterns, specifically electric school buses (ESBs), often deployed at specific times and remaining idle for extended periods, making them practical for delivering vehicle-to-grid (V2G) ancillary services. It introduces a V2G model centered on ESBs in various schools within a single community, formulating the problem as a noncooperative game where the utility company (UC) determines the optimal incentive price for schools to discharge energy, minimizing additional costs during the peak demand period. Schools negotiate for the optimal discharged energy to maximize benefits during the peak period. The optimal energy-price (OEP) algorithm is also introduced to achieve equilibrium, which is proven to be unique and always existent.

The third scheme, inter-community energy sharing management for fully moving energy storage (eFMES), proposes a three-level energy-sharing model: utility company (UC) level, community energy aggregators (CEAs) level, and electric vehicles (EVs) level. In the smart grid, multiple communities exist, each with EVs inside. EVs possess the unique capability to travel between communities and engage in energy sharing through charge/discharge activities. The model is a three-level game, where UC at the upper level, supplies/buys electricity to/from the multi-community system and sets the multi-communities energy sharing price. CEAs, in the middle level, set optimal community energy sharing prices within their community. At the bottom level, each EV determines optimal charging and discharging energy, responding to energy sharing prices. All players aim to maximize their utility functions by choosing their best strategies. The scheme presents the optimal three-level energy-price (3OEP) algorithm to obtain an equilibrium that is proven to be unique and always existent.

The evaluation studies for the proposed three schemes of the hMESH framework were performed through simulations using MATLAB. The simulation results demonstrate the effectiveness of the proposed framework. The simulation on eNMES shows a reduction in energy loss and a significant decrease in energy storage capacity. Furthermore, the simulation on ePMES shows a reduction in the peak-to-average ratio and the bills for

schools possessing ESBs, which help discharge energy to the grid during peak periods. Finally, the results for the eFMES scheme indicate a reduction in the peak caused by charging EVs, with a significant decrease in the peak-to-average ratio and the electricity bills of EV owners. This also leads to a much flatter load profile compared to the original charging profile, where there is no multi-communities energy sharing management system.

Acknowledgments

First and foremost, I would like to express my deepest gratitude to my supervisor, Associate Professor **Yuto Lim**, whose invaluable advice, guidance, time, and unwavering motivation have been instrumental throughout my Ph.D. journey. He has shared profound lessons both in academia and life, consistently aiding me through physically and mentally challenging times. Words alone cannot sufficiently convey my gratitude.

I extend heartfelt thanks to Associate Professor **Chalie Charoenlarpnopparut** for his invaluable advice and support during the latter stages of my Ph.D. studies.

My sincere appreciation goes to the dedicated examining committee members, including Professor **Yasuo Tan**, Associate Professor **Razvan Beuran**, and Associate Professor **Itthisek Nilkhamhang**, for their invaluable comments and suggestions. Their insightful feedback and expert guidance have been crucial in significantly enhancing the quality and depth of my dissertation.

I am truly grateful to Assistant Professor **Saher Javaid** for her insightful suggestions and comments throughout this study. Additionally, I would like to express my sincere gratitude to Assistant Professor **Somsak Kittipiyakul** for his guidance and support during the early stages of my Ph.D. studies.

I would like to acknowledge the support and friendship extended to me by the TAN and LIM laboratory members at JAIST, whose collaboration has been invaluable. I also wish to thank the advisees of Professors Somsak and Chalie at SIIT for their friendship and counsel.

Lastly, I wish to express my deepest appreciation to my family for their unwavering and unconditional financial and emotional support throughout this journey. I would also like to especially thank Dr. **Rujiret Seweepong** for her continuous emotional support, the medicines, and the comforting meals she provided during challenging times.

Contents

This dissertation was prepared according to the curriculum for the Collaborative Education Program organized by Japan Advanced Institute of Science and Technology and Sirindhorn International Institute of Technology, Thammasat University.

List of Figures

List of Tables

List of Abbreviations

2LV	two-level game
3OEP	Three-level optimal energy-price
AC	Air conditioning
AGG	Aggregator
BLE	Bluetooth low energy
CAU	Charge-after-use
CEA	Community energy aggregator
CEN	Centralized approach
CS	Charging station
DER	Distributed energy resources
DPFA	Distributed power-flow assignment
eNMES	Energy sharing management for non-moving energy storage scheme
ePMES	Critical hour energy sharing management for patially moving energy storage scheme
eFMES	Inter-community energy sharing management for fully moving energy storage scheme
EB	Electric bus
ESB	Electric school bus
ESS	Energy storage system
ET	Electric taxi
EV	Electric vehicle
FC	Fuel cell
G2V	Grid-to-vehicle
hMESH	hierarchical multicommunities energy-sharing management framework
ICEV	Internal combustion engine vehicle
ICT	Information and communication technology
IoT	Internet of Things
MPFA	Multiple-load power-flow assignment
MPFA/SG	Multiple-load power-flow assignment: single generator to storage
MPFA/MG	Multiple-load power-flow assignment: multiple generators to storage
OEP	Optimal energy-price
P2P	Peer-to-peer
PAR	peak-to-average ratio
PFA	Power-flow assignment
PG	Power generator

PL	Power load
PLC	Power-line communication
PoE	Power over Ethernet
PS	Power storage
PV	Photovoltaic
QoES	Quality of energy service
RE	Renewable energy
SDR	Supply-to-demand ratio
SoC	State of charge
SPFA	Single-load power-flow assignment
SPE	Single-pair ethernet
SPFA	Single load Power-Flow Assignment
SPFA/S	Single load Power-Flow Assignment: Storage source
SPFA/GS	Single load Power-Flow Assignment: Generator and Storage sources
UC	Utility company
V2G	Vehicle-to-gird
VF	Ventilation fan
WT	Wind turbine

List of Symbols

Chapter 3

$\mathcal{H}$	A set of power storage units
$\mathcal{M}$	A set of power generators
$\mathcal{N}$	A set of power loads
$\varphi(X, Y, t)$	Logical power-flow connections from X to Y at time t
DE	Demanded energy of shifting HADs
ED	Energy deliverable to shifting HADs
$EC_h^{loss}(t)$	Charging loss of hth power storage unit at time t
$EDC_h^{loss}(t)$	Discharging loss of hth power storage unit at time t
$EG_m^f(t)$	Energy generation level of mth fluctuating power generator at time t
$EL_n^f(t)$	Energy demand level of nth fluctuating power load at time t
$ES_h(t)$	Charge or discharge energy of hth power storage unit at time t
ESS_h	Capacity of hth power storage unit
$SE_h(t)$	Stored energy of hth power storage unit at time t
$ES_h(t)$	Charge or discharge energy of hth power storage unit at time t
h	hth power storage
H_{DE}	Total number of operating hours of the energy loads
H_{ED}	Total number of operating hours of the energy deliverables
$I(t)$	Total charging energy at time t
$L(t)$	Total lacking energy at to be discharged time t
m	mth power generator
n	nth power load
$O(t)$	Total discharging energy at time t
$P_{demand}(t)$	Total demanded energy at time t
$P_{battery}(t)$	Total battery energy at time t
$P_{supply}(t)$	Total supplied energy at time t
$pg_m^{f,max}$	Maximum instantaneous power level limitations of mth fluctuating power generator
$pg_m^{f,min}$	Minimum instantaneous power level limitations of mth fluctuating power generator
$pg_m^f(t)$	Instantaneous power level of mth fluctuating power generator at time t
$pl_n^{f,max}$	Maximum instantaneous power level limitations of nth fluctuating power load
$pl_n^{f,min}$	Minimum instantaneous power level limitations of nth fluctuating power load

e_n^t	Remaining energy in the electric school buses in school n that can be further utilized after discharging energy for peak shaving service at time slot t
h_d	Number of hours used in driving service each round
N	Number of schools
n	nth school
p^t	Unit dynamic electricity price at time slot t
p_{avg}^t	Average charging price per unit of energy constituting the current amount of stored energy at time slot t
p_{uc}^t	Incentive price for peak shaving service paid by utility company to schools at time slot t
p_{uc}^{max}	Maximum incentive price that utility company can provide
p_{uc}^{min}	Minimum incentive price that utility company will provide
s_1^t	Charging state of electric school bus at time slot t
s_2^t	Discharging state of electric school bus at time slot t
s_3^t	Traveling state of electric school bus at time slot t
SoC_n^{max}	Maximum state of charge of battery of nth school
SoC_n^{min}	Minimum state of charge of battery of nth school
SoC_n^t	State of charge of battery of nth school in time slot t
SoC_n^{t+1}	State of charge of battery of nth school in the next time slot
t	tth time slot
U_n^t	Utility function of school n at time slot t
U_{uc}^t	Utility function of utility company at time slot t
x_n^t	Discharged energy from school n at time slot t
$\boldsymbol{x_{-n}^t}$	Strategies of all the schools in time slot t except for the school n
x_n^{max}	Maximum discharged energy from school n at time slot t
x_n^{min}	Minimum discharged energy from school n at time slot t

Chapter 5

$\mathcal{M}$	A set of communities in multi-communities system
$\mathcal{N}$	A set of electric vehicle in a community
$\mathcal{T}$	A set of time slots
$\psi_{m,n}^t$	Satisfaction faction of electric vehicle m,n of having the amount of stored energy at time slot t
$\lambda_{m,n}$	Preference parameter of electric vehicle m,n distinguishing it from others
$\theta_{m,n}$	Quadratic function's predefined constant of of electric vehicle m,n
α^t	New defined parameter related to quadratic function's predefined constant
β^t	New defined parameter related to preference parameter of electric vehicle
γ^t	New defined parameter related to total charge/discharge energy from electric vehicle
δ^t	New defined parameter related to total fixed demand of communities

a	Coefficient of the generation cost function
b	Coefficient of the generation cost function
C_{gen}^t	Cost required to generate the energy to serve all demand in the multi-communities at time slot t
$D_{CEA,m}^t$	Aggregated net energy inside community m at time slot t
D_{uc}^t	Total net energy in the multi-communities system
$E_{CEA,m}^t$	Total charge/discharge energy from electric vehicle inside community m at time slot t
$E_{m,n}^t$	Remaining energy in the EV that can be further utilized at time t before deciding to charge or discharge
L_m^t	Total fixed demand of community m at time slot t
M	Number of community in multi-communities system
m	mth community
N_m^t	Number of electric vehicle in community m
n	nth electric vehicle
$\boldsymbol{p_{CEA}^t}$	Set of the strategies of all community m in time slot t
$p_{CEA,m}^t$	Community energy sharing price in community m at time slot t
p_{CEA}^{max}	Maximum single community energy sharing price
p_{CEA}^{min}	Minimum single community energy sharing price
p_{uc}^t	Multi-communities energy sharing price in the multi-communities system at time slot t
p_{uc}^{max}	Maximum multi-communities energy sharing price
p_{uc}^{min}	Minimum multi-communities energy sharing price
T	Number of time slots in a single day
t	tth time slot
$U_{CEA,m}^t$	Utility function of community energy aggregator m at time slot t
U_{uc}^t	Utility function of utility company at time slot t
$U_{m,n}^t$	Utility function of electric vehicle m,n at time slot t
$\boldsymbol{x^t}$	Set of the strategies of all electric vehicles in the multi-communities system in time slot t
$\boldsymbol{x_m^t}$	Set of the strategies of all the EVs in community m in time slot t
$\boldsymbol{x_{-m,n}^t}$	Set of the strategies of all the EVs in community m in time slot t except the EV m,n
x_n^t	charging/discharging energy of the m,nth electric vehicle at time slot t
x_n^{min}	Minimum charging/discharging energy of the m,nth electric vehicle at time slot t
x_n^{max}	Maximum charging/discharging energy of the m,nth electric vehicle at time slot t

Chapter 1

Introduction

1.1 Today and Future Electrical Grid

1.1.1 Today Electrical Grid

In our traditional society, electricity is predominantly generated by large power plants and transmitted through extensive networks to various end-users, constituting what we commonly refer to as the electrical grid. This grid has historically operated on a unidirectional model, with power flowing from centralized generation facilities to passive consumers.

Comprising four primary components: generation, transmission, distribution, and end-users. The grid has long functioned as a centralized, top-down system. Generation involves the production of electricity at large-scale power plants, followed by transmission across long distances via high-voltage lines. Distribution networks then deliver electricity to homes, businesses, and institutions, where it is consumed by end-users. The traditional power system is shown in Figure1.1.

However, a notable transformation is underway. The proliferation of distributed energy resources (DERs) and renewable energy (RE) technologies has shifted away from centralized generation towards a more decentralized model. Advancements in RE technologies, coupled with declining installation costs, have drived their widespread adoption globally. The increase of RE in the world energy supply is shown in Figure 1.2.
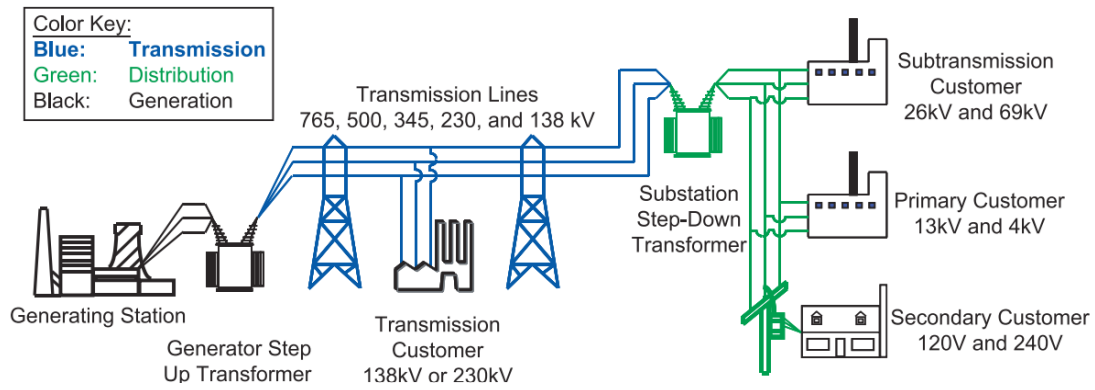
Figure 1.1: Traditional electrical power system [1].
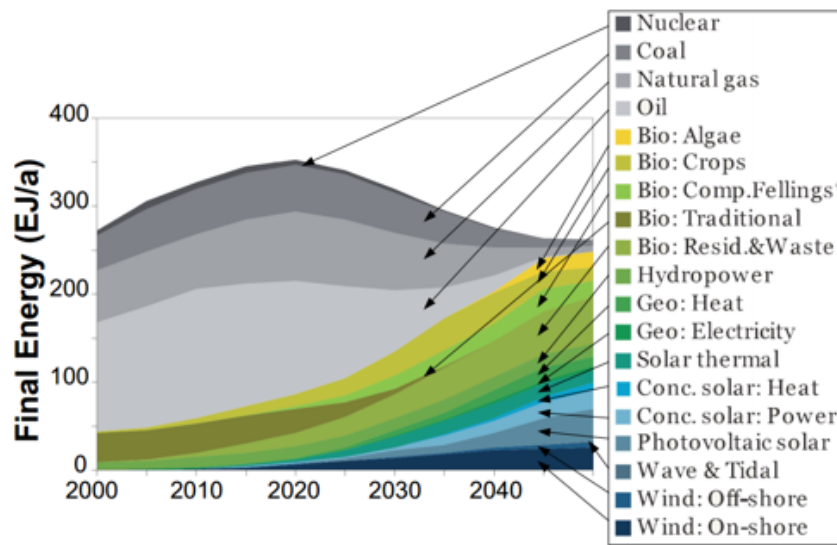
Figure 1.2: World energy supply by source [2].

This transition towards decentralization signifies a departure from the traditional one-way power flow, empowering end-users to become prosumers who actively engage in energy generation and consumption. By leveraging technologies such as solar panels and wind turbines, individuals and communities can generate electricity, thereby contributing to a more dynamic, cooperative, collaborative energy ecosystem.

Consequently, the modern electrical grid finds itself needs to embrace these changes and adapt accordingly. As we strive towards a more sustainable and resilient energy system, the grid must evolve to accommodate decentralized energy generation, fostering inclusivity and innovation along the way. Ultimately, this transition holds the promise of a greener, more sustainable future for generations to come.

One of the significant challenges facing the electrical grid is the necessity to match demand in real-time. As electricity consumption fluctuates throughout the day, grid operators must continuously adjust the supply to meet the peak demand periods. To accomplish this, they often rely on peak power plants, which are designed to quickly ramp up production to meet surges in electricity usage. However, these peak plants come with their own set of drawbacks. Not only are they technically and economically inefficient compared to base-load power plants, but they also contribute to harmful emissions, posing risks to both environmental and public health. The reliance on such plants not only intensify pollution levels but also adds strain to the grid infrastructure. As the global push for sustainability intensifies, finding viable alternatives to these peak power plants becomes necessary for the long-term health and resilience of the electrical grid.

1.1.2 Green and Sustainable Future Electrical Grid

In recent years, a transformative shift has occurred in the landscape of the electrical grid, giving rise to what is now known as "The smart grid." This new paradigm represents a significant departure from the traditional, centralized model of grid operation, instead embracing a digitally enabled framework facilitated by advancements in information and communication technology (ICT), smart metering, and home energy management systems (HEMS). The smart grid fundamentally reimagines how energy is produced, distributed, and consumed, introducing a dynamic and interactive platform that facilitates two-way communication between grid operators and end-users. A conceptual illustration of the smart grid is shown in Figure1.3

At the heart of the smart grid concept lies on the notion of bidirectional energy flow changing from the conventional top-down, one-way energy transmission model. Rather than passively receiving electricity from centralized power plants, consumers become active participants in the energy ecosystem, capable of both consuming and generating power. This bottom-up approach not only decentralizes energy production but also enhances grid resilience and efficiency by optimizing resource allocation and reducing reliance
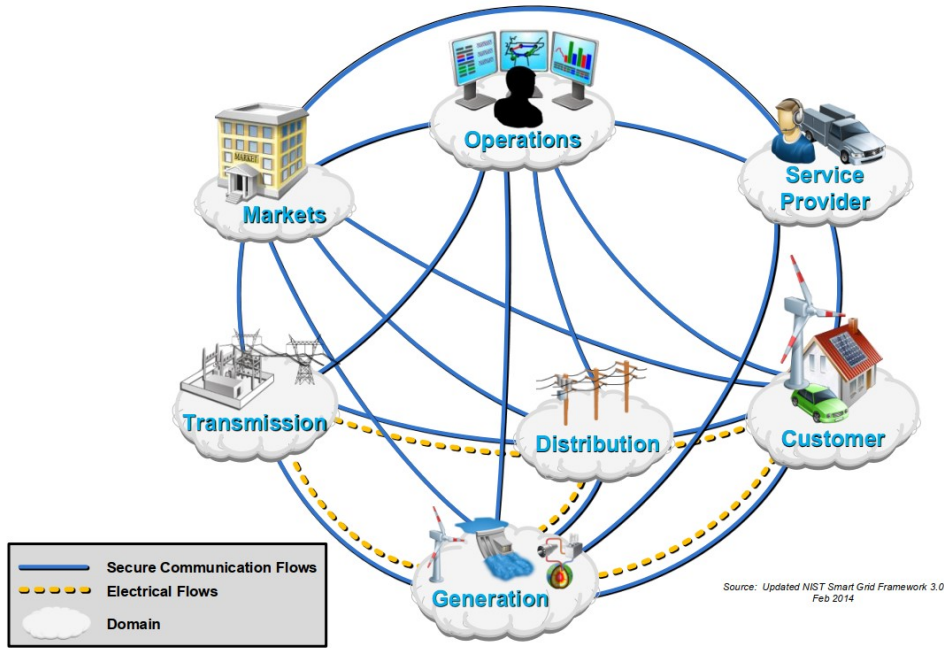
Figure 1.3: conceptual illustration of the smart grid [3].

on traditional fossil fuel-based generation.

Central to the functionality of the smart grid are smart meters, which enable real-time monitoring and communication between consumers and grid operators. These devices provide insights into energy usage patterns, allowing for more precise demand forecasting and load management strategies. Coupled with home energy management systems, which empower consumers to monitor and control their energy consumption, smart meters form the foundation of a more responsive and adaptive grid infrastructure.

Moreover, the integration of renewable energy (RE) sources such as solar and wind power into the smart grid further supports its capabilities. With their intermittent nature, RE resources pose unique challenges to grid stability and reliability. However, advancements in energy storage systems (ESS) offer promising solutions by providing a means to store excess renewable energy for use during periods of high demand or low generation. By coupling RE generation with ESS deployment and smart grid technologies, the grid becomes more flexible, resilient, and sustainable, reducing reliance on fossil fuels and mitigating greenhouse gas emissions.

In essence, the emergence of the smart grid represents a paradigm shift in the way

we conceptualize and manage our energy infrastructure. By leveraging advancements in ICT, RE integration, electric vehicles (EVs), and energy storage, the smart grid promises to revolutionize the energy sector, leading to an era of greater efficiency, reliability, and sustainability. As we continue to embrace the opportunities presented by this transformative technology, the smart grid holds the potential to reshape our energy future for the better, paving the way towards a more resilient, decentralized, and environmentally conscious grid ecosystem.

1.2 Energy Sharing in Electrical Grid

The recent advancements in smart grid technology have lead to a new era where consumers are empowered to take on more active roles within the power system. These new active users, often referred to as prosumers, have the capability to not only consume electricity but also generate and share it within their communities. Through distributed energy resources (DERs), electric vehicles (EVs), and energy storage systems (ESS), prosumers can contribute to the energy generation process, adjusting their supply based on factors like cheap pricing periods and storing excess energy for later discharge or sale.

One notable development in this realm is the emergence of energy sharing platforms, allowing prosumers to share their excess generation with others in the community. Energy sharing can be categorized into two main approaches: fully peer-to-peer (P2P) and mediated sharing. In P2P sharing, participating users directly engage with one another to negotiate energy prices and quantities, eliminating the need for intermediaries. Conversely, mediated sharing involves the presence of a third-party entity that serves as an intermediary interface between energy buyers and sellers, facilitating the energy sharing process. Figure 1.4 shows both types of energy sharing.

While P2P sharing offers a direct and potentially more cost-effective approach, the complexity involved in negotiating energy transactions among multiple peers may necessitate the use of a mediator or a platform. These intermediary entities streamline the negotiation process, ensure fair pricing, and provide a centralized platform for energy transactions.

As community energy sharing continues to evolve, it is expected that mediated sharing mechanisms will play an increasingly essential role in facilitating efficient and fair energy exchanges among prosumers within smart grid communities.

(a)   (b)
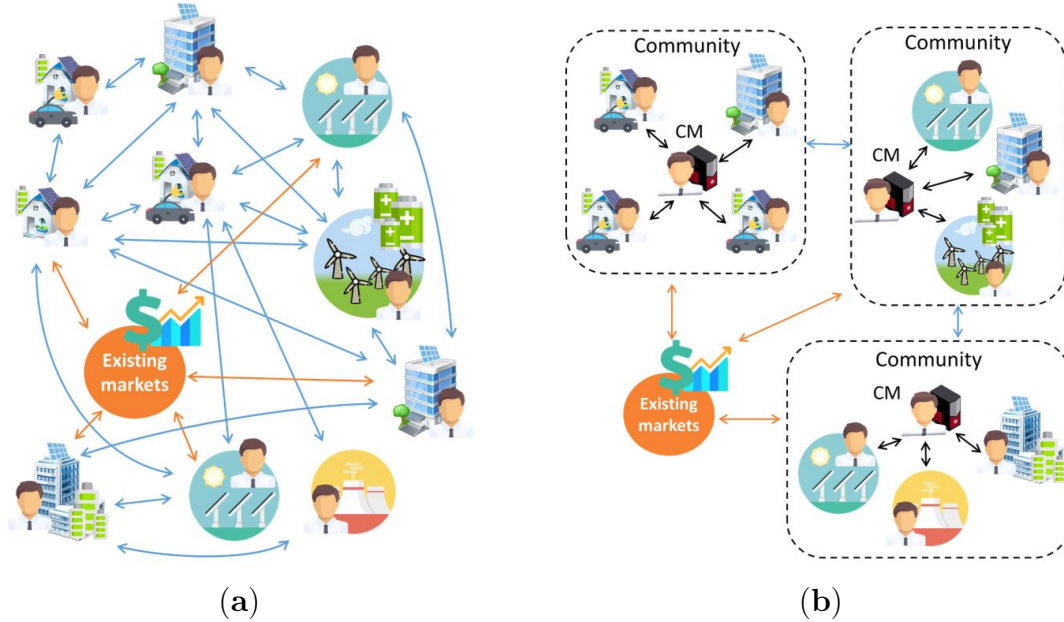
Figure 1.4: Two types of energy sharing [4]: (**a**) P2P and (**b**) Community-based.

1.3 Problem Statement

The traditional energy landscape has long been characterized by centralized power generation, with large-scale power plants supplying electricity to passive consumers. However, recent advancements in renewable energy (RE) technologies, along with the decrease in installation costs, have led to their widespread adoption. This shift is transforming the energy sector into a new era, moving away from centralized power generation and empowering consumers to become prosumers who can both generate and consume electricity. However, despite the positive benefits that prosumers can derive from producing and utilizing their own electricity from RE, its intermittent nature influenced by variable weather conditions, poses challenges to their reliability as energy sources. Moreover, irregular human behavior and the widespread adoption of high-demand loads lead to significant fluctuations in energy demand and generation. This results in immediate peak

periods during which electricity must be sourced from conventional peak power plants. These plants are not only technically and economically inefficient but also release harmful emissions, posing risks to health.

To address these challenges and promote a more resilient and sustainable energy infrastructure, the integration of energy storage systems (ESS), for example, stationary ESS and movable energy storage like electric vehicles (EVs) in the smart home layer, a single community layer, and a macro multi-community layer, emerges as a crucial solution. ESS exhibits the distinctive capability of providing fast response times, allowing for the efficient management of surplus energy during off-peak demand periods and the discharge of stored energy during peak-demand periods. By strategically deploying ESS in conjunction with energy sharing and demand-side management, smart grid communities can harness the benefits of energy storage to balance supply and demand, mitigate the effects of fluctuations in energy demand and generation, and reduce reliance on costly and environmentally harmful peak power plants.

Typically, the electricity market is a hierarchical structure with multiple layers. The first and lowest layer consists of end-users and prosumers, such as smart homes equipped with various appliances, and other prosumers, like electric vehicle owners utilizing public charging facilities. Since small prosumers have limited demand and supply capacity, they need to belong to aggregators in order to provide energy sharing to the system. The higher layer, or middle layer, comprises community aggregators that consolidate all demand and supply within the community or region and facilitate exchanges with other communities in different regions and utility companies for energy and information. In some cases, they may be called ancillary service providers or demand response service providers. Additionally, this layer could include significant prosumers who do not need to go through the aggregators, such as commercial and industrial buildings, as well as public places with high demand, like schools. The highest layer is occupied by the market operator or the utility company, which centrally manages electricity production to meet the demands of a multi-community power system. In each layer, there are challenges that should be investigated.

1.3.1 Basic Community Energy Sharing for Storage Loss Problem

Energy storage systems (ESS) play a crucial role in smart homes powered by RE resources. However, ESSs face several challenges that need to be addressed for effective integration. Energy loss is an important consideration, and minimizing energy loss should be prioritized to preserve system efficiency. Without proper management, energy loss can adversely impact the overall efficiency of the system. Determining the appropriate capacity for the ESS is crucial when designing an energy system integrated with RE resources. The capacity directly influences the system's ability to handle surplus and shortage energy. An improperly sized ESS can lead to system instability, reducing the capability of the ESS to manage fluctuating generation and demand. An effective method to reduce energy loss and decrease the size of the energy storage capacity is to implement load shifting. Load shifting involves adjusting the demand of home appliances and devices (HADs) to align with the generated energy from RE sources, thereby enhancing the overall system efficiency.

1.3.2 Single Community Energy Sharing for Peak Shaving Problem

Typically, generated electricity needed to be matched all the time with the electric demand. When multiple high-consumption electric appliances are simultaneously activated, it can result in a surge in overall energy demand, leading to peak periods. During these peak periods, UC are required to operate peak-generation power plants, incurring significant expenses to meet the additional demand. To tackle this challenge, a potential solution involves offering peak shaving services to various groups of EVs or battery packs. The UC can leverage the fast response capabilities of energy storage units on the demand side to discharge stored energy into the grid. This approach assists the UC in mitigating peak demand and reducing additional costs. Electric vehicles, for instance, can be charged at lower prices during non-peak demand periods and discharge energy back to the grid during peak-demand periods, such as early evening, offering benefits for their

participation in this program. However, the majority of G2V and V2G research primarily concentrates on personal passenger EVs. These vehicles, designed for individual transportation with diverse schedules and purposes, typically have smaller battery capacities, resulting in lower willingness and interest to participate in ancillary services. Real-world implementation of V2G programs with this type of EV may prove challenging. In contrast, ESBs follow specific schedules and routes, often remaining parked in idle mode. Schools that own ESBs would find participation in V2G programs beneficial, so it ensures high willingness to engage in ancillary services. Due to their predictability and substantial battery storage capacities, ESBs are well-suited for providing V2G services. This makes them a compelling choice for contributing to grid stability and benefiting both schools and the UC. However, a single ESB may not be capable of discharging a sufficient amount of energy to participate in such a program. Therefore, it is essential for a school, which can aggregate the discharged energy from multiple ESBs within its location, to act as the participant in the peak shaving program.

1.3.3   Muti-Communities Energy Sharing for Energy-Pricing Problem

In a multi-community smart grid, the demand profile for each community is different. Normally, the unit price of electricity depends on the net energy demand consumed. To promote fairness between each community, different pricing is used, depending on the net energy of that region. In order to achieve a better energy profile and reduced unit electricity price in each community in a multi-communities system, mobile energy storage such as electric vehicles could be interesting to use for charging and discharging energy while traveling to/from different places in different communities. It could help in cases where there is a difference in energy profiles between communities; for example, Community 1 may have a very sunny day and can produce a lot of surplus energy from PV, while Community 2 may be facing heavily cloudy or rainy days where energy from PV is almost impossible to generate. In this case, electric vehicles that are already planned

to travel from Community 1 to Community 2 may be able to charge surplus electricity at a low price and discharge it at Community 2, where the selling price per unit will be very high. This will result in the EV owner gaining economic benefits, while other prosumers in Community 2 will benefit from the reduced price due to the reduced amount of energy within their community. In a case like this, the game theoretical approach is highly suitable to implement, where there are many stakeholders, including electric vehicle owners, community energy aggregators, and utility companies. The utility of every entity will be maximized, resulting in a win-win-win situation.

1.4 Research Purpose and Objectives

The purpose of this dissertation is to introduce a "hierarchical Multi-communities Energy SHaring management (hMESH)" framework with integrated energy storage for multi-layer multi-communities, determining optimal strategies of various entities, along with minimizing the energy loss and optimal storage capacity in a smart grid. The main objectives are as follows:

- To study the energy sharing management in a smart home in order to design optimal storage capacity with minimum energy loss through distributed power flow assignment.

- To study the critical hour energy management in a single community in order to determine the optimal critical hour strategies of electric school buses.

- To propose and study novel inter-communities energy sharing management model for movable energy storage, i.e., electric vehicles, and determine the optimal energy-price strategies.

1.5 Structure of Dissertation

The rest of the dissertation is organized as follows:

- Chapter 2: Hierarchical Multi-Communities Energy Sharing Management Framework (hMESH)

  Chapter 2 explains the key components associated with the proposed hMESH framework, including renewable energy resources, energy storage systems, electric vehicles, and smart homes. It further presents and describes the proposed hMESH framework for future smart grid communities, which integrates various kinds of energy storage.

- Chapter 3: Energy Sharing Management for Non-Noving Energy Storage (eNMES) Scheme

  In Chapter 3, an energy sharing management for non-moving energy storage in smart home environments comprising multiple renewable energy sources, home appliances, and multiple energy storage system units is introduced. It utilizes distributed power flow assignment coordinated with a load-shifting algorithm to minimize energy loss and determine the optimal energy storage capacity.

- Chapter 4: Critical Hour Energy Sharing Management for Partially Moving Energy Storage (ePMES) Scheme

  In Chapter 4, a critical hour energy sharing management model for partially moving energy storage, specifically electric school buses (ESBs), is proposed. The ESB is highly suitable for performing vehicle-to-grid (V2G) ancillary services as it is deployed at specific times and remains idle for extended periods. The single community V2G model is introduced, where a non-cooperative game is formulated between a utility company (UC) trying to minimize additional costs from generating peak demand during critical hours and schools that possess a number of ESBs. These buses can help the UC by discharging stored energy from their batteries to mitigate peak demand. Schools try to negotiate with the UC to maximize their benefits, resulting in the optimal interval and month for discharging energy.

- Chapter 5: Inter-Community Energy Sharing Management for Fully Moving Energy Storage (eFMES) Scheme
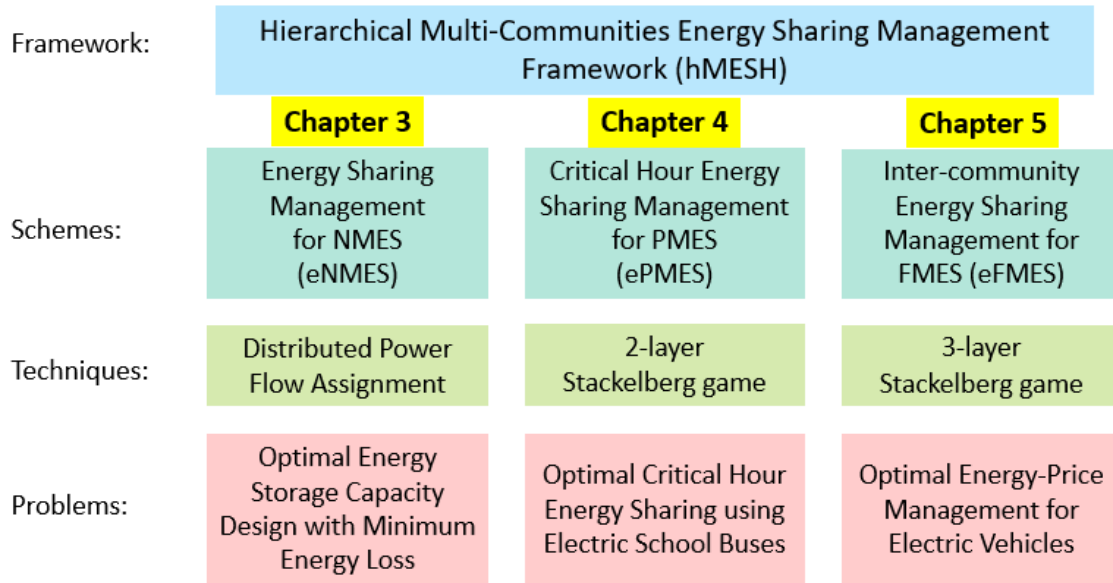
Figure 1.5: Proposed conceptual framework for multi-communities energy sharing management system.

In Chapter 5, a novel multi-communities energy sharing management model is proposed and studied. The model consists of three types of players across three hierarchical levels: the utility company (UC) at the upper level, community energy aggregators (CEAs) at the middle level, and electric vehicles (EVs) at the bottom level. In smart grid communities, EVs can move between multiple communities with different load profiles and energy prices, performing charging and discharging in different areas. At each level, players try to maximize their benefits by selecting strategies in response to other players. The UC will set the optimal multi-community energy-saving price, CEAs will set the optimal community energy sharing prices, and EVs will set the optimal charging/discharging strategies.

- Chapter 6: Conclusions and Future Works

  In Chapter 6, conclusions and future research directions are provided.

The proposed conceptual framework for multi-communities energy sharing management system can be illustrated in Figures 2.2.

Chapter 2

Hierarchical Multi-Communities Energy Sharing Management Framework (hMESH)

2.1 Components of the Framework

2.1.1 Renewable Energy Resources

Renewable Energy Resources (RE) such as solar Photovoltaic cells (PV), Fuel cells (FC), and wind turbines (WT) play a crucial role in the integration of smart home environments and smart grid and are widely installed in residential households and smart grid communities to supply electricity [5]. Several factors contribute to this trend, including the significantly reduced installation costs of solar PVs due to advancements in solar cell technology [6]. Moreover, the environmentally friendly nature of these renewable sources, compared with conventional power plants that rely on fossil fuels, releasing harmful emissions, has driven the adoption of RE [7]. Despite the benefits, the intermittent, uncertain, and fluctuating nature of RE, primarily dependent on weather conditions, poses challenges to the reliability of RE as an energy source [8]. This variability can reduce the stability of electricity and presents a significant obstacle to seamlessly integrating RE into electrical

systems. In addition to the fluctuating nature of RE, the various types of power loads with unplanned human activities and user preferences can also contribute to the dynamic behavior of load demand in electrical systems [9].

2.1.2   Energy Storage Systems

In today's power system landscape, renewable energy (RE) resources play a pivotal role, particularly within the residential sector. Despite the significance of these resources, the intermittent nature of RE resources, influenced by variable weather conditions, poses challenges to their reliability as energy resources. Addressing this challenge, the integration of an energy storage system (ESS) emerges as a viable solution, enabling the storage of surplus energy during peak-generation periods and subsequent release during shortages. In order to fully utilize RE together with ESS, an efficient system design for integrating REs with ESSs is highly needed. Today, the design of energy systems in a distributed way that incorporates RE resources and human activities is essential. As people's activities in a house are becoming more complicated, it is necessary to ensure a balanced, reliable, and safe energy supply to all electrical loads from RE resources. The ESS becomes an indispensable component to address the intermittent nature of RE and the dynamic fluctuations in loads' demand. In smart home environments and smart grids, ESS integration is necessary to provide uninterrupted electricity availability to satisfy demand in real-time.

2.1.3   Electric Vehicles

Today, the number of internal combustion engine vehicles (ICEVs) on the road is steadily being replaced by electric vehicles (EVs) . This shift is facilitated by the decreasing prices of EVs, making them more affordable. EVs offer numerous advantages over ICEVs, such as their environmentally friendly nature, energy efficiency, high performance, and low maintenance costs. In the U.S.A., approximately 58% of harmful greenhouse gas emissions come from the power and transportation sectors [10]. ICEVs contribute to emissions that are not only detrimental to the environment, causing climate change issues, but also pose

health risks to humans, leading to various diseases [11].

The development of information and communication technology (ICT) has led to the transformation of the traditional grid into a smart grid [12], enabling various entities to communicate and be controlled efficiently. An important aspect of this transformation is the integration of EVs, which possess the capability of charging and discharging from/to their battery storage. As the number of EVs on the road continues to rise, coupled with advancements in modern 2-way communication and control systems, the charging and discharging of EVs can be effectively controlled and managed.

2.1.4 Smart Homes

Nowadays, smart homes represent a promising and increasingly prevalent trend in the residential sector. The phrase "smart home" was first introduced in 1984 by the American Association of House Builders, as F. K. Aldrich remarked [13]. These smart homes typically integrate renewable energy (RE) resources, like solar photovoltaics (PVs), fuel cells (FCs), and more [14], to power various home appliances and devices (HADs). The concept of smart homes has evolved significantly in recent decades, driven by advanced technologies, such as the internet of things (IoT). This technological integration allows HADs to be fully interconnected for both energy and information communication through a central controller. The introduction of the IoT, power-line communication (PLC), and power over ethernet (PoE) has transformed the traditional way of managing energy usage in HADs. These technologies enable the controller to communicate with diverse home appliances, collecting and monitoring the energy generated by RE sources and the consumption profiles of HADs. Employing PoE is an excellent choice for quickly and directly controlling home equipment, encompassing the capability to both supply energy and send/receive information via Ethernet cables. Single-pair ethernet (SPE) is an evolved version of PoE that emerges as a promising option for future IoT applications. Compared with traditional PoE, SPE utilizes only two twisted wires, making this technology suitable for small-scale deployment and reducing installation costs [15]. SPE still serves the dual

purpose of carrying information and electrical energy within the system. In addition to wired communication technologies like PoE, wireless communication technologies are also extensively employed for IoT purposes. Examples include Bluetooth low energy (BLE), ZigBee, WiFi, LoRaWAN, WiSUN, and others. These wireless technologies contribute to the seamless connectivity and communication of smart home devices, enhancing the overall efficiency and control of these systems.

2.2 Related Work on Energy Sharing in Smart Grids

For community-based energy sharing management, the literature explores two main categories: energy sharing within a single community with and without EV integration, and energy sharing across multiple communities.

Several studies have made efforts toward energy sharing within single communities without considering EVs [16–19]. In [16], a novel energy sharing model is proposed by utilizing the supply-to-demand ratio (SDR) to determine internal buying and selling prices, facilitating energy sharing among PV prosumers within a single community. The simulation reveals the model's effectiveness in reducing prosumers' costs and improving the sharing economy. A game-theoretic approach for energy sharing management is proposed in [17], where it is used to find the optimal energy price and consumption of prosumers. A novel profit model of the microgrid operator, utility model of prosumers, and billing mechanism are introduced. The results show increased benefits for all players. A. Paudel et al. [18] introduced a novel peer-to-peer energy trading model among prosumers in a single community. The Stackelberg game is formulated for the interaction between sellers and buyers, where the sellers are the leaders and the buyers are the followers of the game. The results confirm the effectiveness of the model in improving both technical and financial benefits for the community. In [19], a community-based energy trading model is proposed, where a coordinator helps facilitate the trading process between market participants. Demand-side management is also implemented using a non-cooperative game. The findings show that the model can increase prosumers' profits and greatly reduce peak

energy demand.

On the Other hand, Some work has focused on a single community energy sharing integrating EV [20–24]. In [20], a peer-to-peer energy trading model among plug-in hybrid electric vehicles (PHEVs) is proposed. The model provides incentives for PHEVs to discharge energy to balance the energy profile of the system. Agreed-upon energy and electricity prices are determined using a double auction. Simulation results reveal that the model can achieve maximum social welfare. J. Kim et al. [21] presented an energy trading and demand response system for electric vehicles in a single isolated microgrid system. In the model, sellers and buyers submit transaction prices, and buyers determine optimal results. Revenue and energy are allocated according to payments and sales. Results show that participants can maximize their profit while stabilizing energy supply and demand. A framework for peer-to-peer energy trading among electric vehicles, charging stations, and office buildings is introduced in [22]. Electricity price depends on the price of stored energy in the battery. Analysis shows that the model can help reduce prosumers' costs by 23%, improve PV self-consumption by 10%, and guarantee willingness to participate. In [23], an energy dispatching model for a microgrid and EVs is introduced, where the microgrid aims to balance supply and demand while EVs aim to lower energy costs. Results show an increase in microgrid profit and a reduction in EV costs In [24], a novel power scheduling scheme for electric vehicle (EV) charging facilities is proposed, utilizing a two-level Stackelberg game between charging facilities and EVs within a single community. The results demonstrate improved financial profits for both EV users and charging facilities.

There is limited research on energy sharing in multi-community smart grid [25–29]. With the increasing installation of distributed energy resources, F. Moret et al. [25] present the concept of a community-based energy market structure called 'energy collectives,' where prosumers can share energy at a community level. Additionally, the community manager can further facilitate energy sharing with other communities under the market or system operator. A peer-to-peer energy-sharing system with multiple regions is studied in [26], where the large scale of PV prosumers is considered. The distributed network can

be divided into multiple energy-sharing regions where the electricity price varies. Prosumers can choose the region they want to join and can provide demand response to the system, with profit maximization formulated, taking into account electricity prices and fees. The results show an increase in prosumer profit compared to scenarios without divided regions. A novel charging scheme for EVs inside smart communities integrated with RE is proposed in [27]. The authors consider three parties in the model: the grid, aggregators (AGGs), and EVs, where a trust model is introduced to enable EVs to select an AGG for charging, as information needs to be shared between each entity involved. The analysis results show that the proposed scheme is effective compared with traditional schemes. In [28], the authors proposed a planning strategy framework to optimize and manage optimal EV charging and discharging operations in multiple charging stations at different locations, aiming to enhance the flexibility and efficiency of the microgrid. The problem was formulated as a non-cooperative game involving the distribution company, charging stations, and EVs. The findings reveal that the proposed framework can increase the flexibility and efficiency of a microgrid by 0.3% and 67.4%, respectively, compared to a case study. In [29], an optimal vehicle-to-grid pricing strategy is introduced, employing a two-level Stackelberg game between multiple aggregators and EVs. However, the work considers only V2G operations and excludes G2V interactions. The results show an improvement in EV users' benefits while taking into account user satisfaction and inconvenience.

However, to the best of our knowledge, there is no research that introduces hierarchical multi-community energy sharing management systems integrating movable energy storage, such as electric vehicles, while considering the interests of multiple entities involved in the multi-community systems. The properties of movable energy storage in EVs are particularly interesting to study due to their high potential impact on the grid in multi-community systems in the future. Moreover, considering the benefits for each and every entity is highly important in order to implement these systems in the real world as well.

The summaries and comparisons of the above main related works are shown in Figure 2.1.

Ref	Proposed Solution	Method	Communities	RE/ESS/Loads	Results
[16] 2017 N. Liu	An energy-sharing model with price-based demand response is proposed	Supple-to-demand ratio	Single community	• PV • Residential loads	• Saving PV prosumers' costs • Improving the sharing of the PV energy
[18] 2018 A. Paudel	A novel game-theoretic model for peer-to-peer energy trading among the prosumers in a community	2-level Stackelberg game: Seller Prosumers, Buyer prosumers	Single community	• PV • Residential loads • Battery Storage	• Provide significant financial (cost is greatly reduced)
[19] 2021 M. Zhang	A community-based energy trading model using blockchan	Non-cooperative game: Suppliers, Prosumers	Single community	• PV • Residential loads	• Increase prosumers' profits • Greatly reduce peak energy demand
[24] 2022 J. Kim	A novel power scheduling scheme for EV charging facility	2-level Stackelberg game: Charging facility, EVs	Single community	• EV	• Improve financial profit of EV users and charging facility
[26] 2020 L. Chen	An energy sharing framework for distributed network with multi-energy-sharing region	2-level Stackelberg game: Energy sharing provider, Prosumers	Multiple regions	• PV • Prosumer loads (No ESS/EV)	• ESP profit and prosumers are be increased (compare without regional)
[27] 2019 Y. Wang	A charging scheme for EVs in a Smart communities integrated with RES	Non-cooperative Game: Microgids, EVs	Multiple microgrids	• PV • Buildings • EVs (only charging)	• Utilities of EV are improved
[28] 2022 E. Shokouh mand	A planning strategy for managing and optimizing electric vehicles G2V/V2G	Non-cooperative Game: Parking lots, EVs	Multiple charging stations in a single community	• Parking lots • EVs	• The flexibility and efficiency of the microgrid increase by 0.29% and 67.37% compared to demand response program case study
[29] 2023 P. Chen	An optimal V2G pricing strategy	2-level Stackelberg game: Aggregators, EVs	Multiple aggregators	• EVs (only V2G)	• Improve EV users benefit while considering satisfaction/inconvenience
This Work	A hierarchical multi-communities energy sharing management framework in smart grid by utilizing ESS and EV, where EVs are able to share energy at different places	3-level hierarchical including: prosumers, single communities, and multi-communities level	Multiple communities (EVs are movable to different communities)	• UC • Aggregators/Schools • EVs • Smart home	• Win-Win situation for every entity • Reduce cost/improve profit • Reduce peak, fill valley, reduce PAR • Not only EV who provide, but others prosumer in the system will benefit as well

Figure 2.1: Comparisons of the main related works in the energy sharing field.

19

2.3 Proposed hMESH Framework

In this dissertation, a novel framework called the Hierarchical Multi-Communities Energy Sharing Management Framework (hMESH) is introduced, which considers various energy storage integrations into the smart grid for the future electrical grid. The overview structure of the framework, which aligns with the electrical grid, is shown in Figure 2.2. This dissertation aims to address three problems at different levels of the structure.
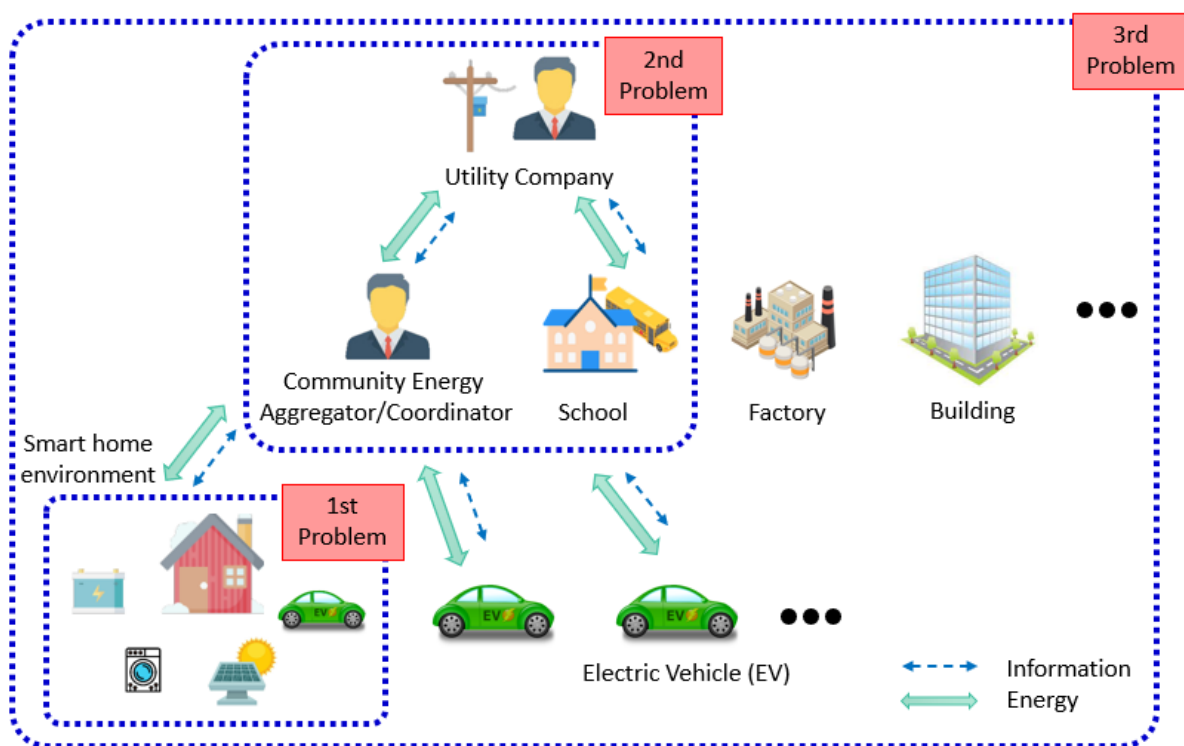
Figure 2.2: Illustration of hMESH framework with research problems in smart grid.

Renewable energy resources are expected to be widely installed. As previously mentioned, one solution to address the intermittent nature of renewable energy (RE) is integrating energy storage systems with RE installations. Additionally, the number of electric vehicles (EVs) on the road has significantly increased due to their lower prices and numerous advantages over internal combustion engine cars. These advantages include environmental friendliness, energy efficiency, high performance, and low maintenance costs. Energy storage systems are capable of functioning as a load when charging and as a source when discharging. Because of the reasons mentioned above, various types of energy stor-

age will be widely deployed and used in future smart grids, significantly transforming the current grid structure. Existing studies on energy sharing mainly consider a single community and do not account for movable energy storage, such as EVs, which can travel to multiple places across smart grid communities. This framework focuses on integrating various kinds of energy storage, including non-moving energy storage, partially moving energy storage, and fully moving energy storage, into smart grid multi-communities. The energy storage is integrated into three levels of smart grid communities. The proposed framework can help understand and project the future of energy sharing management in the electrical grid. Three schemes are proposed and studied in this framework to address various problems at different levels and structures: energy sharing management for non-moving energy storage in smart home environments, critical hour energy management for partially moving energy storage in a single community, and inter-community energy sharing management for fully moving energy storage in hierarchical multi-communities.

The distribution network of the proposed framework is illustrated in Fig 2.3. The low voltage network consists of end-users and prosumers, such as electric vehicles and smart homes, which comprise various appliances. Meanwhile, the medium voltage network may include users with larger energy demands, such as buildings, factories, and schools.
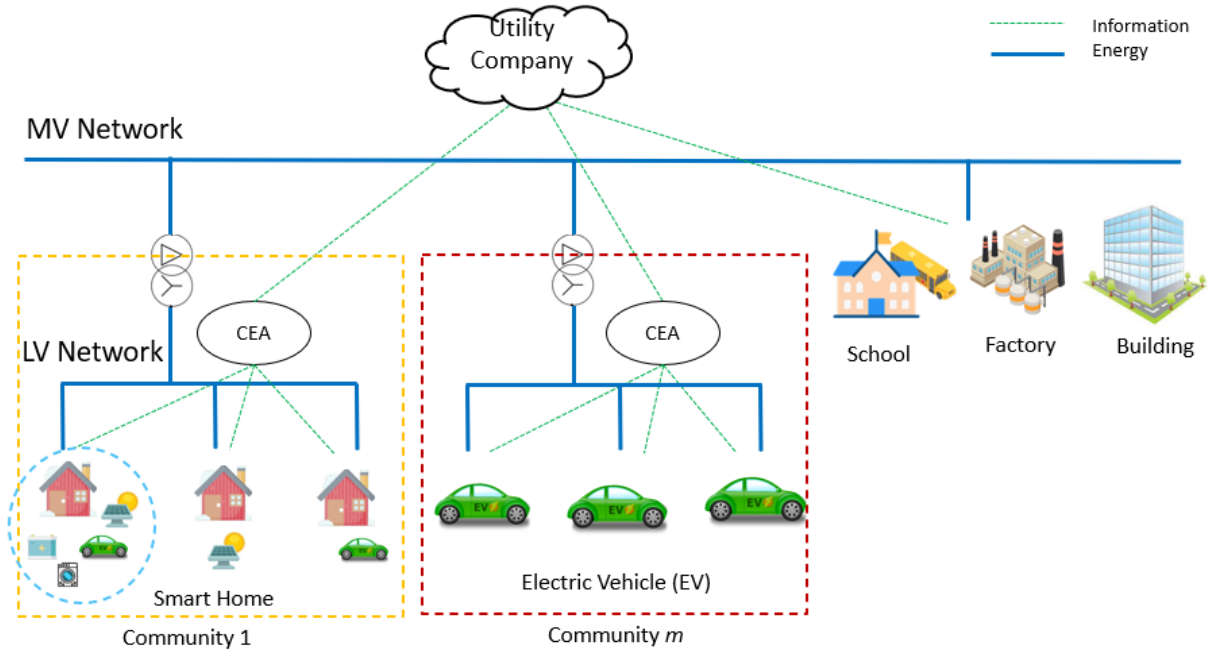
Figure 2.3: Topology of distribution networks of the proposed framework.

A proposed energy-sharing management model is structured with three hierarchical levels: utility company (UC) level, community energy aggregator (CEAs) level, and prosumers and electric vehicle (EVs) level. Within the smart grid, multiple communities exist, and each community comprises a number of EVs and prosumers. The EVs possess the unique capability to travel across the multi-community system and engage in energy sharing through charge/discharge activities. Each entity in each level of the framework is explained as follows:

- 3rd level:

  - Electric Vehicles (EVs) : Each electric vehicle is capable of charging and discharging energy through CEA. We assume that all EVs are equipped with a smart energy management system, through which they can communicate with CEA via charging facilities. The SEMS sends consumption data and receives shared price information. It is able to perform necessary computational tasks and control charging and discharging. The EV is located within the low voltage network inside a community.

– Smart Home : Smart homes are situated within the low voltage network and may have their own renewable energy resources, such as PV solar panels. They consume energy primarily through various home appliances.

- 2nd level:

  – Community Energy Aggregator (CEA) : Each CEA facilitates energy sharing within the community by engaging in two-way communication with EVs within its community. It also communicates with UC for the purpose of energy sharing between communities and determines the energy sharing prices within the community. The CEA ensures payment and energy balance for the community in which it sells or buys energy to or from EVs within the community and the utility company. If the generated energy within the community is insufficient, the CEA is responsible for purchasing the energy from the utility company.

  – High-demand Consumers : High-demand consumers, such as factories, buildings, and schools that possess a number of electric school buses, consume a significant amount of energy and are typically located within the medium voltage network. These consumers purchase substantial amounts of energy from the utility company.

- 1st level:

  – Utility Company (UC) : The UC generates and sells energy to CEAs or high-demand consumers at the price according to the net aggregated energy from the communities.

The increase of RE sources along with EVs enables consumers to both consume and generate electricity independently, adding complexity to the electrical grid. This complexity requires advanced technology and protocols for efficient management and successful implementation of the system. This framework can be implemented by utilizing the following advanced technologies:

- Advanced metering infrastructure (AMI): Smart meters are crucial components in the smart grid, playing an essential role not only in accurately measuring electrical parameters but also in facilitating communication and control. They might even be capable of providing timely forecasts of energy demand, either day-ahead or during the day. Smart meters for users and prosumers will be installed at sites where the demand and generation occur, such as homes, charging stations, and buildings. The communication capabilities of smart meters can be enhanced through various technologies. Wireless options like WiMAX or wired solutions through power line communication (PLC) enable efficient two-way communication between different entities in the system. This connectivity is essential for real-time data exchange and grid management. Effective operation of the smart grid requires specific functionalities from AMI, such as bidirectional energy measurement and communication, seamless connectivity, and adequate memory storage. These capabilities ensure that all parts of the grid are integrated and that data flows smoothly to support grid management and optimization.

- Communication protocol: In the future complex smart grid network, there will be a high frequency of communication, including numerous requests and acknowledgments between entities. The communication between sensors and smart meters can be achieved using wireless communication technologies or PLC. These methods enable efficient data exchange and monitoring within the smart grid infrastructure. The communication between smart meters and aggregators or operators can utilize wireless networks such as WiMAX, 3G, and 4G. These technologies provide reliable and rapid data transmission, essential for effective grid management and operations. The selected communication technologies should be capable of covering wide areas, offer connectivity at any time, and incur low operational costs. The standard for EV charging station communication is ISO/IEC 15118, which outlines the protocol for communication between electric vehicles and charging stations. Meanwhile, the standard for communication between charging stations and the grid is IEC 61850,

which is used for substation automation and enables interoperability and communication between various grid components.

2.3.1 Energy Sharing Management for Non-Moving Energy Storage Scheme

The energy sharing management for non-moving energy storage scheme (eNMES) is proposed to address the optimal energy storage capacity design with minimal energy loss in a smart home environment by utilizing a newly introduced distributed power flow assignment (DPFA). DPFA assigns power flow paths from energy sources, such as renewable energy (RE), to household loads. Additionally, in eNMES, DPFA is integrated with a load shifting algorithm to further reduce energy loss and the required battery storage capacity.

2.3.2 Critical Hour Energy Management for Partially Moving Energy Storage Scheme

The critical hour energy management for partially moving energy storage scheme (ePMES)is proposed to address the problem of optimal critical hour energy using partially moving energy storagee, such as electric school buses (ESBs). In this scheme, a vehicle-to-grid model is introduced between the utility company (UC) and schools that possess ESBs. Typically, ESBs are used at specific times and often remain parked and idle, making them highly suitable and practical for providing peak shaving services. During critical hours, such as peak periods, the UC sends an incentive price signal to schools within a community. Each school can discharge the stored energy in its ESBs to perform peak shaving and receive monetary benefits. The UC also benefits from reduced additional generation costs due to the lowered peak demand. The model utilizes a non-cooperative game between the players to determine the optimal incentive price and the optimal amount of discharge energy. Moreover, during periods of low demand or "valleys," ESBs can help the UC by charging and flattening the energy profile curve. Ultimately, the peak-to-average ratio of the system can be reduced.

2.3.3 Inter-Community Energy Sharing Management for Fully Moving Energy Storage Scheme

Inter-community energy sharing management scheme for fully moving energy storage is proposed to address the problem of optimal energy-price when hierarchical multi-communities integrated with electric vehicles. In the future, the number of EVs on the road will be very high. EVs can act as significant loads consuming high power and energy, and as sources capable of discharging energy back to the grid. They can also move across different communities within a smart grid, each community has its own energy profile and electricity pricing. Therefore, EVs can be managed using energy sharing prices from the utility company to help with charging or discharging, ultimately flattening the grid profile. Without proper management, from typical human behavior, typical human behavior tends to involve charging EVs upon returning from work in the evening, causing a very high demand. In this scheme, the problem is formulated as a three-level Stackelberg game involving three entities: the utility company, community energy aggregators, and EVs. All players aim to maximize their benefits. Consequently, they receive monetary benefits and can also reduce the peak-to-average ratio.

2.4 Summary

This chapter details key components associated with the proposed hMESH framework, including renewable energy resources, energy storage systems, electric vehicles, and smart homes. The hMESH framework for future smart grid communities, which integrates various kinds of energy storage, is presented and described. Additionally, the three proposed schemes within the framework are introduced and explained.

Chapter 3

Energy Sharing Management for Non-Moving Energy Storage Scheme

3.1 Introduction

World energy demand is continuously increasing [30]. Since it is not environmentally friendly, constructing more fossil fuel power plants is not an excellent answer to deal with such a problem. On the other hand, renewable energy resources such as solar panels, wind turbines, and fuel cells do not produce harmful CO_2 emissions [7]. The development of advanced technologies and the decrease in renewable energy (RE) costs make RE very interesting for many involved parties. However, the intermittent nature of RE makes it an unstable energy resource that cannot be utilized fully. Thus, energy storage systems (ESSs) are a viable solution for mitigating this issue. Especially in the residential sector, people are becoming more interested in producing their energy by using RE integrated with an ESS. These days, not only has the cost of RE decreased, but the installation cost of ESSs has also decreased by 60% from 2014 to 2017. Moreover, it is predicted to further decrease up to 61% by 2030 compared to 2017 [6].

Energy storage systems (ESSs) play a crucial role in smart homes powered by RE resources. However, ESSs face several challenges that need to be addressed for effective integration. Energy loss is an important consideration, and minimizing energy loss should

be prioritized to preserve system efficiency [31]. Without proper management, energy loss can adversely impact the overall efficiency of the system. Determining the appropriate capacity for the ESS is crucial when designing an energy system integrated with RE resources. The capacity directly influences the system's ability to handle surplus and shortage energy. An improperly sized ESS can lead to system instability, reducing the capability of the ESS to manage fluctuating generation and demand [32]. An effective method to reduce energy loss and decrease the size of the energy storage capacity is to implement load shifting. Load shifting involves adjusting the demand of HADs to align with the generated energy from RE sources, thereby enhancing the overall system efficiency. In a distributed power-flow system (DPFS), ensuring balanced, reliable, stable, and safe energy supply from all power generators or RE sources to all power loads (PLs) or HADs is crucial. The ESS becomes an indispensable component to address the intermittent nature of RE and the dynamic fluctuations in HADs' demand. Therefore, ensuring a steady, dependable, and secure energy flow in the DPFS is crucial, in addition to achieving a balance between power generation and consumption in home energy management systems and control [33]. In smart home environments, ESS integration is necessary to provide uninterrupted electricity availability to satisfy demand in real time.

In this chapter, our objective is to study the energy loss of ESSs for single and multiple power load fluctuating DPFAs in a smart home. Further, the investigation is extended by applying two types of MPFA and incorporating a load-shifting algorithm to minimize energy loss and reduce energy storage capacity. Additionally, the aim is to determine the optimal energy storage capacity by formulating the problem as a linear optimization problem. In particular, a novel approach is proposed which combines multiple-load power-flow assignment with a load-shifting algorithm to minimize energy loss and determine the optimal energy storage capacity.

The main contributions of this chapter can be summarized as follows:

- Introduce a system model of fluctuating DPFA to study balancing RE resources and power loads with the presence of ESSs in a smart home.

- Propose power-flow assignment algorithms for the energy system to efficiently assign the required power for single and multiple power loads, i.e., single-load power-flow assignment (SPFA) and multiple-load power-flow assignment (MPFA) algorithms, respectively.

- Reveal through simulation results that the proposed PFA algorithms ensure that the total energy from PGs from RE resources are completely supplied to all the PLs in order to reduce energy loss due to ESSs.

- Introducing a scheme consists of a load-shifting algorithm incorporated with the MPFA algorithm. This scheme aims to minimize energy loss and optimize energy storage capacity in the DPFS within smart homes.

- Examining the MPFA algorithm in the DPFS coupled with a load-shifting algorithm by using a real experimental dataset of a smart home environment, *i*House, and confirming the design and performance of the proposed scheme, which can efficiently and directly assign the required power to multiple PLs with the lowest energy loss.

3.2   Related Works

The literature review explores various aspects related to ESSs: integration of RE resources, optimal energy storage capacity design, energy efficiency and energy loss during charging/discharging, and integrated load-shifting algorithms.

There are many works on energy loss when integrating RE resources with ESSs [34–36]. In [34], P. Fortenbacher et al. use multi-period optimal power flow to schedule optimal battery storage operations. Their findings show that the proposed method can reduce battery losses by 30%. Additionally, a novel algorithm for optimal control and placement of ESSs for minimizing energy losses using a genetic algorithm is proposed in [35]. J. Sardi et al. [36] manage to obtain the optimal ESS capacity and analyze the energy loss reduction of an RE system integrated with an ESS through load leveling.

Several studies have focused on determining the optimal capacity of energy storage [37–41]. In [37], a method was introduced for the optimally sizing, placing, and daily charging and discharging of storage systems. The cost function considered energy loss, and the results indicated a decrease in energy loss. J. Xiao et al. [38] proposed an optimization model to find the optimal size and installation location of an ESS with the goal of minimizing the total net present value of the system, while also considering battery lifetime. The proposed method was proven to be effective. The optimal siting and sizing of distributed storage systems were addressed in [39], and the paper considered factors such as voltage support, energy loss, and the cost of energy flow in the model. A heuristic technique was employed to solve the problem, resulting in improvements in all considered terms. In [40], A.V. Sackin et al. presented control strategies for charging and discharging a large-scale ESS integrated into a wind farm. The aim was to determine the optimal capacity of all energy storage units, considering operating constraints, system capital, and operational cost while also prolonging battery life. The study used real data from an actual wind farm, and simulation results demonstrated the effectiveness of the proposed method. Additionally, an observation was made that with an increase in the number of storage units, the optimal capacity of the battery decreased. The authors in [41] proposed a method to determine the capacity of distributed energy sources, including generators and storage, to meet energy demand. The approach considers optimization for both annual and hourly operations of distributed energy systems. The results demonstrate reductions in energy consumption, operation costs, and losses.

In the research studies [42–44], the specific focus is on investigating energy losses during the charging and discharging processes of ESSs. In [42], an optimal lithium-ion battery charging strategy is introduced to minimize charging losses, employing a dynamic programming algorithm. Experimental results demonstrate the efficiency of the proposed approach, achieving minimum energy loss throughout the charging process. Research in [43] proposes a novel charging algorithm designed to reduce energy loss during the charging process. Experiments reveal a significant reduction in the energy loss of the ESS with the application of the proposed method. In [44], the authors present a novel

multi-objective optimization framework for achieving economical charging management of ESSs. The framework considers factors such as charging time; electrical energy loss; and the overall cost of charging, including battery degradation. The results conclude that the cost associated with battery degradation is considerably higher than the cost incurred from energy loss.

On the other hand, certain research studies [45–49] concentrate on optimal power assignment, aiming to enhance the overall efficiency of electrical systems incorporating ESSs. In [45], a power-flow distribution strategy is proposed for a utility-scale second-life ESS, with the goal of increasing energy system efficiency by minimizing the operational time and energy loss of the ESS. Experimental results demonstrate that the PFDS effectively improves the efficiency of multiple-battery energy systems, reducing energy loss by 24%. It achieves a 4.4% cost saving over the system's lifetime. A novel hierarchical structure for power sharing in multiple-battery ESSs is proposed in [46], aiming to increase overall system efficiency by employing an algorithm for proper control selection. Results indicate an improvement in the overall efficiency of the system. The authors in [47] introduce an operational algorithm to enhance the efficiency of multiple-unit ESSs. Efficient operation is achieved through a combination of operating points in a lookup table incorporated with a genetic algorithm to perform frequency regulation. The model is explored in different power assignment scenarios for an ESS, revealing that optimal assignment demonstrates improved system efficiency and reduced energy loss. In [48], a multi-objective optimization algorithm for power assignment and resource allocation in multiuser and multiserver edge computing is proposed to minimize costs and energy consumption. The results verify the effectiveness of the algorithm compared with the baseline method. The authors in [49] presented control strategies for power-flow control between fluctuating PVs and ESSs to ensure stable energy delivery to loads considering battery degradation and system reliability. The results demonstrate the efficiency of the proposed control scheme in managing battery operation.

Some research efforts are directed towards load shifting integrated into ESSs to minimize energy loss and determine optimal storage capacity [50–55]. In [50], the study indicates

31

that shifting domestic loads to off-peak time periods has the potential to reduce electrical losses and carbon emissions. The problem of the optimal scheduling of 24 h electric loads is explored in [51] to minimize electricity generation costs while considering system losses. Results demonstrate a reduction in average generation costs by more than 34% compared with traditional systems. However, the decrease becomes less significant as the number of loads increases. The authors in [52] consider the effects of peak load shifting on storage capacity in hybrid power systems while also considering energy losses during power conversion, transfer, and storage, developing shifting heuristics to achieve optimal storage size. The results show effective reduction in storage size, minimizing the cost of energy storage. A load-shifting allocative method for hybrid energy storage is proposed in [53] to determine the capacity of energy storage in district energy planning based on peak values for different electrical load seasons. In [54], an innovative electricity demand forecasting framework is developed to calculate the optimal battery capacity. The goal is to maximize the profit of an electricity retailer by using battery storage in electrical load scheduling. Results indicate significant annual cost savings with real electricity price market conditions and reasonable battery costs, with the optimal capacity size depending on the battery cost. A scheduling approach for the optimal charging/discharging time of battery energy storage integrated with renewable generators to reduce energy loss and dependence on the grid is proposed in [55]. The coordination operation of battery storage and renewable energy sources is considered. The results demonstrate a reduction in power loss and energy supply from the grid of up to 40%.

However, to the best of our knowledge, no research has been observed attempting to study the MPFA algorithm along with the load-shifting algorithm to reduce energy loss and energy storage capacity in a smart home environment. This combination holds high potential for decreasing energy loss and optimizing the size of battery storage in smart homes.

3.3   System Model

In Figure 3.1, the system model illustrates a simple architecture for distributed power-flow assignment (DPFA) in a smart home environment. Two power storage units (PS units), two power generators (PGs), and two power loads (PLs) are incorporated in this model. Each PG possesses the capability to provide power to both PLs and PS units.

Within the framework of basic research analysis, intentional selection of an FC and a PV system as the PGs was made. The PLs, represented by an air conditioning (AC) unit and a ventilation fan (VF), are configured to receive power from both PGs and PS units. The goal is to investigate the energy loss and determine the optimal energy storage capacity of the ESS within the power-flow system (PFS) while following the state-of-charge (SoC) boundary constraints of the PS system.

The word "fluctuating" in this work particularly relates to the unpredictability of PGs and PLs. Additionally, the term "PS system" is used interchangeably with the term "energy storage system".

The charging of an ESS is facilitated by the energy supplied by PGs, and conversely, the device can discharge energy to PLs. To logically illustrate power-flow connections among PGs, PS units, and PLs, a tripartite graph model is employed, as depicted in Figure 3.2. This graphical representation involves denoting connections between two devices through pairs of power devices. For instance, (PG_m, PL_n) indicates the connection between the m-th power generator (PG_m) and the n-th power load (PL_n).
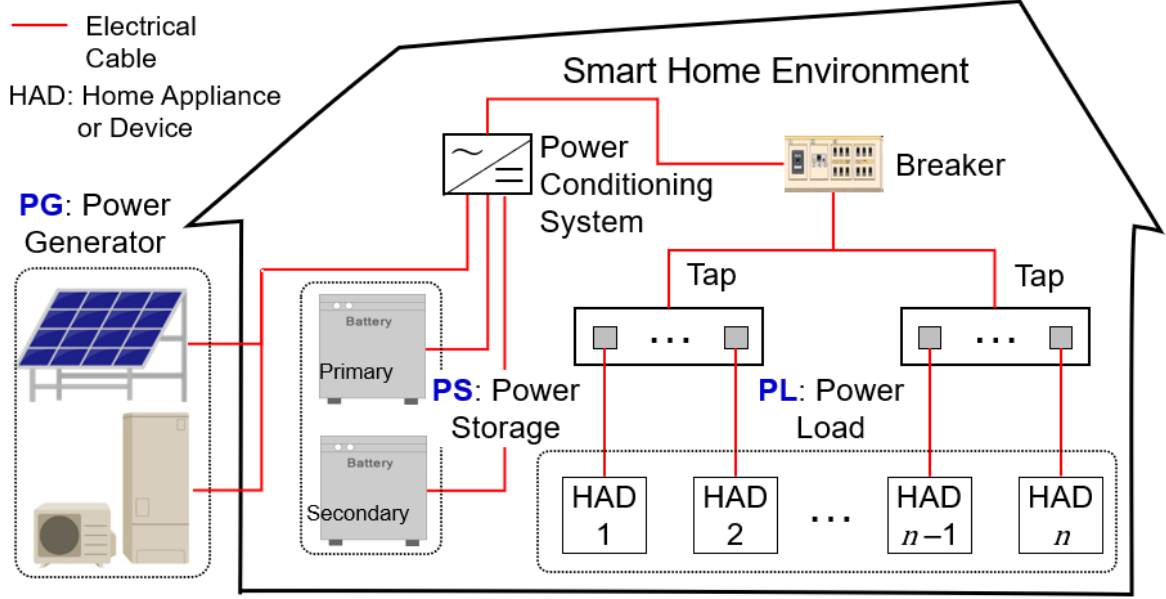
Figure 3.1: System architecture of DPFS in a smart home environment.
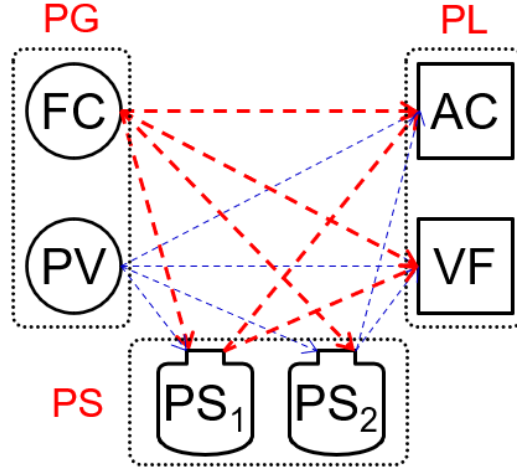
Figure 3.2: All the possible logical connections in the DPFS.

Let $\mathcal{M}$ represent the set of PGs, $\mathcal{N}$ represent the set of PLs, and $\mathcal{H}$ represent the set of PS units. Define $EG_m^f(t)$ as the set of time-varying energy generation levels at time t served by the fluctuating PGs in set $\mathcal{M} = 1, 2, \ldots, M$, where $m \in \mathcal{M}$. Denote $EL_n^f(t)$ as the set of time-varying energy load levels at time t associated with the fluctuating PLs in $\mathcal{N} = 1, 2, \ldots, N$, where $n \in \mathcal{N}$. In addition, the parameters $SoC_h(0)$, SoC_h^{min}, SoC_h^{max}, $SE_h(t)$, $EC_h^{loss}(t)$, and $EDC_h^{loss}(t)$ define a set of active PS units. Here, h varies

34

within $\mathcal{H} = 1, 2, \ldots, H$, representing the initial SoC, minimum SoC, maximum SoC, stored energy in the PS system at time t, and energy loss resulting from charging efficiency and discharging efficiency at time t, respectively.

Consider $\varphi = 1, 2, \ldots, \phi \in \phi$ to be a set representing logical power-flow connections, where the active connections at time t between the set of PL, Y, and the set of PGs, X, are indicated by the symbol $\varphi(X, Y, t)$.

After the PS system is integrated, $\varphi(PG, PL, t)$ can be reformed as a flow path that depends on connections between PGs and PS units and between PS units and PLs [56,57], i.e.,

$$\varphi(PG, PL, t) \subseteq \varphi(PG, PS, t) \cup \varphi(PS, PL, t) \tag{3.1}$$

There is a corresponding energy level for every power-flow assignment, which can be expressed as

$$\varphi(EG_m^f, EL_n^f, t) \subseteq \varphi(EG_m^f, ES_h, t) \cup \varphi(ES_h, EL_n^f, t) \tag{3.2}$$

In simpler terms, $\varphi(EG_m^f, EL_n^f, t)$ denotes the energy transferred from a PG to a PL at time t. These energy flows within the power-flow assignment of the energy system align with the following conditions:

(i) The total energy of PGs from RE sources is completely supplied.

(ii) The total energy of PLs from HADs is absolutely consumed.

(iii) The SoC limitations of PS units are securely constrained by the total energy of both PGs and PLs.

3.3.1 Power Generators and Loads

The instantaneous power of power generators and power loads is represented by $pg_m^f(t)$ and $pl_n^f(t)$, respectively. By integrating the instantaneous power, the total energy produced by each m-th power generator and the total energy consumed by each n-th power load

during time t can be represented as [56, 58]

$$EG_m^f(t) = \int_0^t pg_m^f(t)dt \tag{3.3}$$

$$EL_n^f(t) = \int_0^t pl_n^f(t)dt \tag{3.4}$$

Each PG and each PL have power limitations, as indicated below.

$$pg_m^{f,min} \leq pg_m^f(t) \leq pg_m^{f,max} \tag{3.5}$$

$$pl_n^{f,min} \leq pl_n^f(t) \leq pl_n^{f,max} \tag{3.6}$$

where $pg_m^{f,min}$ and $pg_m^{f,max}$ represent the minimum and maximum power level limitations of the m-th power generator, while $pl_n^{f,min}$ and $pl_n^{f,max}$ denote the minimum and maximum power level limitations of the n-th power load, respectively.

3.3.2 Power Storage Systems

The input power and output power of a power storage system are denoted by the variables $ps_h^{in}(t)$ and $ps_h^{out}(t)$, respectively. The SoC of the PS system is calculated using the integral of energy in the following equations [56, 59, 60].

$$SoC_h(t) = SoC_h(0) + \frac{\eta_c}{ESS_h} \int_0^t ps_h^{in}(t)dt - \frac{1}{\eta_d ESS_h} \int_0^t ps_h^{out}(t)dt \tag{3.7}$$

The PS capacity is denoted by ESS_h, while the charging efficiency and discharging efficiency are denoted by η_c and η_d, respectively. The SoC of the PS system must stay within a specific operating range to avoid overcharging and overdischarging [56, 61]:

$$SoC_h^{min} \leq SoC_h(t) \leq SoC_h^{max} \tag{3.8}$$

Therefore, the stored energy in PS system h at any given moment t is

$$SE_h(t) = SoC_h(t) \times ESS_h \tag{3.9}$$

where $ps_h^{in}(t)$ and $ps_h^{out}(t)$ have minimum and maximum power levels as follows:

$$ps_h^{in,min} \leq ps_h^{in}(t) \leq ps_h^{in,max} \tag{3.10}$$

$$ps_h^{out,min} \leq ps_h^{out}(t) \leq ps_h^{out,max} \tag{3.11}$$

3.3.3 Energy Loss of Power Storage System

In a distributed power-flow system (DPFS), energy losses occur during the charging and discharging of power storage units. Energy loss is investigated in this study using the following equations, where the energy loss resulting from charging efficiency (η_c) and discharging efficiency (η_d) may be written as follows:

Energy loss while the PS system is being charged:

$$EC_h^{loss}(t) = (1 - \eta_c) \left(\sum_{m \in \mathcal{M}} EG_m^f(t) - \sum_{n \in \mathcal{N}} EL_n^f(t) \right) \tag{3.12}$$

Energy loss while the PS system is being discharged:

$$EDC_h^{loss}(t) = (\frac{1}{\eta_d} - 1) \left(\sum_{n \in \mathcal{N}} EL_n^f(t) - \sum_{m \in \mathcal{M}} EG_m^f(t) \right) \tag{3.13}$$

3.3.4 Operating Hours of HADs

The energy load (EL) parameter for HADs can be utilized to calculate the number of operating hours in a whole day. For instance, the energy demand of HADs can be computed by using the total number of operating hours of the energy loads, denoted by H_{DE}. The parameter $SD_i(t)$ is defined to indicate the state of demand, where $SD_i(t) = 1$ means that the HADs demand energy, while $SD_i(t) = 0$ means that the HADs do not require

energy.

$$H_{DE}(i) = \sum_{t=0}^{T} SD_i(t) \tag{3.14}$$

where

$$SD_i(t) = \begin{cases} 1 & , EL_i(t) > 0 \\ 0 & , EL_i(t) = 0 \end{cases} \tag{3.15}$$

On the other hand, the parameter of energy supply (ES) for a renewable energy source can be used to determine the number of operating hours in a whole day. For example, the energy supply of a solar panel can be computed by using the total number of operating hours of the energy deliverables, denoted by H_{ED}. The parameter $SS_i(t)$ is defined to indicate the state of supply, where $SS_i(t) = 1$ means that the PG has supplied energy, while $SS_i(t) = 0$ means that the PG has no supplied energy.

$$H_{ED}(i) = \sum_{t=0}^{T} SS_i(t) \tag{3.16}$$

where

$$SS_i(t) = \begin{cases} 1 & , ES_i(t) > 0 \\ 0 & , ES_i(t) = 0 \end{cases} \tag{3.17}$$

3.4 eNMES Scheme

This section provides a detailed description of the energy sharing management for non-moving energy storage in a smart home (eNMES) scheme. The scheme consists of three main parts. The first part is admission control. The second part involves logical power assignment algorithms using MPFA and a load-shifting algorithm. The third part focuses on optimal energy storage capacity design using linear programming.

The flowchart of the overall scheme is illustrated in Figure 3.3. First, the proposed scheme gathers data from a real experimental dataset of a smart home named *i*House, along with resident activities, and initializes all necessary parameters. Subsequently, the multiple-load power-flow assignment algorithm is applied to establish power-flow connec-
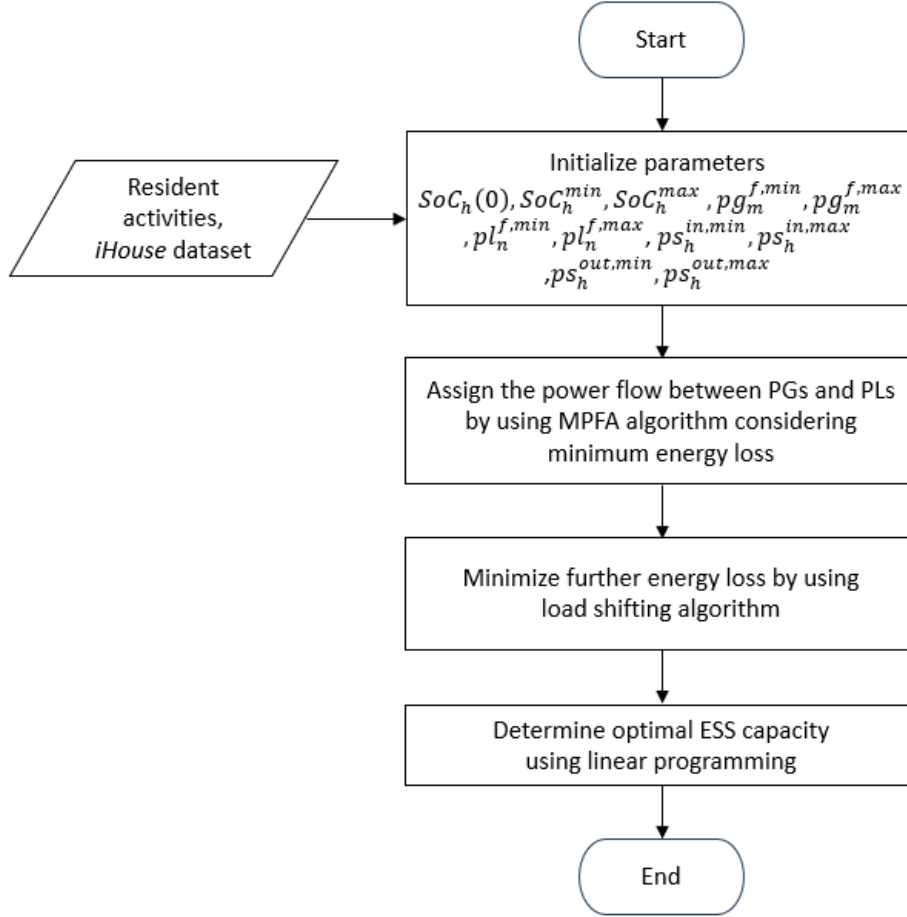
Figure 3.3: Flowchart of the overall proposed scheme.

tions between PGs and PLs. After that, the load-shifting algorithm to reduce energy loss is applied. Finally, the reduced optimal ESS capacity is determined using linear programming.

3.4.1 Admission Control

In a DPFS within a smart home environment, a controller engages in message exchange with all PGs and HADs. The controller may calculate the overall energy supply from power generators and the total energy requests from PLs after receiving these communications. Figure 3.4 shows the state change of the admission control scheme.

The figure illustrates three main entities: the controller, HADs, and RE sources, which communicate through a communication channel, interacting with each other. The first
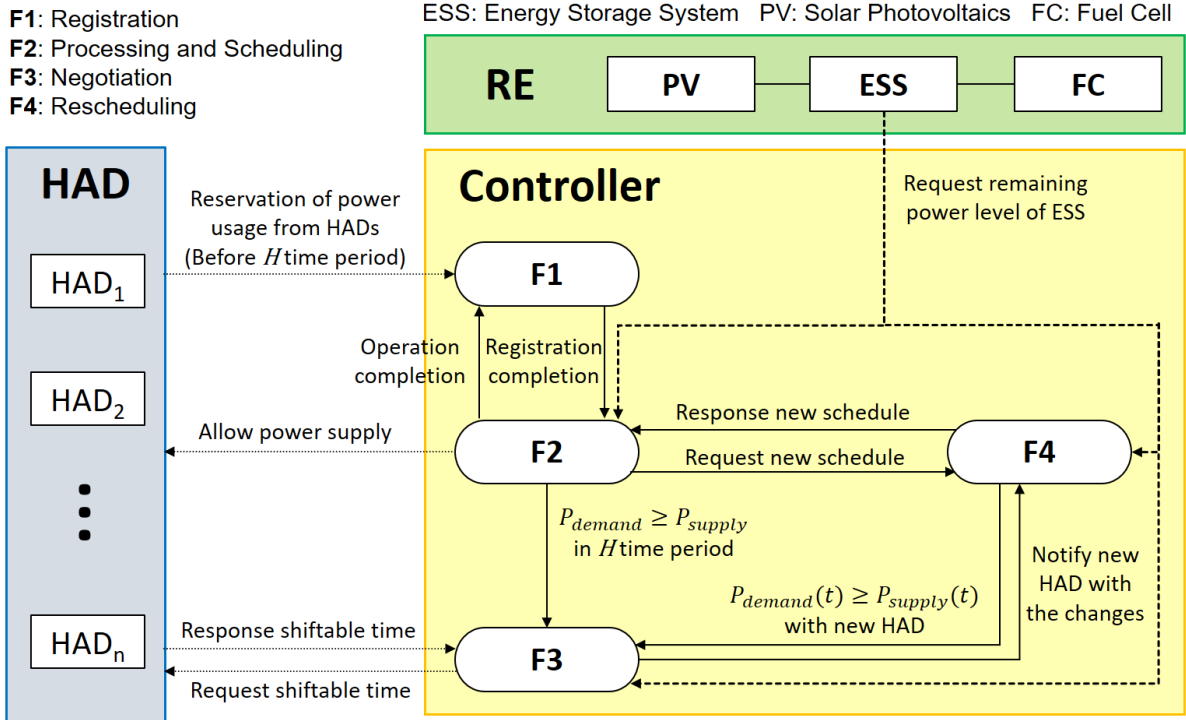
Figure 3.4: State transition of admission control scheme for a controller.

operation, in F1, when HADs require energy to operate, involves sending a signal to the controller. Subsequently, the controller registers the HADs' information and requests. Then, in F2, the controller performs calculations and scheduling based on the demand of HADs. If the demand cannot be met (F3), the controller initiates negotiations with HADs using the proposed scheme to shift their operating time to a new time slot. In the F3 stage of admission control, algorithms are proposed to negotiate the lowest energy loss for the entire distributed power-flow system. If the new schedule can be settled, the controller performs rescheduling in F4. Moreover, tailoring the admission control mechanism to the demand and preferences of users is possible by indicating the priority energy class of any of the HADs. For instance, HADs with a shiftable mode can be programmed to operate during times when energy supply exceeds energy needs. In this chapter, further examination will be conducted on this criterion for a DPFS in a smart home environment.

3.4.2 Fluctuating Distributed Power-flow Assignment

This subsection introduces the details on how fluctuating distributed power-flow assignment (DPFA) works with its algorithms when a single power load and multiple power loads are considered.

Single-Load and Multiple-Load Power-flow Assignment

In Figure 3.5, fluctuating DPFA can be divided into two types. One is single-load power-flow assignment (SPFA), which indicates the logical connection that a single PL can obtain its power from a PS only or both a single PG directly and a PS. Another is multiple-load power-flow assignment (MPFA), which represents the logical connection of each PL that can obtain its power both from multiple PGs directly and from a PS or multiple PSs. The amount of charging energy of a PS depends on the remaining power after the PGs supply multiple loads.

In SPFA, when a single PL obtains its power from the basic logical power-flow connection, e.g., $\varphi(PS, PL, t)$, we define SPFA/S as a single PL that only receives its power from a PS. Likewise, when a single PL obtains its power from two basic logical power-flow connections, e.g., $\varphi(PG, PL, t)$ and $\varphi(PS, PL, t)$, we define SPFA/GS as a single PL that receives its power from both a single PG directly and from a PS.

In MPFA, multiple PLs obtain their power both from multiple PGs and from a single or multiple PSs. When the PS receives the remaining power from a single PG (SG) only through the basic logical power-flow connection, e.g., $\varphi(PG, PS, t)$, we define MPFA/SG as multiple PLs receiving their power under the condition that the PS receives the power remaining from a single PG. Likewise, when multiple PLs obtain their power both from multiple PGs and multiple PSs, and the PS receives the power remaining from multiple PGs (MG) through the basic logical power-flow connection, e.g., $\varphi(PG_m, PS_h, t)$, we define MPFA/MG to mean multiple PLs receive their power under the condition that the PS receives the power remaining from multiple PGs.

Single-load Power-flow Assignment

Since SPFA/S involves simple and very straightforward assignment, there is no algorithm for SPFA/S power-flow. However, an algorithm is needed for SPFA/GS. The objective of the SPFA/GS algorithm is to ensure that the total energy of the PG is directly supplied first to the corresponding PL. Then, the remaining energy from the PG will charge the single PS.
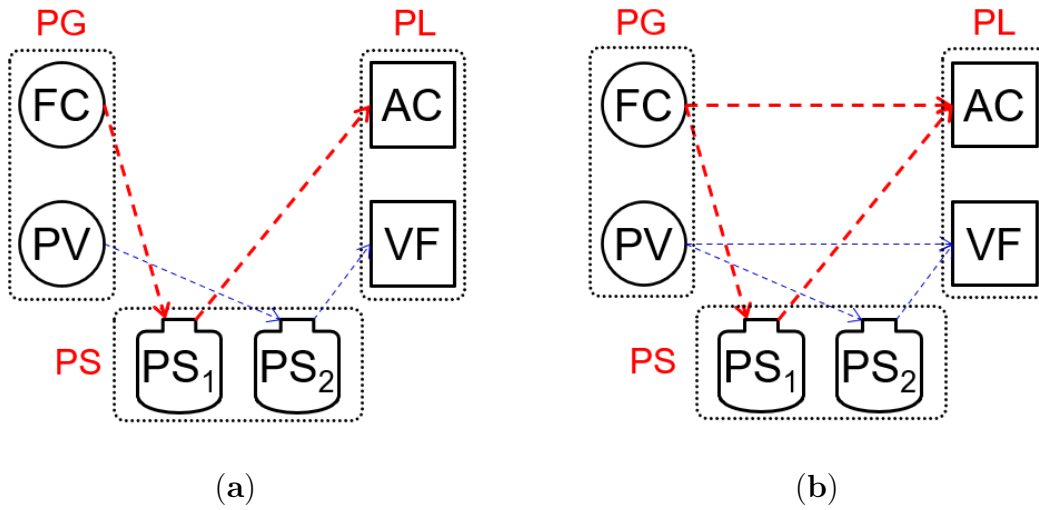
Figure 3.5: Logical power connections of two different SPFA types: (**a**) SPFA/S and (**b**) SPFA/SG.

Multiple-load Power-flow Assignment

This subsection provides details on how MPFA works. In MPFA, each PL draws power from multiple PGs and, additionally, from either a single or multiple PS units. The surplus energy is stored either in a single PS unit or multiple PS units, depending on whether the system is MPFA/SG or MPFA/MG. The logical connections of these MPFA types are illustrated in Figure 3.6.

In the MPFA/SG configuration, several PLs receive energy based on the circumstance under which each PS unit acquires the remaining energy from a single corresponding PG (SG). Subsequently, each PS unit further supplies only a single corresponding PL. To illustrate, both the FC and PV sources can simultaneously provide energy to the HADs, namely, the AC unit and the VF. However, the FC can only store generated power in
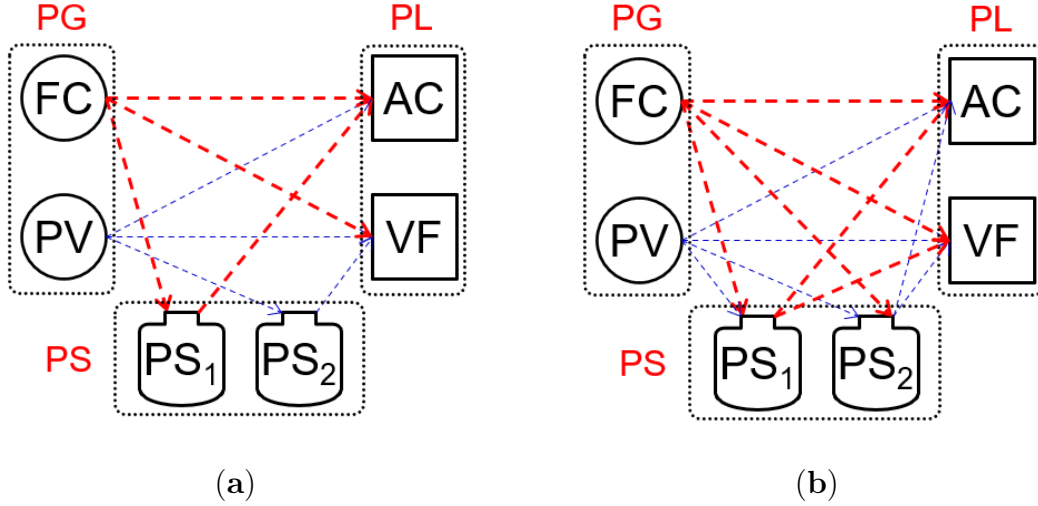
Figure 3.6: Logical power connections of two different MPFA types: (**a**) MPFA/SG and (**b**) MPFA/MG.

PS_1, and similarly, the PV system can only store power in PS_2. In scenarios where the FC generates insufficient energy for the AC unit, PS_1 can discharge the stored energy to turn on the AC unit. Similarly, in the case of the PV system supplying energy to the VF, PS_2 helps provide the required energy, as shown in Figure 3.6a. The goal of the MPFA/SG algorithm is to guarantee the direct supply of the total energy from the PG to all PLs. The remaining energy of the PG is then utilized to charge the single PS unit. Figure 3.7 illustrates the flow chart of MPFA/SG.

Conversely, in MPFA/MG, multiple PLs draw energy from both multiple PGs and multiple PS units. Each PS unit obtains the remaining energy from multiple PGs (MGs) and further supplies multiple PLs. For example, energy can be supplied to the AC unit and the VF by both the PV system and the FC simultaneously. Then, both PS_1 and PS_2 can equally store the excess energy from both the FC and the PV system. Additionally, energy can be concurrently obtained by the AC unit and the VF from both PS_1 and PS_2, as shown in Figure 3.6b. The aim of the MPFA/MG algorithm is to prioritize the direct supply of the total energy from the PG to all PLs. The residual energy of the PG is evenly distributed to charge multiple PS units. Figure 3.8 depicts the flow chart of MPFA/MG.
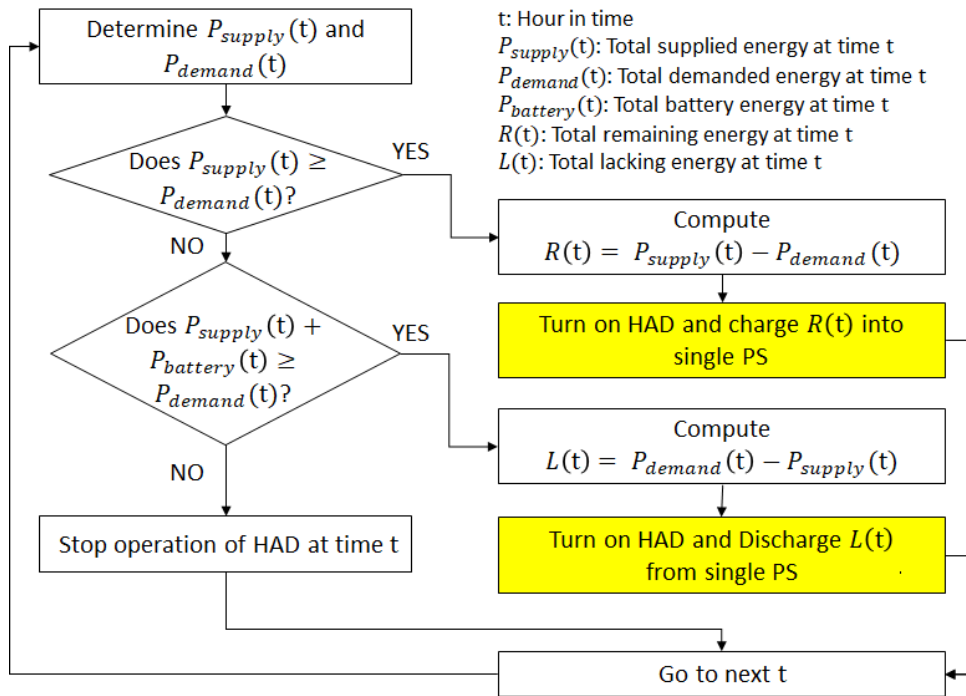
Figure 3.7: Flowchart of the MPFA/SG algorithm.
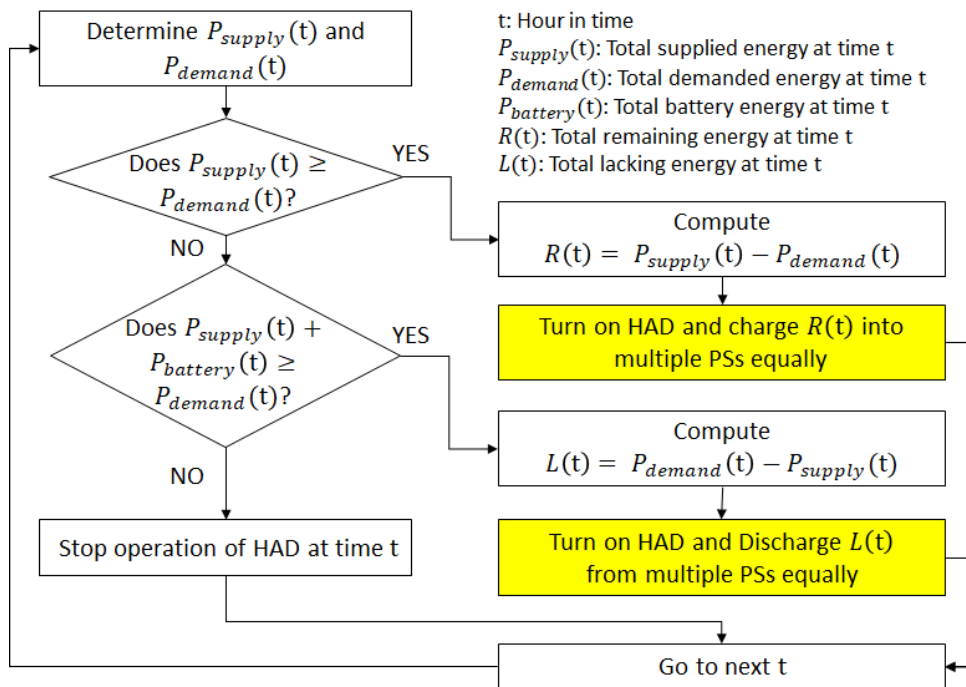
Figure 3.8: Flowchart of the MPFA/MG algorithm.

3.4.3 Load-Shifting Algorithm

The load-shifting algorithm's flowchart is shown in Figure 3.9. The algorithm first estab-lishes for how many hours shifting HADs may operate. The operating time of shifting HADs is thus moved into different time slots while minimizing energy loss in the PS system. Lastly, the controller notifies all shifting HADs with the new time slots.

We further define additional parameters used in executing the proposed scheme, as these parameters will be used in the upcoming flowcharts: $P_{supply}(t)$ is the total supplied energy at time t; $P_{demand}(t)$ is the total demanded energy at time t; $P_{battery}(t)$ is the total battery energy at time t; DE is the demanded energy of shifting HADs; ED is the energy deliverable to shifting HADs; $R(t)$ is the total remaining energy at time t; and $L(t)$ is the total lacking energy at time t.
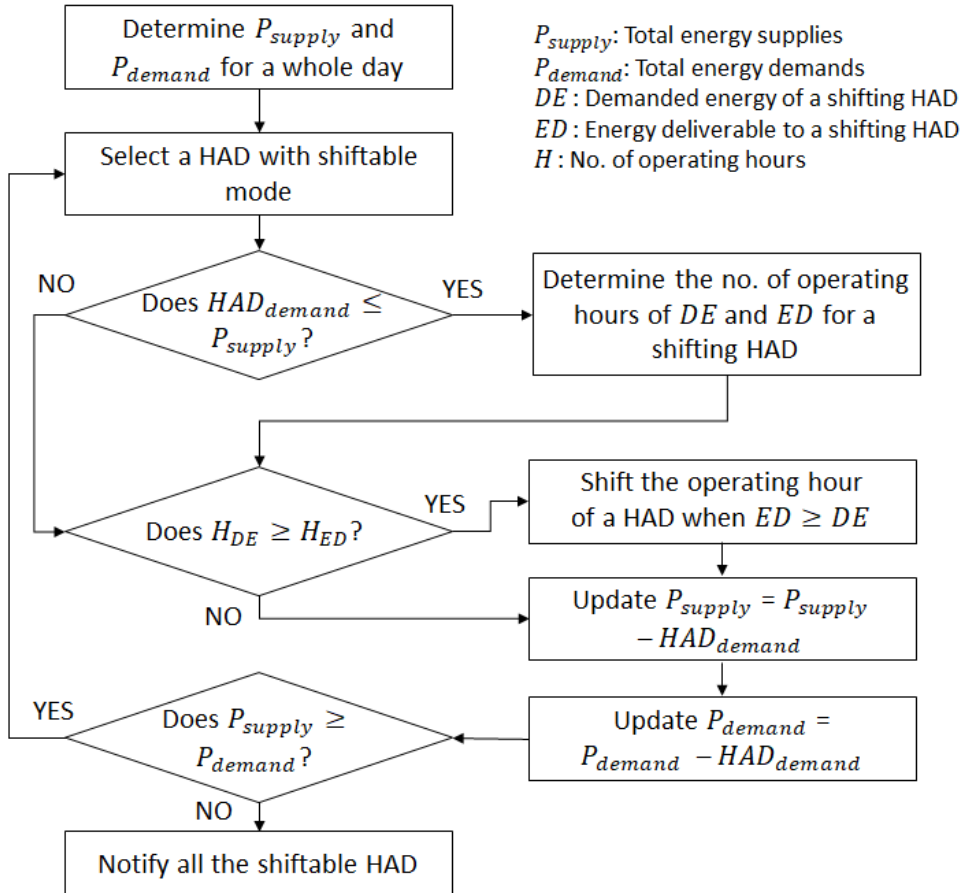
Figure 3.9: Flowchart of the load-shifting algorithm.

3.4.4 Optimal Energy Storage Capacity Computation

The optimal energy storage capacity is determined by formulating a linear programming minimization problem constrained by two assignment conditions [32, 33]. These conditions ensure the normal operation of PS systems by maintaining energy generation and consumption within SoC bounds.

$$minimize \sum_{h \in \mathcal{H}} ESS_h(t) \qquad (3.18)$$

Condition 1:

$$\sum_{m \in \mathcal{M}} EG_m^f(t) \leq \sum_{n \in \mathcal{N}} EL_n^f(t) + \sum_{h \in \mathcal{H}} (SoC_h^{max} - SoC_h(0)) \cdot \frac{ESS_h(t)}{\eta} \qquad (3.19)$$

Condition 2:

$$\sum_{m \in \mathcal{M}} EG_m^f(t) \geq \sum_{n \in \mathcal{N}} EL_n^f(t) + \sum_{h \in \mathcal{H}} (SoC_h^{min} - SoC_h(0)) \cdot \frac{ESS_h(t)}{\eta} \qquad (3.20)$$

3.5 Evaluation Studies

3.5.1 Simulation Setup

In this section, we investigate the performance of single- and multiple-load power-flow assignment algorithms for fluctuating DPFA in a smart home. We also further evaluate the effectiveness of MPFA with and without the load-shifting algorithm in a smart home environment is performed, aiming to minimize energy loss and identify the optimal energy storage capacity. The study involves two power generators, namely, a PV system and an FC; two power loads, namely, an AC unit and a VF; and two PS units. Simulations are conducted for two different seasons, summer and winter, chosen due to high demand, especially for heating, ventilation, and air conditioning.

For the PV system and the FC, real experimental datasets obtained from a smart home named *i*House in Ishikawa, Japan [62], are utilized, where the rated voltage is 110 V and
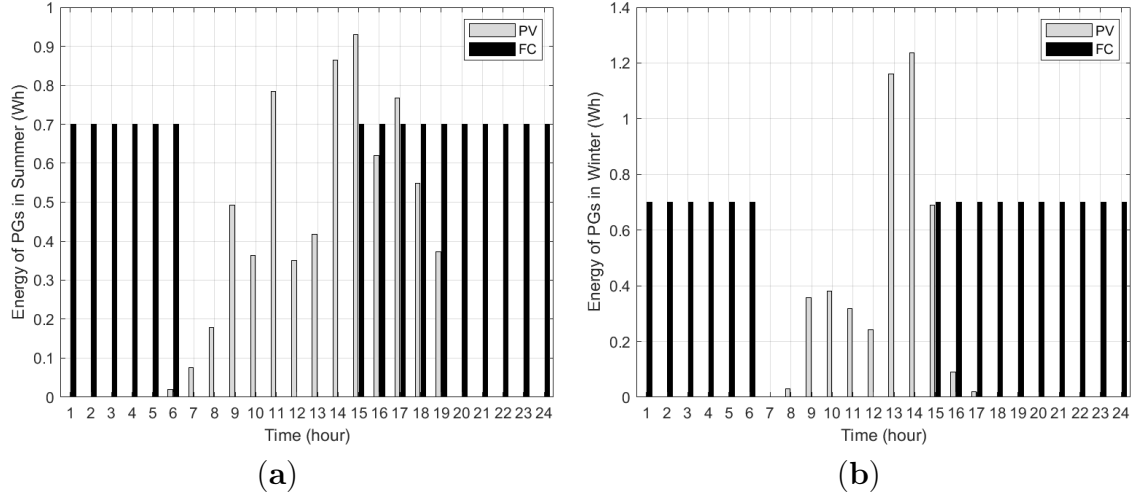
Figure 3.10: Energy generation of PV system and FC in two different seasons: (**a**) summer and (**b**) winter.

the frequency is 50 Hz. The data for the two seasons correspond to 14 June 2016 (summer) and 11 January 2017 (winter). The FC model is based on ECOFARM [63], with specified operation times from 00:00 to 06:00 and from 14:00 to 24:00 for both seasons. The energy generation of the PV system and the FC in summer and winter are shown in Figure 3.10a and Figure 3.10b, respectively. The AC unit and VF work together to regulate the temperature in the smart home, ensuring thermal comfort mode. These PLs follow a 24 h schedule based on the daily activities of a four-member household (father, mother, and two children) [64]. The members in the household intend to use the AC unit during the intervals 00:00–04:00 and 05:00–24:00 in summer and during the intervals 00:00–04:00 and 08:00–24:00 in winter. The VF operates three times a day, i.e., 05:00–06:00, 12:00–13:00, and 17:00–18:00 in both seasons. Regarding the PS parameters, the initial SoC, minimum SoC, and maximum SoC are set to 21%, 20%, and 94% of the capacity, respectively.

For optimal energy storage capacity design, the optimization problem is solved using the linear programming solver *linprog* in MATLAB.

3.5.2 Four Different Logical Power Connections

The different logical power connections shown in Figure 3.11 require different power-flow assignment algorithms. These four different logical power-connection scenarios can be

Table 3.1: Simulation parameters and settings

Parameter	Value (unit)
Simulation time	24 hours
PV peak power	1500 W
FC rated power	700 W
AC demand power	790 W (Summer), 890 W (Winter),
VF demand power	27.8 W (Summer), 16.5 W (Winter)
AC operation time (Summer)	00:00-04:00 and 05:00-24:00
AC operation time (Winter)	00:00-04:00 and 08:00-24:00
VF operation time for both seasons	05:00-06:00, 12:00-13:00, and 17:00-18:00
Initial SoC of PS	21%
Minimum SoC of PS	20%
Maximum SoC of PS	94%
Charging and discharging efficiency of PS	92%

divided into two categories based on power-flow assignment (PFA). The first category is single-load power-flow assignment (SPFA), which consists of SPFA/S and SPFA/GS to handle a single PG and supply its power to a single PL. The second category is multiple-load power-flow assignment (MPFA), which are MPFA/SG and MPFA/MG to handle multiple PGs and supply their power to multiple PLs via a single PS or multiple PSs, respectively.

In Figure 3.11a, a single PG always stores its power in a single PS first; then, a single PL obtains its power directly from the corresponding PS. For example, FC stores energy directly to PS_1, and PV also directly stores energy to PS_2. Then, PS_1 can only supply its power to AC, and PS_2 can only supply to VF. In Figure 3.11b for the SPFA/GS algorithm, a single PG always supplies its power directly to a single PL first; then, the remaining energy is stored in a single PS. A single PL can also obtain its power directly from the corresponding PS. In particular, FC can directly supply power to the AC, and if there is energy left, it is stored in PS_1. PV supplies energy to the VF first and stores the remaining energy in PS_2. PS_1 and PS_2 can still only supply a single load: AC and VF, respectively.

In Figure 3.11c for MPFA/SG, multiple PGs supply their power directly to all PLs first; then, the remaining energy is stored in a single PS. A single PL can only obtain its
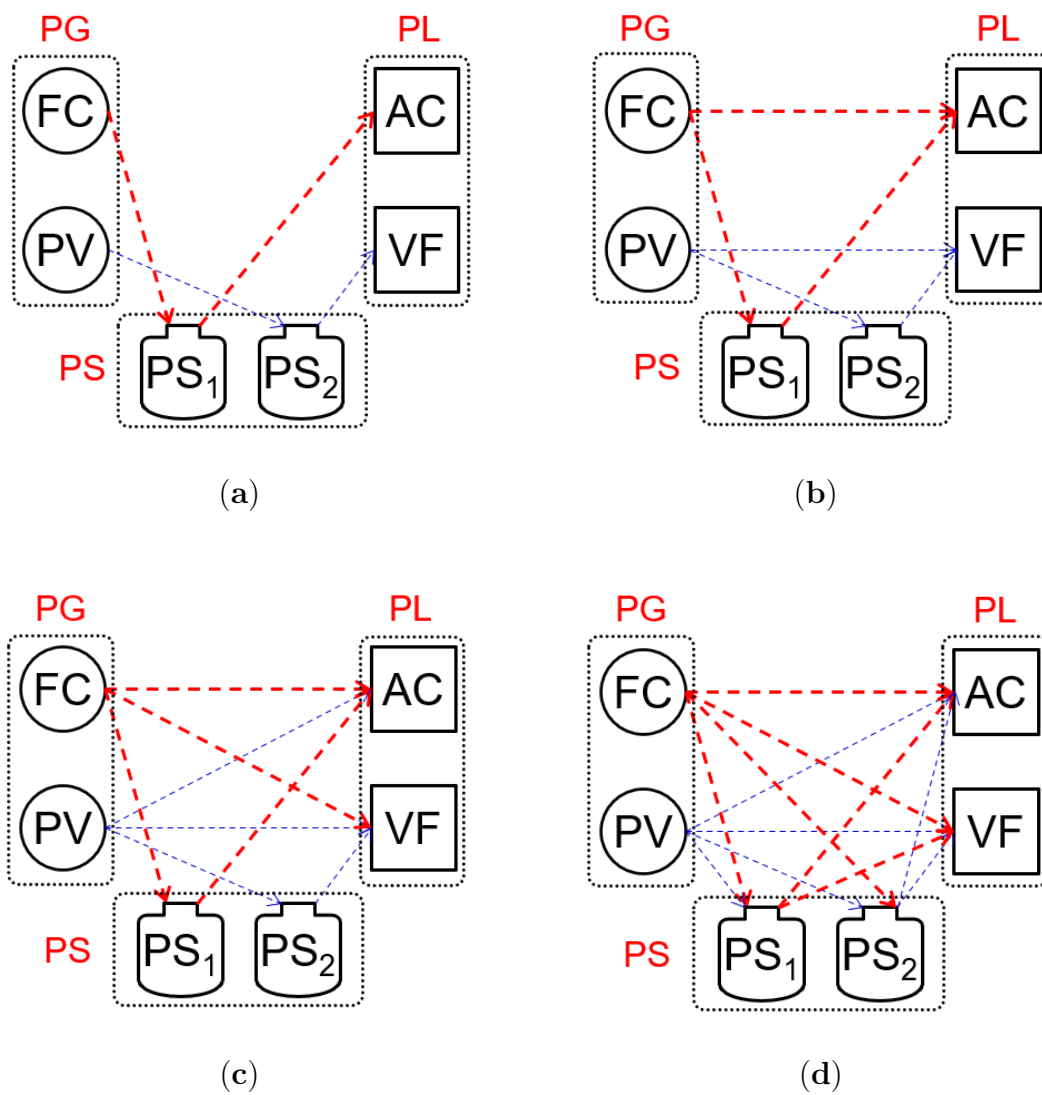
Figure 3.11: Logical power connections of four different PFAs: (**a**) SPFA/S, (**b**) SPFA/GS, (**c**) MPFA/SG, and (**d**) MPFA/MG.

power directly from the corresponding PS. For example, FC and PV can supply power to both loads, AC and VF, at the same time. However, FC can only store its power in PS_1, similar to PV, which can only store its power in PS_2. When FC or PV generate insufficient power for AC or VF, PS_1 and PS_2 can discharge the stored energy to a single load: AC and VF, respectively. Finally, in Figure 3.11d for MPFA/MG, multiple PGs supply their power directly to all PLs first; then, the remaining energy is stored in multiple PSs equally. Any PL can obtain its power from multiple PSs. For instance, both FC and PV can provide their power to both AC and VF at the same time. The energy remaining from both FC and PV can be stored in both PS_1 and PS_2 equally. Further, both AC and VF can retrieve their energy from both PS_1 and PS_2 simultaneously.

3.5.3 Results and Discussions on Energy Profile Applying DPFA

Figures 3.12 and Figures 3.13 show the energy profiles of four different PFAs in winter and summer, respectively. The different PFAs may have different energy profiles because AC and VF loads need to consume the full amount of energy in order to turn themselves on, which is the result of the amount of energy generated and the condition of the ESSs; otherwise, the load is not turned on, and the remaining energy is stored in an ESS instead. Note that t = 1 on the horizontal axis means time 0:00–1:00.

The energy profiles of winter and summer show similar demand patterns. Around 08:00–14:00, there are no PFAs that can satisfy the required demand because AC consumes such a high amount of energy that both FC and PV cannot supply enough for the entire operation time. Even MPFA/MG, with the help of both PSs, cannot satisfy all PLs during the day. However, during the operation time, the PLs in MPFA/SG and MPFA/MG are met for more hours than in SPFA/S and SPFA/GS since both PGs help supply the PLs. On the other hand, in SPFA/S and SPFA/GS, each PG can only supply one load; thus, the AC load cannot be fulfilled when FC is not generating energy even when PV generates energy sufficient for both PLs.
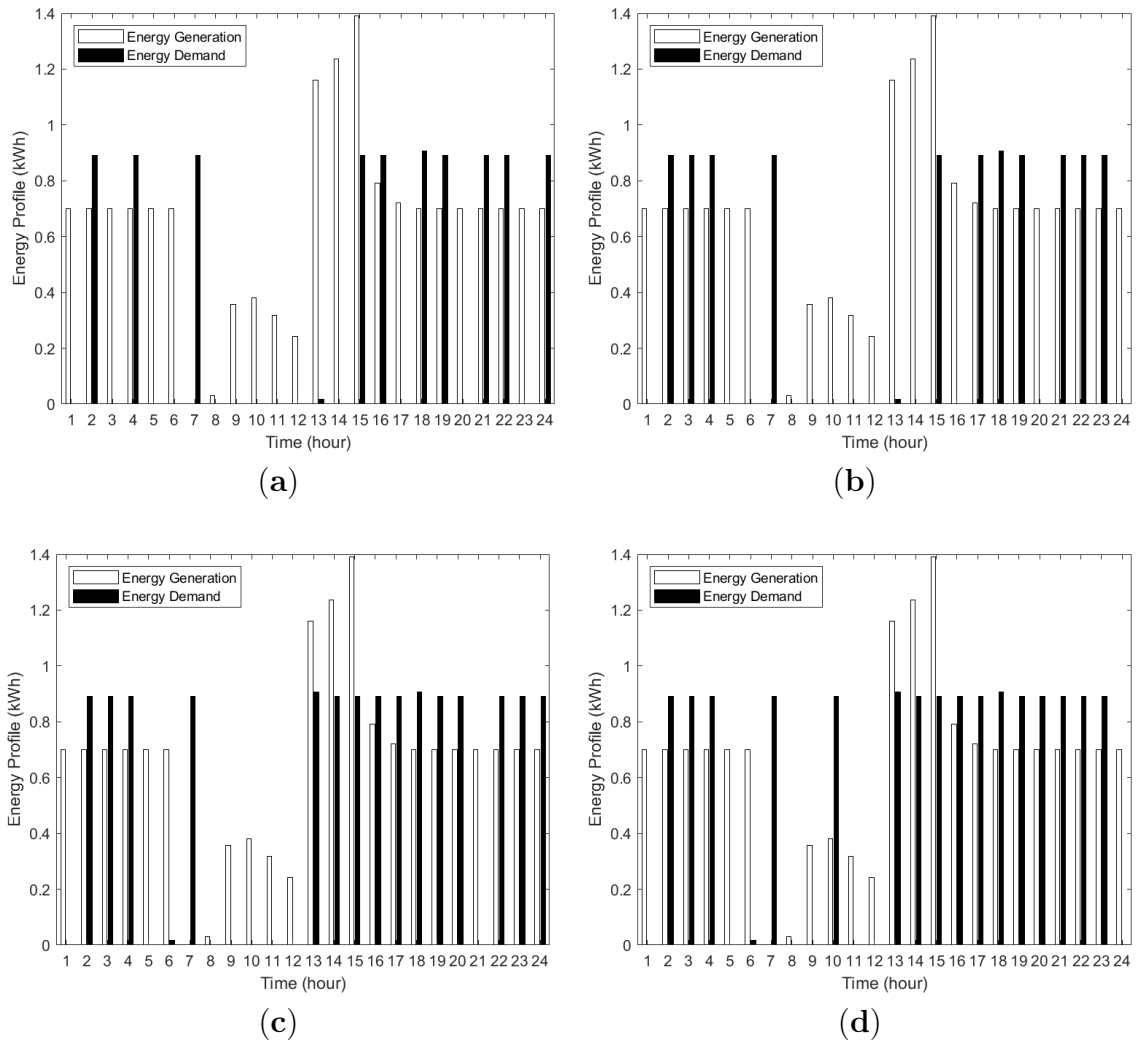
Figure 3.12: Energy profiles of four different PFAs in winter: (**a**) SPFA/S, (**b**) SPFA/GS, (**c**) MPFA/SG, and (**d**) MPFA/MG.
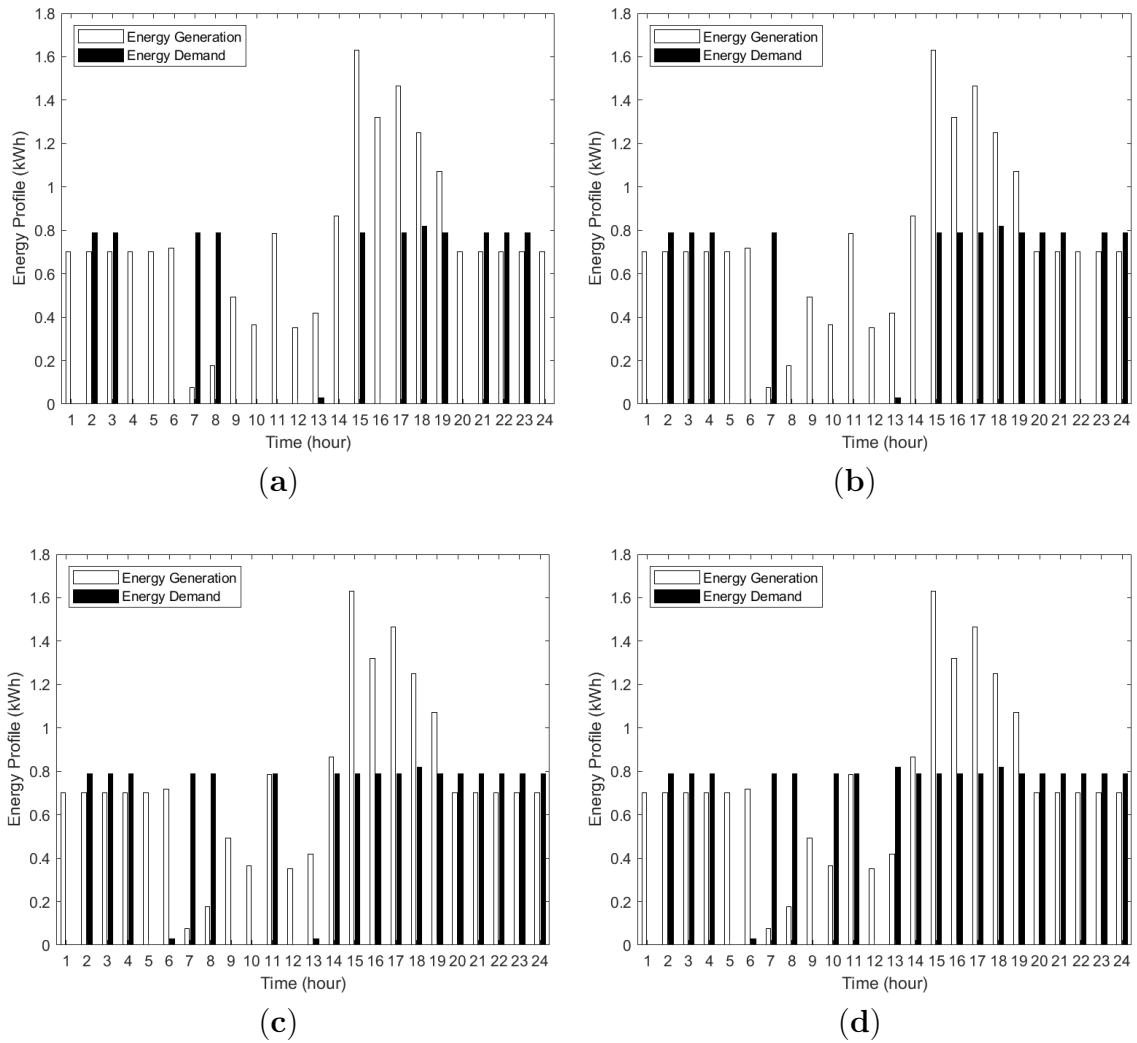
Figure 3.13: Energy profiles of four different PFAs in summer: (**a**) SPFA/S, (**b**) SPFA/GS, (**c**) MPFA/SG, and (**d**) MPFA/MG.

3.5.4 Results and Discussions on Energy Storage Applying DPFA

Figures 3.14 and Figures 3.15 show the energy loss of winter and summer, respectively. In SPFA/S, the PGs always store energy in PSs first; then, PSs supply energy to PLs. Thus, there are always charging and discharging losses, which results in the highest total storage energy loss for all the seasons. The energy loss results for all seasons further show that SPFA/GS comes in second place with the highest energy loss, in which the energy loss is higher than that of MPFA/SG and MPFA/MG. This is because in SPFA/GS, the PGs can only supply a single load rather than multiple loads, which results in high remaining energy charged to the PS. Hence, higher charging loss occurs. However, in MPFA/SG and MPFA/MG, the loads can receive energy from both PGs, which results in less charging loss from less surplus energy.

Table 3.2 shows that SPFA/S has the highest total 24-h storage energy loss from charging and discharging, as we mentioned before. In winter, the loss from MPFA/SG is the lowest and is 67% lower than that of SPFA/S. For MPFA/MG, the energy loss is very close to that of MPFA/SG and is 66.5% less than that of SPFA/S for winter. Lastly, when comparing SPFA/GS with SPFA/S, the loss in SPFA/GS is 53.7% less than that of SPFA/S for winter. Similar descriptions are applied to summer season. The results further show that summer possesses higher energy loss in ESSs compared to winter. This is because AC load in the summer consumes less energy compared to winter and there is high PV generation, so the energy remaining to be stored in ESSs and discharged from ESSs is higher than in winter. Hence, the energy loss in the summer is higher.
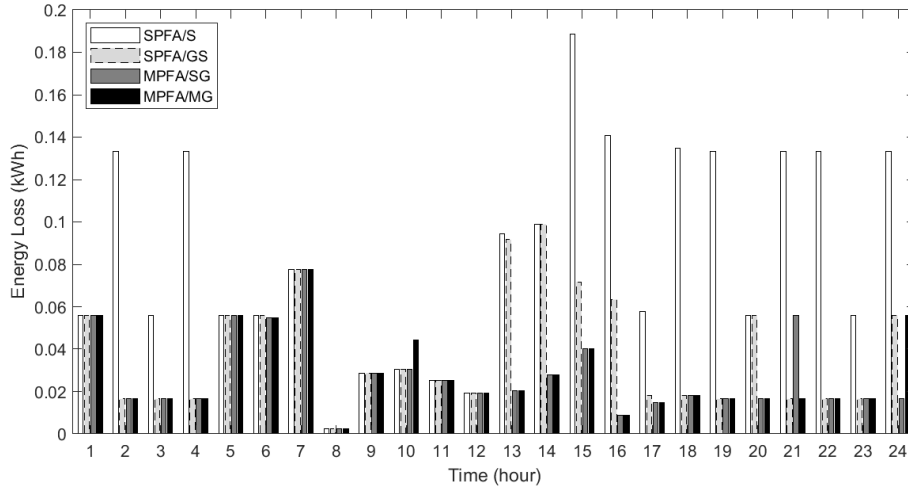
Figure 3.14: Energy loss of PS systems in winter.
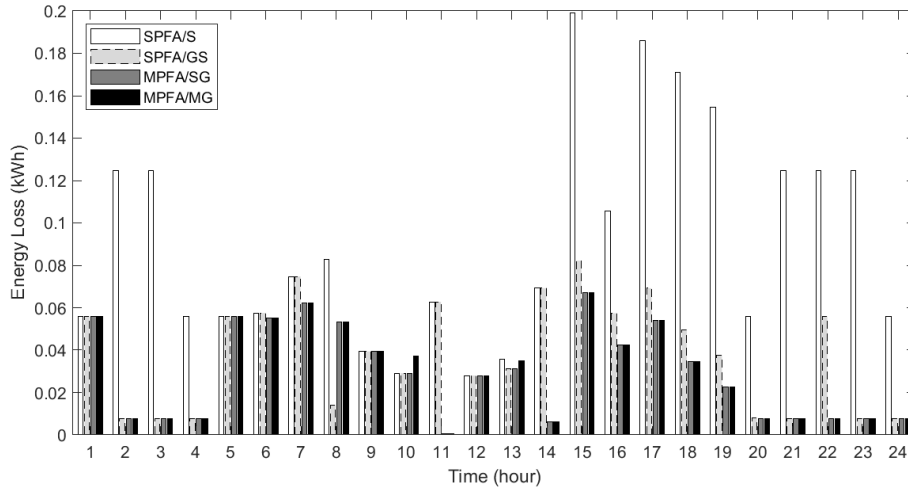
Figure 3.15: Energy loss of PS systems in summer.

When comparing energy loss between SPFAs and MPFAs, the latter demonstrates greater efficiency, with MPFAs achieving energy loss that is 55.2% lower than that of SPFAs.

Table 3.2: Total energy storage loss (kWh)

Season	SPFA/S	SPFA/GS	MPFA/SG	MPFA/MG
Winter	2.035	0.941	0.668	0.682
Summer	2.199	0.925	0.700	0.712

Figures 3.16 and Figures 3.17 show the stored energy in ESS of winter and summer, respectively. The stored energy in both seasons have a similar pattern. The graphs illustrate that when stored energy increases over time, we can clearly see the difference

54

between stored energy in single-load PFAs (SPFA/S and SPFA/GS) and multiple-load PFAs (MPFA/SG and MPFA/MG). The reason is that each PG in SPFA can only supply a single load, unlike in MPFA, where each PG supplies multiple loads. Hence, there is higher surplus energy to be charged and stored in a PS for SPFA. Therefore, the stored energy of SPFA is higher than that of MPFA. Furthermore, the stored energy of MPFA/SG and MPFA/MG in winter and summer are different since PG in MPFA/SG can only charge a single PS and discharge to a single load, while PG in MPFA/MG can charge to multiple PSs, and all PSs can discharge to multiple PLs. Therefore, the stored energy in PS of MPFA/SG is higher than that of MPFA/MG. In winter and summer, the demands satisfied are different for each PFA, so the stored energy results are very different between each PFA over time, especially between SPFA and MPFA. The results further show that summer possesses higher stored energy in ESS compared to winter since in the summer, the AC load consumes less energy and PV produces higher generated energy compared to winter.

Ultimately, we can conclude that energy loss decreases when the number of connections is higher. Especially, all the generated energy should not be stored in battery storage first and supplied to loads later. Loads should be met directly first; then, the remaining energy can be stored to be supplied later. Another thing that should be pointed out is that for SPFA, if a PG is assigned to supply a PL, conversely, the situation could be the worst, since PV alone cannot fulfill the AC load for the entire operation time.
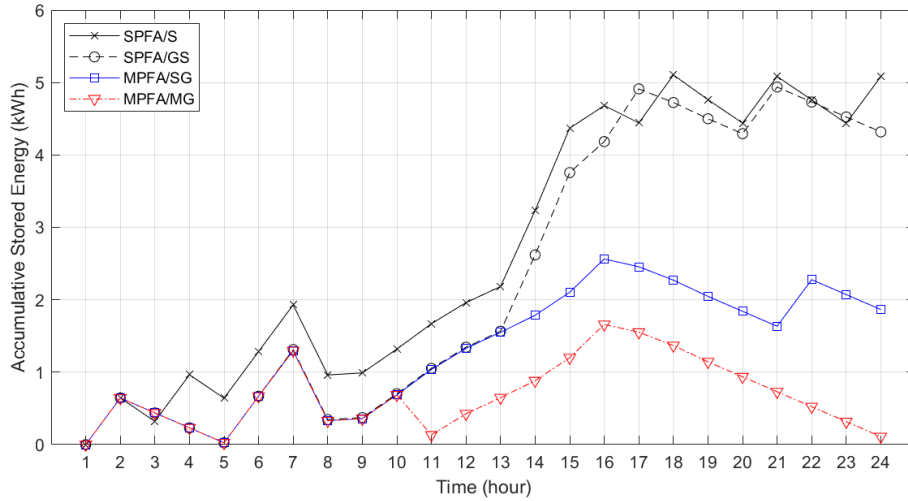
Figure 3.16: Accumulated stored energy of PS systems in winter.
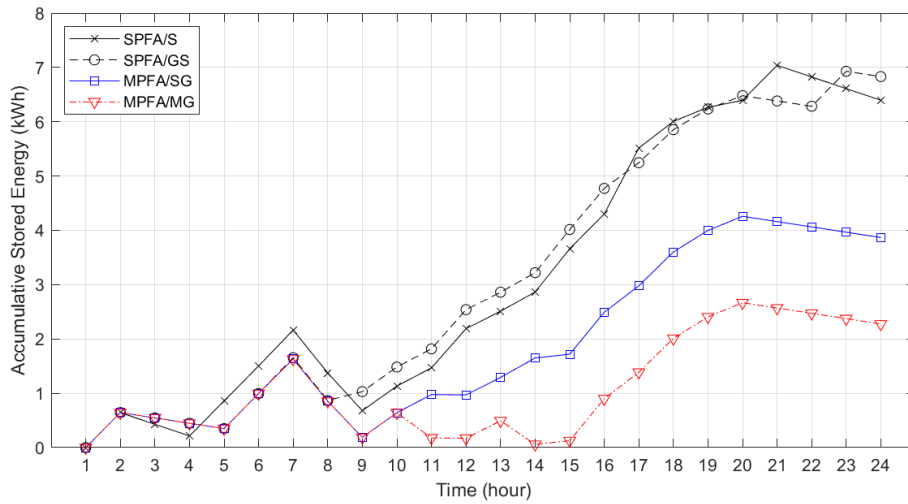
Figure 3.17: Accumulated stored energy of PS systems in summer.

3.5.5 Results and Discussions on Energy Profile Incorporating Load Shifting Algorithm

Figures 3.18–3.21 illustrate the energy profiles over 24 h for MPFA/SG and MPFA/MG during both winter and summer. The white bars represent the total generated energy from power generators, while the gray bars represent the total consumed energy of PLs without the load-shifting algorithm. The black bars depict energy demand when the load-shifting algorithm is applied. The results vary between the seasons due to fluctuations in energy generation and demand.

56
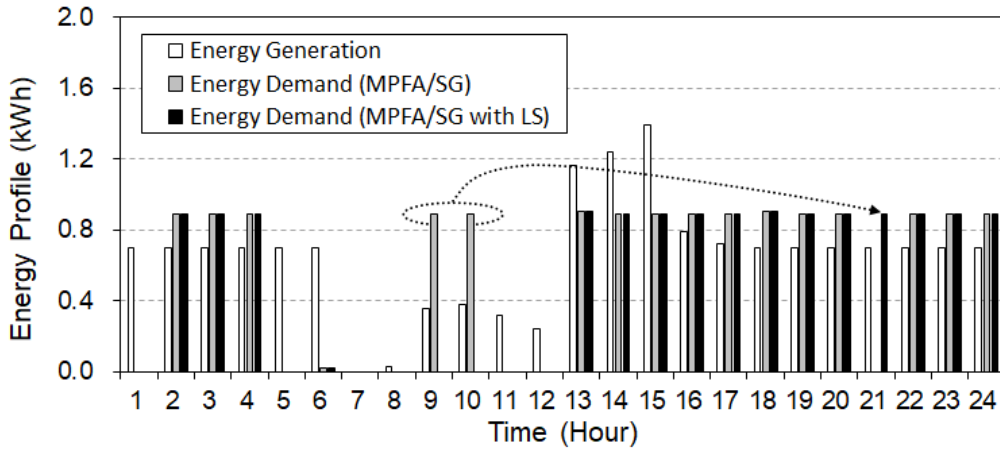
Figure 3.18: Energy profile for MPFA/SG with and without load shifting in winter.
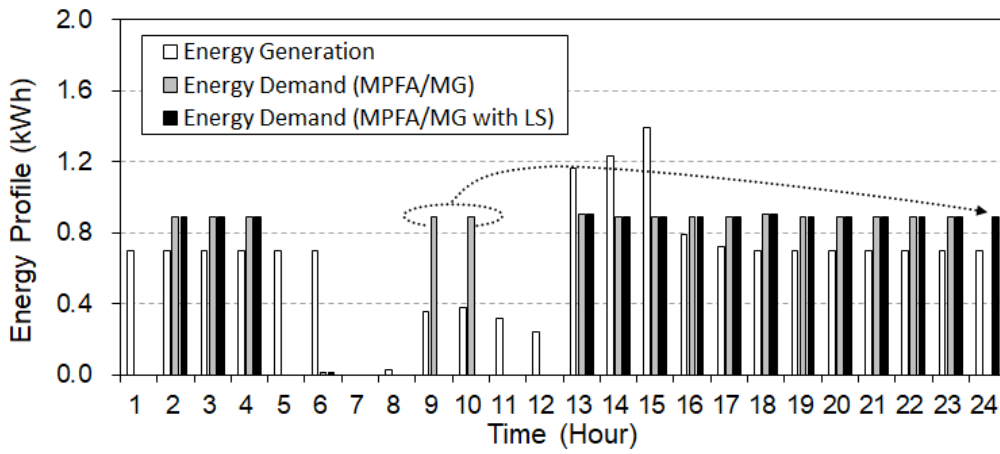
Figure 3.19: Energy profile for MPFA/MG with and without load shifting in winter.
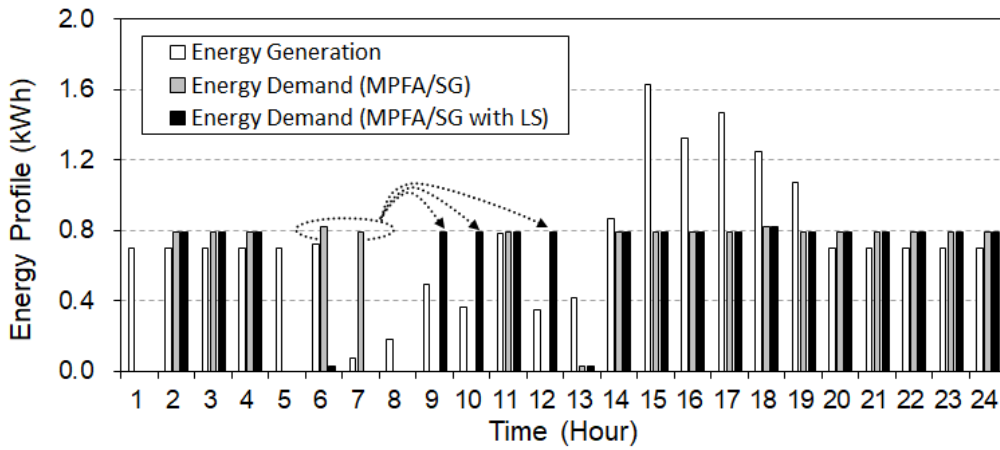
Figure 3.20: Energy profile for MPFA/SG with and without load shifting in summer.
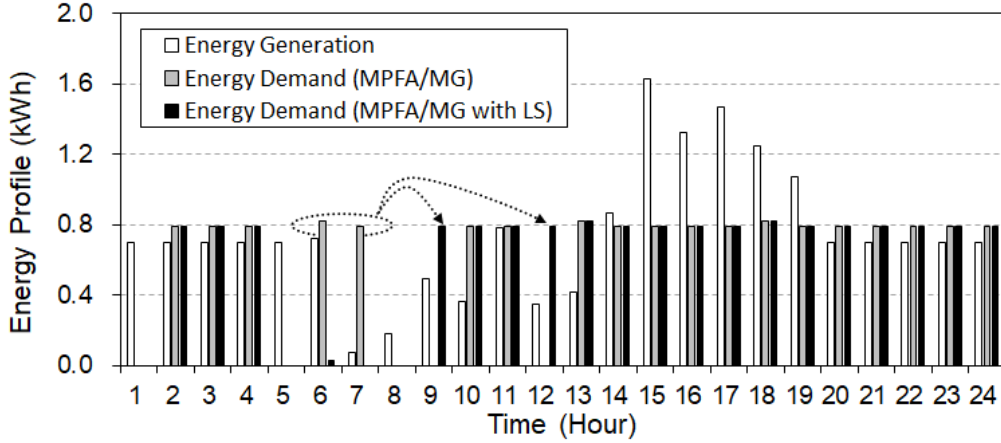
Figure 3.21: Energy profile for MPFA/MG with and without load shifting in summer.

In Figures 3.18 and 3.19, the energy profiles for winter are displayed for both MPFA/SG and MPFA/MG, with and without the load-shifting algorithm. Both profiles exhibit a similar demand pattern, where no power-flow assignment (PFA) can satisfy all the energy demand throughout the day. This is primarily due to the high energy demand of the AC unit, for which the PV system and the FC do not generate enough energy to cover the entire day. Even MPFA/MG with multiple PS units cannot meet all PL demand during that day.

Figures 3.20 and 3.21 display the energy profiles in summer for MPFA/SG and MP-FA/MG, respectively. These results reflect similar patterns as in the winter season, with both MPFA/SG and MPFA/MG struggling to meet all energy demand throughout the entire day.

When comparing the results between the cases of applying and not applying the load-shifting algorithm in winter, the results show that the load-shifting algorithm adjusts the operating hours of the AC unit to reduce energy loss. This shift enables the AC unit to operate continuously in the early evening, as the demand is shifted from the morning. On the other hand, when the load-shifting algorithm is applied in summer, it can be observed that the demand tends to shift from early morning to mid-morning.

3.5.6 Results and Discussions on Energy Storage Incorporating Load Shifting Algorithm

Figures 3.22 and 3.23 display the energy loss comparison in both winter and summer seasons with and without the load-shifting algorithm for MPFA/SG and MPFA/MG, respectively. Figures 3.24 and 3.25 illustrate the optimal energy storage capacity comparison in both winter and summer seasons with and without the load-shifting algorithm for MPFA/SG and MPFA/MG, respectively.
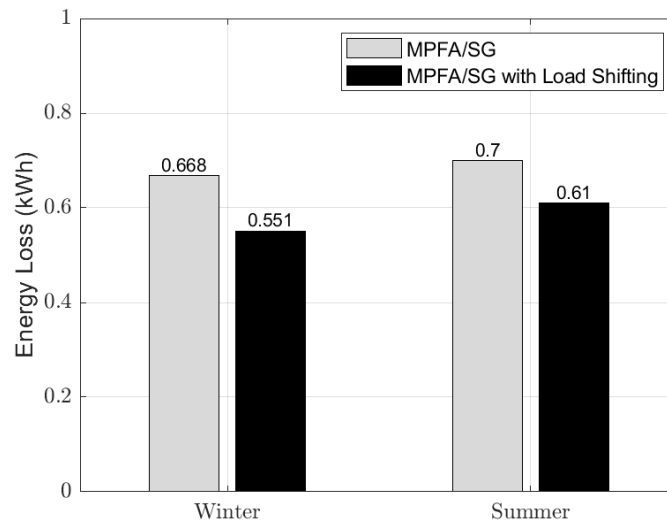
Figure 3.22: Energy loss for MPFA/SG with and without load shifting.
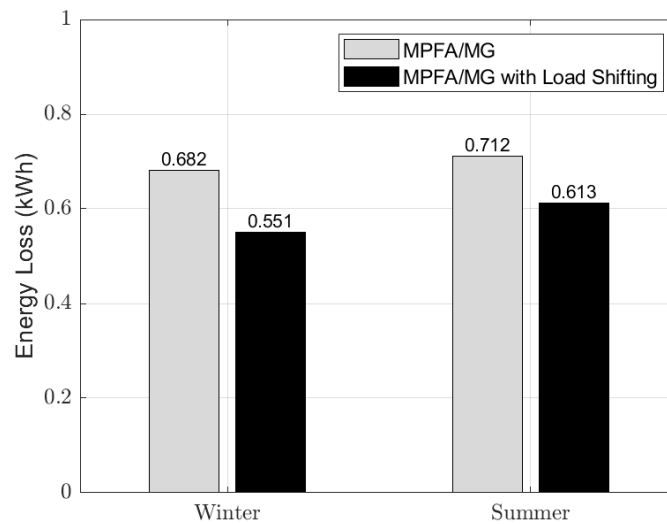
Figure 3.23: Energy loss for MPFA/MG with and without load shifting.
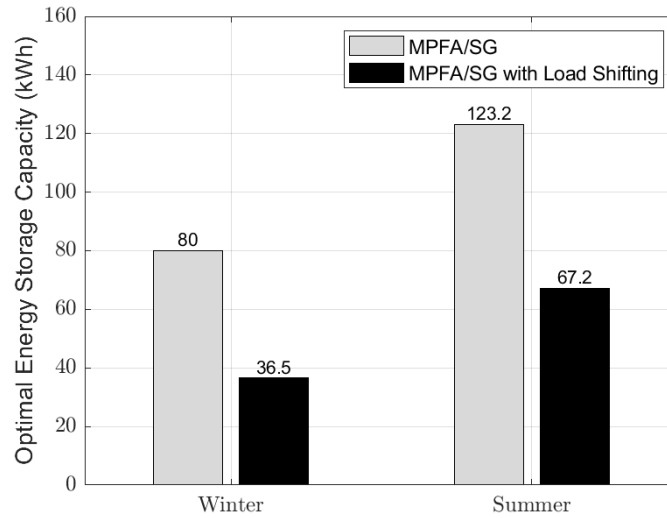
Figure 3.24: Optimal storage capacity for MPFA/SG with and without load shifting.
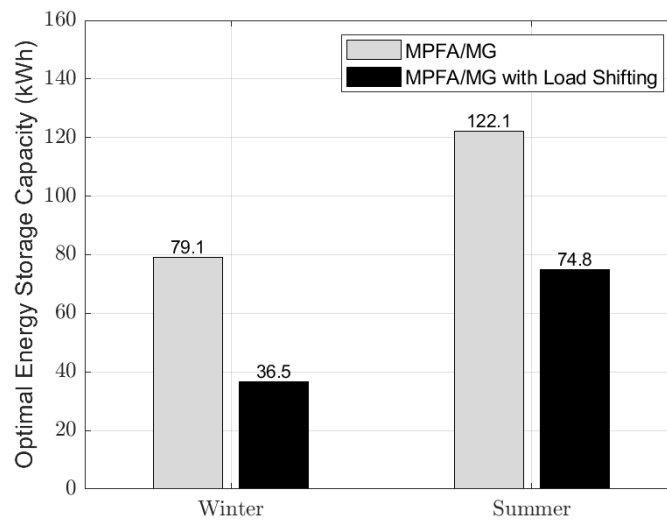
Figure 3.25: Optimal storage capacity for MPFA/MG with and without load shifting.

When comparing the cases of applying and not applying the load-shifting algorithm, the results demonstrate that the shifted profiles for both seasons have lower energy loss, reduced by approximately 1.4% and 11.4% for summer and winter, respectively. Reductions also occur for the optimal energy storage capacity when applying load shifting, with reductions of 6.7% in summer and 62.1% in winter.

Comparing the results between the two seasons, in terms of the difference in energy loss when not applying the load-shifting algorithm, there is not a significant distinction. However, in cases where the load-shifting algorithm is applied, the winter season experiences a substantial reduction in energy loss, with approximately 9.9% lower energy loss

compared with summer.

When selecting an ESS for a smart home, it is essential to consider its performance throughout the entire year. Specifically, one should take into account the worst-case scenario or, in other words, the maximum value of energy loss from both seasons. The results indicate that the energy loss is reduced by 1.9% and 2.1% for MPFA/SG and MPFA/MG, respectively, when comparing applying the load-shifting algorithm to not applying it. Similarly for energy storage capacity, the worst-case scenario is defined as the maximum value of optimal energy storage capacity from both seasons. The results indicate that the optimal energy storage is reduced by 21.9% and 29.6% for MPFA/SG and MPFA/MG, respectively, when comparing applying the load-shifting algorithm to not applying it.

In summary, MPFA/MG in winter demonstrates the highest reduction in both energy loss and optimal energy storage capacity. This is credited to the effective load-shifting algorithm, supported by multiple PS units, which appropriately shifts the AC demand. Additionally, higher energy demand in the winter season leads to lower energy loss and a smaller optimal energy storage capacity due to a lower amount of surplus energy available for charging in the PS system, while in the summer season, reductions in both energy loss and energy storage capacity also occur, although not to the same extent as in the winter season.

3.5.7 Comparison of the proposed scheme with existing work

In this section, the proposed multiple power flow assignment (MPFA) and the proposed eNMES scheme, which incorporates a load-shifting algorithm into MPFA, are compared to an existing work [57]. This work is the first to introduce the term "distributed power flow assignment" in 2022.

From table 3.3, the results show that when comparing MPFA with SPFA/S, the proposed MPFA effectively reduces energy loss by 66.8% in winter and by 67.9% in summer. When MPFA is incorporated with the load-shifting algorithm, the energy loss is further

Table 3.3: The energy loss comparison for each type of DPFA in two seasons (kWh)

DPFA type	Winter	Summer
SPFA/S	2.035	2.199
MPFA/SG	0.668	0.700
MPFA/MG	0.682	0.712
MPFA/SG + LS	0.551	0.610
MPFA/MG + LS	0.551	0.613

Table 3.4: The optimal energy storage capacity comparison for each type of DPFA in two seasons (kWh)

DPFA type	Winter	Summer
SPFA/S	84.9	147.6
MPFA/SG	80.0	121.2
MPFA/MG	79.1	122.1
MPFA/SG + LS	36.5	67.2
MPFA/MG + LS	36.5	74.8

reduced, achieving a reduction of 72.9% in winter and 72.2% in summer.

Table 3.4 shows the optimal energy storage capacity for different DPFA types. The results illustrate that the MPFA introduced in this work can reduce energy storage capacity by 5.8% in winter and by 16.9% in summer compared to the existing work that uses SPFA/S. The optimal energy storage capacity is further decreased when the load-shifting algorithm is applied together with MPFA, resulting in a reduction of 57% in winter and 51.9% in summer compared to SPFA/S.

3.6 Summary

In this chapter, we studied the effects of energy loss and stored energy in ESS related to the frequency of charging and discharging for all seasons for designing logical power connections for distributed power-flow assignment in a smart home. We further investigates the minimization of energy loss in an ESS within a smart home environment. This study employs a load-shifting algorithm incorporated with two types of DPFA, namely, MPFA/SG and MPFA/MG. This study also explores the optimal energy storage capacity when applying the load-shifting algorithm, formulated as a linear programming prob-

lem. Real experimental data from a smart home environment called *i*House in winter and summer are utilized for design, performance, and investigation. Through numerical studies, we can conclude that both MPFA/SG and MPFA/MG algorithms ensure the power generated by PGs is supplied directly to be consumed by PLs, and the remaining power from the PGs is stored in PS systems for PLs to operate at other times. As a result, both MPFA/SG and MPFA/MG achieved low energy loss with efficient energy storage during the day. The proposed DPFA algorithms can reduce energy loss up to 67% compared to power-flow assignment for which all the generated power is stored in the ESS directly (SFPA/S) in the winter. The design of a power-flow assignment that links high PG to high PL, e.g., FC to AC, is essential to ensure low energy loss for the entire energy system. We can observe that both SPFA/S and SPFA/GS cannot perform more efficiently when the logical power connections of FC to AC and PV to VF become FC to VF and PV to AC, respectively. To address this complicated design for distributed power-flow assignment, both MPFA/SG and MPFA/MG are highly recommended. The results further show that summer possesses the higher energy loss and stored energy in ESSs compared to winter. When applying the load-shifting algorithm with MPFA during winter, it results in a significant reduction in energy loss, approximately 11.4%. Additionally, the optimal energy storage capacity experiences a substantial reduction, 62.1%, benefiting from the support provided by multiple PS units to meet energy demand. On the other hand, in the summer season, reductions in both energy loss and optimal energy storage capacity also occur, although not as much as in the winter season. In summer, energy loss is reduced by approximately 1.4%, and there is a 6.7% decrement in optimal battery storage capacity. The analysis and findings suggest that higher energy demand, as observed in the winter season, leads to lower energy loss and smaller optimal energy storage capacity due to a lower amount of surplus energy available for charging in the PS system. Recommendations include shifting the operation of the loads to the time when the amount of energy supply closely matches energy demand in order to reduce energy loss and optimize the energy storage capacity of smart homes.

Chapter 4

Critical Hour Energy Sharing Management for Partially Moving Energy Storage Scheme

4.1 Introduction

Currently, research in Electric Vehicle (EV) technology is gaining widespread attention, with a particular focus on Grid-to-Vehicle (G2V) and Vehicle-to-Grid (V2G) systems, both of which can be considered part of energy sharing management schemes that incorporate EVs into the smart grid. In G2V research, the emphasis is on understanding the behavior of EVs and developing methods to manage and control the charging operations of EV batteries. This involves utilizing energy from sources such as the utility grid and renewable energy resources (RE). On the other hand, V2G research explores the potential of EVs to provide ancillary services to the grid by discharging energy from their batteries back into the grid. The battery storage in EVs serves as an excellent supply source capable of responding almost in real-time and can address the problem of the intermittent nature of RE [57]. V2G has the potential to support the grid with various ancillary services, including peak shaving, frequency regulation, voltage regulation, and spinning reserve [65]. EV owners can derive benefits by charging their batteries during non-peak periods when

electricity prices and generation costs are low. Subsequently, they can provide V2G services to assist the grid during peak periods when electricity prices and generation costs are high.

However, the majority of G2V and V2G research primarily concentrates on personal passenger EVs. These vehicles, designed for individual transportation with diverse schedules and purposes, typically have smaller battery capacities, resulting in lower willingness and interest to participate in ancillary services [66]. Real-world implementation of V2G programs with this type of EV may prove challenging. In contrast, electric school buses (ESBs) follow specific schedules and routes [67, 68], often remaining parked in idle mode. Schools that own ESBs would find participation in V2G programs beneficial, so it ensures high willingness to engage in ancillary services. Traditionally, school buses have been powered by diesel engines, emitting harmful pollutants that can negatively impact the health of students [69] , particularly young children in primary schools. However, there is a positive shift in the transportation sector. The price of electric buses (EBs) has decreased significantly compared to several years ago, particularly in the early 2000s [10]. This reduction in cost, coupled with growing environmental awareness, has led to initiatives in the USA aimed at transforming 500,000 diesel buses into electric ones [70].This transformative effort aligns with the broader goal of fostering cleaner and more sustainable school transportation. Due to their predictability and substantial battery storage capacities, ESBs are well-suited for providing V2G services. This makes them a compelling choice for contributing to grid stability and benefiting both schools and the UC.

Typically, generated electricity needed to be matched all the time with the electric demand. When multiple high-consumption electric appliances are simultaneously activated, it can result in a surge in overall energy demand, leading to peak periods. During these peak periods, UC are required to operate peak-generation power plants, incurring significant expenses to meet the additional demand. These peak power plants are not only inefficient economically but also environmentally harmful [56].

To tackle this challenge, a potential solution involves offering peak shaving services to various groups of EVs or battery packs. The UC can leverage the fast response capabilities

of energy storage units on the demand side to discharge stored energy into the grid. This approach assists the UC in mitigating peak demand and reducing additional costs. Electric vehicles, for instance, can be charged at lower prices during non-peak demand periods and discharge energy back to the grid during peak-demand periods, such as early evening, offering benefits for their participation in this program. Given the suitability of ESBs for providing peak shaving services, they should play an important role in the peak shaving program. However, a single ESB may not be capable of discharging a sufficient amount of energy to participate in such a program. Therefore, it is essential for a school, which can aggregate the discharged energy from multiple ESBs within its location, to act as the participant in the peak shaving program.

In this chapter, we introduce a novel V2G model for peak shaving problem that incorporates ESBs inside schools within a community. The problem is formulated as a Stackelberg game, where the UC assumes the role of a leader. The UC issues information about the peak shaving program, particularly the incentive unit price offered to schools for providing the service. The UC aims to minimize the additional cost associated with meeting peak demand. Simultaneously, schools in the community act as followers, negotiating the optimal discharged energy from their ESBs and determining the discharge hours during peak periods to maximize their utility.

The main contributions of this chapter can be summarized as follows:

- A peak shaving model incorporating ESBs in a community is proposed which includes the additional cost model of UC and the utility model of schools that possess a number of ESBs. The UC tries to minimize the additional cost to cover peak demand periods, while schools in a community try to maximize their utility using the stored energy inside their ESBs.

- Two-level Stackelberg game model is introduced to capture the interaction between two types of players, that is UC and schools who possess a number of ESBs both of the players trying to negotiate to establish the optimal incentive price and discharged energy for peak shaving program. Also, the existence and uniqueness of the

Stackelberg equilibrium is proven and guaranteed

- The optimal battery storage capacity of ESB and the best time to discharge during peak-demand periods are also determined.

4.2 Related Works

This section provides a review of the literature related to G2V and V2G research for various types of EVs, including personal passenger EVs, Electric Taxis (ETs), Electric Buses (EBs), and Electric School Buses (ESBs).

Research in the field has predominantly concentrated on personal passenger cars for both G2V and V2G operations. Several studies have explored into G2V research, particularly incorporating personal EVs [24, 27, 71–74]. In [71], the authors proposed a G2V model between the grid and groups of personal EVs using a noncooperative game between the personal EVs and the energy supplier. In this model, the grid aims to maximize its revenue with limited supplied energy, while the personal EVs aim to minimize their charging cost. The proposed algorithm was introduced and assessed through simulations, demonstrating that the EVs in the proposed model can obtain higher utility compared to PSO and equally distributed methods. A power scheduling scheme for an EV charging station (CS) is proposed in [24]. The paper analyzes the benefits for multiple parties by formalizing the problem as a game theory interaction between CS and EV users. The results reveal that the proposed power management scheme is feasible for an actual environment, reducing the electricity cost by up to 8.6%. The authors in [72] proposed a charging scheme focused on public EV CS, aiming to determine the charging time, pairing between CS-EVs, and pricing using game theory along with a matching algorithm. The findings indicate that the proposed scheme can enhance the performance of the charging system. In [73], the study on the EV charging problem in intelligent transportation systems is conducted, consisting of CS and EGVs, where CS aims to maximize its revenue, and EVs aim to find the proper CS with the lowest charging cost, considering the willingness of the EVs. This work proposed the LOBACH algorithm to find the optimal solution, and

it is then compared to existing works, where it has outperformed other approaches. A novel charging scheme for EVs inside smart communities integrated with RE is proposed in [27]. The authors consider three parties in the model: the grid, aggregators (AGGs), and EVs, where a trust model is introduced to enable EVs to select an AGG for charging, as information needs to be shared between each entity involved. The analysis results show that the proposed scheme is effective compared with traditional schemes. The authors in [74] presented a charging strategy for EV CS equipped with Photovoltaic (PV) panels, considering day-ahead pricing. They introduce a profit model for CS operators and a cost model for EVs. This work studies the model using a game-theoretic approach. The proposed model is verified through results that show an increase in CS operator profit and reduced charging cost for EVs.

On the other hand, there is literature work on V2G research [28, 29, 75–77]. The work in [75] presents a utility maximization algorithm for the V2G scheme. The system comprises EVs and an AGG, both aiming to maximize their own utility. The results demonstrate that the proposed algorithm can increase utility by up to 50% compared to conventional methods. In [28], the authors proposed a planning strategy framework to optimize and manage optimal EV charging and discharging operations, aiming to enhance the flexibility and efficiency of a microgrid. The problem was formulated as a non-cooperative game involving the distribution company, CS, and EVs. The findings reveal that the proposed framework can increase the flexibility and efficiency of a microgrid by 0.3% and 67.4%, respectively, compared to a case study. A V2G model is proposed in [76], where the study is conducted between multiple AGGs and a number of EVs to determine the optimal V2G pricing. The game theory model is formulated with the objective of maximizing the utility of both AGGs and EVs. The simulation is verified with 3 AGGs and 2000 EVs, demonstrating the effectiveness of the proposed model. Authors in [29] proposed a V2G pricing model with demand response based on game theory, where the players involved are AGGs and EVs trying to maximize their objectives by setting optimal strategies. The results confirm the feasibility of the proposed model, ensuring the maximum benefit of all parties. In [77], an approach is presented for scheduling household EV usage for V2G and

vehicle-to-home services, using UK data and dynamic electricity pricing. The simulation results show that the proposed approach effectively reduces electricity bills. It was found that the main factors influencing this reduction are the energy price and the number of EVs.

Some work has focused on G2V and V2G applications involving ETs in their system [78–81]. The optimization of dispatch for ETs and CS is studied in [78]. ETs aim to choose a suitable CS for charging while minimizing their cost, and CS sets the charging price. The model is formulated using game theory, and a practical situation is simulated for analysis. Ma et al. [79] studied a charging problem involving CSs and ETs. ETs aim to select a CS with the lowest electricity charging cost, while CS adjusts the charging price based on regional hotspot information of ETs to maximize its revenue. The results confirm that the proposed model effectively reduces the charging cost of ETs and guarantees CS's revenue. In [80], a multi-objective optimization problem is formulated for the coordinated charging strategy of ETs. The goal is to maximize the utilization of charging facilities, minimize load imbalance, and minimize electricity charging costs. The particle swarm algorithm is employed for optimization. The results confirm the improvement in efficiency, better load balance, and electricity cost benefits. In [81], a charging coordination problem for ETs is studied to decrease the charging cost. The goal is to decide when and where to charge ETs by utilizing real-time information with a two-stage decision process. The analysis reveals that the proposed approach can effectively decrease the charging cost of ETs, increase the utilization of CSs, and flatten the charging demand profile for the power grid.

In recent years, there has been research studying G2V and V2G for EBs [82–86] and ESBs [10, 67, 68, 87]. In [82], a novel bus-to-grid concept is introduced, allowing the bus operator to generate revenue from both fare collection and providing ancillary services to the grid. Non-linear optimization problems are formulated to maximize the bus operator's profit and determine the optimal bus charging plan. The simulation employs bus line data and time-of-day pricing to verify the proposed concept. The work proposed by Yang et al. [83] introduced an optimization model for dispatching EBs to participate in carbon trading and the peak shaving market. The goal is to minimize the bus company's

daily cost and also reduce load fluctuations. The results reveal that the daily cost, load fluctuations, and carbon emissions are reduced compared to the disorderly dispatch of EBs. The operation of EBs integrated with dynamic market prices for load congestion management is studied in [84]. Bi-level optimization is employed to determine electricity market clearing and bus planning. The experimental results show that the engagement of EBs can alleviate network congestion and reduce energy loss by 7.2%. Manzolli et al. [85] focus on the charging scheduling problem of EBs. An optimization model is designed to minimize charging costs while also participating in a V2G scheme. This study demonstrates that it is economically viable for EBs to sell electricity back to the grid. Work [86] developed an optimization model for scheduling battery swapping stations for EBs, aimed at minimizing running costs while considering operational requirements. A savings cost index is proposed, which confirms the economic viability of the concept.

There is limited literature on V2G research specifically focused on ESBs. Ercan et al. [10] focus on the environmental benefits of using V2G technology with ESBs instead of producing more electricity through traditional power plants, which release harmful emissions. The results reveal that ESBs can reduce greenhouse gas emissions by 1420 tons of carbon dioxide. In [67], the paper develops an ESBs V2G model to study the effect of integrating the ESBs with V2G capability into the grid. The aim is to minimize peak load periods and reduce carbon dioxide emissions using DC fast chargers in a centralized fashion. The simulation results show that using ESBs with V2G capability can decrease dependency on peak power plants and avoid carbon emissions up to 1,130 tons per day. An analysis to evaluate the cost and benefit of using V2G-capable ESBs is performed in [68]. Many factors are considered, including electricity cost, fuel cost, battery cost, health benefits, and the ancillary service market. The findings reveal that V2G-capable ESBs can save the school expenses by $6,070 per set in net present value. Work [87] explored the integration of ESBs for V2Gpurposes into the US electrical system, which is powered by solar energy, utilizing Geographic Information Systems (GIS) data. The results indicate that the integration of ESBs for V2G purposes can benefit both communities and schools.

For various reasons, it becomes evident that ESBs are the most suitable EVs for per-

forming V2G service to the grid, given their characteristics of predictability, consistent availability, and large storage capacity, as stated above. However, the existing literature primarily focuses on minimizing overall electricity costs through a centralized entity, such as a bus operator or grid operator. To the best of our knowledge, no research study has addressed the V2G problem for ESBs while considering the interests of multiple entities involved in the system. This consideration is crucial for the practical implementation of V2G solutions in the real world, where the interests of various stakeholders must be taken into account to realize the maximum benefits for each entity. Consequently, this work employs a game-theoretic approach to investigate the problem, aiming for a more realistic exploration of the dynamics involving multiple entities.

4.3 System Model

4.3.1 Preliminaries

Figure 4.1 depicts the conceptual illustration of the vehicle-to-grid model in a community. This model comprises a utility company and multiple schools, each possessing several electric school buses. The involved parties can be explained as follows:

- Utility company (UC): It is assumed that the Utility Company (UC) can accurately forecast the upcoming peak demand and predict the additional energy required for generation. However, power plants generating peak energy during peak durations typically incur very high running costs, posing a considerable financial burden for UC if it were to generate all the required energy during peak times independently. In a community comprising several schools, each with multiple ESBs equipped with battery storage, these ESBs can play a crucial role in supplying the needed energy. Consequently, UC initiates communication by sending incentive price signals and peak duration information to schools before the peak period, engaging in negotiations for the provision of discharged energy from their ESBs. The incentive price offered by UC is set lower than the unit cost it would incur to generate all elec-

tricity independently. While UC still needs to generate the remaining energy that ESBs do not cover, the quantity is reduced, resulting in a substantial decrease in unit costs compared to when UC generates all the energy. Therefore, UC can effectively minimize the cost of generating additional energy during peak periods with the assistance of ESBs in schools within the community.

- Schools: Within a community, there exists a collection of schools, each consisting of a number of ESBs. These ESBs possess the capability to offer V2G services to the UC, specifically engaging in peak shaving activities by receiving incentive prices for providing discharged energy to the UC. The unit incentive price that UC sends to schools will be higher than the unit price at which the schools charge their ESBs during non-peak periods, meaning the school will benefit from providing this service to the UC. Upon receiving the incentive signal from UC, each school responds by determining the optimal quantity of discharged energy to submit back to UC. Additionally, the school strategically identifies the most favorable time-duration to provide the V2G service, aiming to maximize their overall benefit from participating in the program.

The proposed V2G model consists of two levels: the UC level and the schools' level. Initially, at the upper level, the UC anticipates the forthcoming peak period and demand. It initiates negotiations for the V2G program by issuing an incentive signal (p_{uc}^t) to schools within the community. This incentive price is related to the projected amount of peak demand. Subsequently, at the lower level, each school in the community responds to the provided incentive prices by determining and submitting the optimal quantity of discharged energy from their ESBs' batteries to maximize their individual benefits through participation in the V2G program.

The set of schools is denoted as $\mathcal{N} = 1, 2, \ldots, N$, where $n \in \mathcal{N}$ and N is the total number of schools in the system. Every school has the ability to offer V2G service by using the energy that is stored in its ESB battery. Prior to the peak period, the UC has the ability to initiate the peak shaving program by sending an incentive pricing signal.
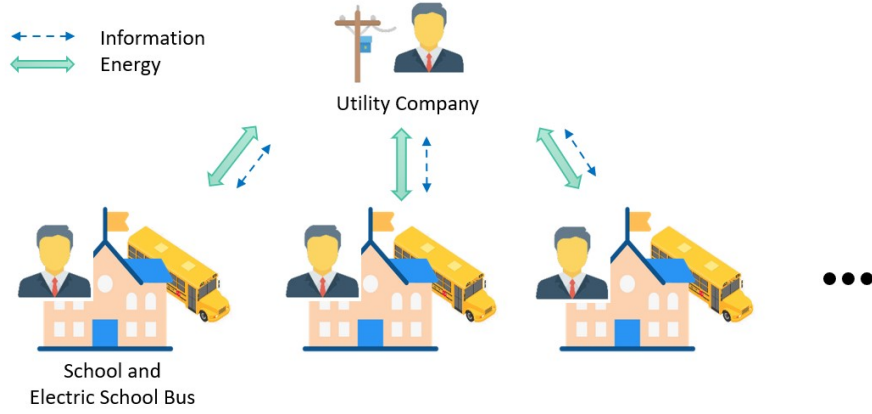
Figure 4.1: Conceptual illustration of vehicle-to-grid model in a community

4.3.2 Utility Company

Energy Cost function

The generation cost, $C_{gen}^t(D^t)$, denotes the cost required to generate the energy to serve all demand loads D^t during time t. The widely used and accepted assumptions for the cost function are as follows:

1) The cost function is an increasing function with the generated energy [88, 89].

$$C_{gen}^t(D_1^t) \leq C_{gen}^t(D_2^t), \quad \forall D_1^t \leq D_2^t, \quad t \in \mathcal{T} \tag{4.1}$$

2) The cost function is strictly convex [90].

$$C_{gen}^t(\theta D_1^t + (1-\theta)D_2^t) < \theta C_{gen}^t(D_1^t) + (1-\theta)C_{gen}^t(D_2^t) \tag{4.2}$$

where $0 < \theta < 1$, $D_1^t, D_2^t > 0$, and $D_1^t < D_2^t$.

In this work, the quadratic cost function that satisfied the above assumption is utilized as follows [88, 89, 91, 92]:

$$C_{gen}^t(D^t) = a(D^t)^2 + bD^t \tag{4.3}$$

where a and b are coefficients of the generation cost function at t, and D^t represents the amount of generated energy.

The unit dynamic electricity price for each t can be calculated by $p^t = \frac{C_{gen}^t(D^t)}{D^t}$, Hence, the unit price is:

$$p^t = aD^t + b \tag{4.4}$$

This price can be employed to calculate the cost of charging ESBs during typically non-peak hours as well.

Utility of UC

The UC aims to fulfill the required demand D_{req}^t by generating energy from its generators, along with procuring discharged energy from ESBs. This is achieved through V2G services, where the UC sends incentive price signals to schools, prompting them to discharge the stored energy in ESBs' batteries.

We define D_{peak}^t, D_{base}^t, and D_{req}^t as the peak demand, base demand, and the required demand resulting from the difference between peak and base demand at time t. This can be written as follows:

$$D_{req}^t = D_{peak}^t - D_{base}^t \tag{4.5}$$

When the peak shaving program is executed, the total amount of discharged energy from ESBs from all the schools for performing peak shaving is:

$$E_{V2G}^t = \sum_{n \in \mathcal{N}} x_n^t \tag{4.6}$$

where x_n^t is the discharged energy from school n at time t.

The new reduced peak demand after ESBs help shave the original peak demand D_{peak}^t can be wrtten as follows.

$$D_{peak,new}^t = D_{peak}^t - E_{V2G}^t \tag{4.7}$$

Hence, the total additional cost incurred by UC from energy generation and the V2G program to meet the total demand in the community D_{peak}^t with a base demand of D_{base}^t is as follows:

$$U_{uc}^t(p_{uc}^t) = p_{uc}^t E_{V2G}^t + C_{gen}^t(D_{peak,new}) - C_{gen}^t(D_{base}^t) \tag{4.8}$$

Here, p_{uc}^t represents the incentive price for providing peak shaving service, paid by UC to schools.

Equation (4.8) comprises three terms. The first term represents the cost of paying incentives to schools for providing the V2G service. The second and third terms denote the generation costs for the new reduced peak demand and base demand, respectively. The subtraction between these two generation cost terms is employed to determine the additional generation cost incurred for producing the extra energy necessary to meet the energy level after subtracting the energy supplied from the V2G program.

Upon substituting (4.3) into (4.8), the total additional cost of UC is reformulated as:

$$U_{uc}^t(p_{uc}^t) = p_{uc}^t E_{V2G}^t + [a(D_{peak,new}^t)^2 + b(D_{peak,new}^t) - a(D_{base}^t)^2 - bD_{base}^t] \tag{4.9}$$

Therefore, the total additional cost of UC consists of two parts: 1) The cost of paying incentives to schools to provide discharged energy from their ESBs. 2) The cost of generating the new reduced peak demand minus the cost that is already incurred at the base demand.

The objective of UC is to minimize this additional cost during peak periods by selecting the proper incentive price p_{uc}^t while ensuring the delivered energy matches the peak demand within the community.

$$\min_{p_{uc}^{min} \le p_{uc}^t \le p_{uc}^{max}} U_{uc}^t(p_{uc}^t) \tag{4.10}$$

4.3.3 Schools

Battery Dynamics

The State-of-Charge (SoC) of a school's ESBs can increase over time during the day by charging the batteries. It can decrease by discharging the stored energy to provide V2G service to the UC and during traveling in the typical schedule of ESBs in the morning and afternoon. The battery dynamics of school n's ESBs can be represented as follows:

$$SoC_n^{t+1} = SoC_n^t + s_1^t \frac{D_{ch}^t}{ESS_n} - s_2^t \frac{x_n^t}{ESS_n} - s_3^t \frac{\omega d_n}{h_d \cdot ESS_n} \tag{4.11}$$

where SoC_n^t and SoC_n^{t+1} represent the SoC at the beginning of time t and the SoC at the beginning of the next time slot for school n's ESBs, respectively. D_{ch}^t denotes the charging energy into the school's ESBs in timeslot t, ESS_n represents the battery capacity of ESBs in school n, ω is the energy consumption rate per distance of ESBs during traveling, d_n is the distance needed to travel of ESBs in school n, h_d is the number of hours used in the driving service each round. s_1^t is the state indicating whether the school's ESB is in charging operation during the timeslot t. s_2^t is the state showing whether the school's ESB is in discharging operation during the timeslot t, and s_3^t is the state representing whether the ESBs is currently in use for travel or not.

The state s_1^t, s_2^t, and s_3^t can be expressed as follows:

$$s_1^t = \begin{cases} 1 \text{ , } charging \\ 0 \text{ , } otherwise \end{cases} \tag{4.12}$$

$$s_2^t = \begin{cases} 1 \text{ , } discharging \\ 0 \text{ , } otherwise \end{cases} \tag{4.13}$$

$$s_3^t = \begin{cases} 1 \text{ , } traveling \\ 0 \text{ , } otherwise \end{cases} \tag{4.14}$$

The SoC of school n at the beginning of the next timeslot SoC_n^{t+1} as in (4.11) can be computed using the following four terms:

1) SoC at the beginning of time slot, SoC_n^t

2) The amount of charged SoC in time slot t

3) The amount of discharged SoC in time slot t

4) The amount of SoC usage for the travel of ESBs in school n in time slot t

Furthermore, it is typically imperative for the SoC to remain within the capacity limitations to extend the battery's lifespan as follows:

$$SoC_n^{min} \leq SoC_n^t \leq SoC_n^{max} \tag{4.15}$$

where SoC_n^{min} and SoC_n^{max} representing minimum SoC and maximum SoC at time t of school n's ESBs.

Each school possesses a number of ESBs that can be utilized to provide the peak shaving program by discharging the stored energy inside their ESBs' battery. Therefore, the maximum available stored energy to be discharged is calculated as the difference between the State-of-Charge (SoC) at that time t and the minimum SoC, which can be converted to kWh by multiplying the battery capacity, ESS_n.

$$E_n^t = (SoC_n^t - SoC_n^{min})ESS_n \tag{4.16}$$

Here, E_n^t is the maximum energy in kWh that can be discharged by school n's ESBs.

Utility of Schools

The utility function of each school n at time t comprises two terms: satisfaction derived from retaining stored energy inside ESBs' batteries and monetary profit from participating in the peak shaving program.

$$U_n^t = \psi_n^t(e_n^t) + (p_{uc}^t - p_{avg}^t)x_n \tag{4.17}$$

where e_n^t is the remaining energy in the school's ESBs that can be further utilized after discharging energy for x_n^t, and the p_{avg}^t is the average charging price per unit of energy constituting the current amount of stored capacity.

$$e_n^t = E_n^t - x_n^t \tag{4.18}$$

$$p_{avg}^t = \frac{1}{\sum_{t=1}^{t-1} D_{ch}^t} \sum_{t=1}^{t-1} p^t D_{ch}^t \tag{4.19}$$

where p^t denotes the dynamic price calculated by (4.4).

We define the satisfaction function $\psi_n^t(e_n^t)$, representing the level of satisfaction obtained from having a certain amount of stored energy in ESBs.

The satisfaction function must satisfy the following properties:

1) The satisfaction function is a non-decreasing function. Each school is always more satisfied with more energy stored inside their ESBs' battery until it reaches the maximum level of stored energy.

$$\frac{\partial \psi_n^t}{\partial x_n^t} \geq 0 \tag{4.20}$$

2) The marginal benefit is a non-increasing function, meaning that the satisfaction level increases less per unit of stored energy as the level of energy in storage increases, eventually reaching a saturated level.

$$\frac{\partial^2 \psi_n^t}{\partial {x_n^t}^2} \leq 0 \tag{4.21}$$

Therefore, in this work, we employ the quadratic satisfaction function, a widely accepted and utilized form in the literature [18, 88, 92].

$$\psi(e_n^t) = \lambda_n e_n^t - \frac{\theta_n}{2}(e_n^t)^2 \tag{4.22}$$

where λ_n is the preference parameter of school n, distinguishing it from other schools,

78

and θ_n stands for the quadratic function's predefined constant.

Therefore, from (4.16),(4.17),(4.18), and (4.22) we can reformulate the utility function of a school n Un as:

$$U_n^t = \lambda_n(E_n^t - x_n^t) - \frac{\theta_n}{2}(E_n^t - x_n^t)^2 + (p_{uc}^t - p_{avg}^t)x_n \qquad (4.23)$$

This utility function represents the trade-off between providing discharged energy to UC for monetary profit and retaining stored energy in the ESBs' battery for satisfaction. In other words, if school n provides more energy to UC, their satisfaction level decreases due to the low remaining energy in the ESBs' battery, but they will earn higher monetary profit. Conversely, if they preserve more stored energy in the ESBs' battery and discharge less, they will make less profit from V2G service, but their satisfaction level stays high. Therefore, each school aims to maximize its utility by determining the optimal value of x_n^t as:

$$\max_{x_n^{t,min} \leq x_n^t \leq x_n^{t,max}} U_n^t(x_n^t) \qquad (4.24)$$

4.4 ePMES Scheme

4.4.1 Game Formulation

The Stackelberg game is a non-cooperative game that examines situations where a hierarchy exists among players. It was first introduced by Heinrich von Stackelberg [93]. In this game, the leader selects the action (strategy) first, and then followers observe the leader's strategy and decide on their own strategies by choosing the "best response strategy" that maximizes their utility function. The leader is also aware of this, so he selects a strategy that maximizes his own utility. The solution to the game is known as the "Stackelberg equilibrium," where no player can increase their utility by unilaterally deviating from their best response strategy. The hierarchical nature of the Stackelberg game makes it highly suitable for modeling the interaction between multiple parties in

smart grid problem.

In this work, a Stackelberg game is formulated, where UC is the leader aiming to minimize its cost function by determining the optimal incentive price (p_{uc}^t). In contrast, schools that own ESBs are the followers trying to maximize their utility function by finding the optimal amount of discharged energy from their ESBs' battery (x_n^t) for V2G service in response to the incentive price issued by UC. The game can be formally defined as:

$$\mathcal{S} = \{(\mathcal{N} \cup \{UC\}), \{\mathcal{X}_n^t\}_n, p_{uc}^t, \{\mathcal{U}_n^t\}_{n \in \mathcal{N}}, U_{uc}^t\} \tag{4.25}$$

which consists of the following components:

1) Players: The set of schools owing ESBs $\mathcal{N}$ as followers determine their optimal discharged energy for the peak shaving program, and UC as the leader decides on the incentive price paid to schools for providing peak shaving service.

2) Strategies: Each shool n decides on the amount of discharged energy, $x_n^t \in \mathcal{X}_n^t$, to maximize its payoff. The UC decides on the optimal incentive price, p_{uc}^t, to minimize its additional cost in meeting the demand within a community.

3) Payoffs: The utility of school n owning ESBs, $U_n^t(x_n^t)$, as described in (4.23), and the additional cost to cover additional peak demand in the community of the UC, $U_{uc}^t(p_{uc}^t)$, as show in (4.9), where the payoffs for both types of players depend on the strategies of the other players.

Definition 1. *For the proposed two-level Stackelberg game in (4.25), a set of strategies $(\boldsymbol{x_n^{t*}}, p_{uc}^{t*})$ constitutes a Stackelberg equilibrium if and only if the following set of conditions is satisfied:*

$$U_n^t(\boldsymbol{x^{t*}}, p_{uc}^{t*}) \geq U_n^t(x_n^t, \boldsymbol{x_{-n}^{t*}}, p_{uc}^{t*}) \tag{4.26}$$

$$U_{uc}^t(\boldsymbol{x^{t*}}, p_{uc}^{t*}) \leq U_{uc}^t(\boldsymbol{x^{t*}}, p_{uc}^t) \tag{4.27}$$

where $\boldsymbol{x_{-n}^{t*}} = \{x_1^{t*}, x_2^{t*}, ..., x_{n-1}^{t*}, x_{n+1}^{t*}, ..., x_N^{t*}\}$ is the optimal strategies of all the schools

in time slot t except for the school n. Hence, the optimal strategies of all the schools in the community in time slot t can be expressed as $\boldsymbol{x^{t*}} = \{x_n^{t*}, \boldsymbol{x_{-n}^{t*}}\}$.

The equation (4.26)-(4.27) implies that when all players are at the Stackelberg equilibrium, no schools can increase its utility by deviating from x_n^{t*}, and the UC cannot reduce more cost by selecting a different incentive price other than p_{uc}^{t*}.

4.4.2 Existence and Uniqueness of the Equilibrium

It is possible that the equilibrium in the game does not always exist. Therefore, investigating whether the equilibrium exists or not is needed for the proposed game model. To examine this, we apply the *backward induction* technique to determine the game's equilibrium. The first step is to find the optimal strategies of each follower. Then, given the optimal strategies from the followers, the existence of the optimal strategy of the leader can be proved. Thus, the existence of the equilibrium will be established.

Theorem 1. *There exists a unique Stackelberg equilibrium in the proposed two-level Stackelberg game among UC and schools that satisfies (4.26)-(4.27)*

Proof. The first step of the proof initiates at the lower level by identifying the best response of each school, which is the optimal discharged energy of the school's ESBs (x_n^{t*}), responding to the UC's strategy (p_{uc}^t) in the upper level. From the best response information of the schools, we can then trace back to determine whether the UC has an existing optimal strategy or not. The mathematical proof is presented as follows:

(1) Lower level: optimal discharged energy of schools

Given the strategy from the leader p_{uc}^t sent from UC in the upper level, the best response strategy for each school n in the lower level can be obtained by taking the first-order derivative of U_n^t in (4.23) with respect to x_n^t:

$$\frac{\partial U_n^t}{\partial x_n^t} = -\lambda_n + p_{uc}^t - p_{avg}^t + \theta_n x_n^t + \theta_n E_n^t \tag{4.28}$$

Let (4.28) equal to zero, the optimal discharged energy of school n that maximizes its

utility function can be obtained as follows:

$$x_n^{t*} = \frac{-\lambda_n + p_{uc}^t - p_{avg}^t}{\theta_n} + E_n^t \qquad (4.29)$$

Then, the second-order derivative of U_n^t is:

$$\frac{\partial^2 U_n^t}{\partial {x_n^t}^2} = -\theta_{m,n} < 0 \qquad (4.30)$$

Since the second-order derivative of U_n^t is always negative as in (4.30) due to $\theta_n > 0$, it means that U_n^t is strictly concave with respect to x_n^t. Therefore, the best response strategy of the school n as in (4.29) is guaranteed to be unique and optimal.

(2) Upper level: optimal incentive price of UC

Given the best-response strategy of followers from the lower level in (4.29), we can calculate the summation of all the discharged energy from the school's ESBs for peak shaving service E_{V2G}^t as:

$$\begin{aligned}
E_{V2G}^t &= \sum_{n\in\mathcal{N}}(\frac{-\lambda_n + p_{uc}^t - p_{avg}^t}{\theta_n} + E_n^t) \\
&= \sum_{n\in\mathcal{N}}(\frac{-\lambda_n - p_{avg}^t}{\theta_n} + E_n^t) + \sum_{n\in\mathcal{N}}\frac{1}{\theta_n}p_{uc}^t
\end{aligned} \qquad (4.31)$$

To simplify the expression, we can define new parameters α and β^t as follows:

$$\alpha = \sum_{n\in\mathcal{N}}\frac{1}{\theta_n} \qquad (4.32)$$

$$\beta^t = \sum_{n\in\mathcal{N}}(\frac{-\lambda_n - p_{avg}^t}{\theta_n} + E_n^t) \qquad (4.33)$$

Therefore, (4.31) can be rewritten as:

$$E_{V2G}^t = \alpha p_{uc}^t + \beta^t \qquad (4.34)$$

The utility function of the UC can be reformulated by substituting the summation

of the optimal strategy of the schools from (4.34) into the UC cost function in (4.9). Therefore, U_{uc}^t can be reformulated as:

$$U_{uc}^t(x_n^t, p_{uc}^t) = p_{uc}^t(\alpha p_{uc}^t + \beta^t) + [a(D_{peak}^t - (\alpha p_{uc}^t + \beta^t))^2 + b(D_{peak}^t - (\alpha p_{uc}^t + \beta^t))]$$
$$- [a(D_{base}^t)^2 + bD_{base}^t]$$

(4.35)

We can determine the first and second-order derivatives of (4.35) with respect to p_{uc} as follows:

$$\frac{\partial U_{uc}^t}{\partial p_{uc}^t} = 2\alpha p_{uc}^t + \beta^t - 2a\alpha(D_{peak}^t - \alpha p_{uc}^t - \beta^t) - \beta^t \qquad (4.36)$$

$$\frac{\partial^2 U_{uc}^t}{\partial p_{uc}^{t\,2}} = 2(a\alpha^2 + \alpha) > 0 \qquad (4.37)$$

Since the value of a and α is positive, the second-order derivative of U_{uc}^t is always positive, as shown in (4.37). This means that U_{uc}^t is strictly convex with respect to p_{uc}^t. Thus, the optimal solution of the UC is guaranteed to be unique and optimal.

From the above proof, we can see that once the unique and optimal strategy of UC (p_{uc}^{t*}) is found, the unique and optimal strategy of each and every school n can be calculated. Hence, the unique Stackelberg equilibrium in the form of ($\boldsymbol{x^{t*}}, p_{uc}^{t*}$) exists for the proposed two-level Stackelberg game model, and it will be found as soon as the optimal UC's incentive price is determined. $\qquad \square$

4.4.3   Optimal Energy-Price (OEP) Equilibrium Algorithm

In this section, we introduce and describe the proposed optimal energy-price (OEP) equilibrium algorithm, designed to achieve game equilibrium in a distributed manner. In this approach, schools are required only to disclose the discharged energy to the UC and nothing else, thereby preserving their privacy. We can see from the previous subsection that the objective function of UC is strictly convex with respect to p_{uc}^t. Hence, enumerating

the incentive price p_{uc}^t will lead to the minimum of the UC cost, meaning it is always guaranteed to reach the unique and optimal solution. In the nature of the leader-follower game, to find the Stackelberg equilibrium, we have to find the optimal solution of the leader. To do that, we can enumerate the leader strategy p_{uc}^t from $p_{uc,min}^t$ to $p_{uc,max}^t$, and the optimal solution is the one that minimizes the cost of UC. When the UC's optimal incentive price p_{uc}^{t*} is found, the optimal discharged energy of every n-th school x_n^{t*} will also be found by (4.29). Hence, the strategy profile $(\boldsymbol{x^{t*}}, p_{uc}^{t*})$ for the Stackelberg equilibrium is found.

In Algorithm 1, the UC iteratively updates p_{uc}^t from $p_{uc,min}^t$ to $p_{uc,max}^t$. The UC first issues the incentive price p_{uc}^t to all schools. Upon receiving the announced incentive price, each school n calculates the optimal discharged energy it will provide to UC for peak shaving service (x_n^t) that maximizes its utility given p_{uc}^t by (4.29) and sends this response information back to the UC. The UC gathers all the responses from the schools, then calculates the total discharged energy from schools in the community (4.6). The UC further calculates the total additional cost it needs to pay to cover the community's demand by (4.9). It then compares the results with the previously recorded utility of the previous recorded incentive price that makes the utility lowest so far. If the new one is lower, indicating an improvement, UC updates the recorded utility value U_{uc}^{t*}. However, if the new one is not less than the recorded utility, UC ignores the newly calculated utility value and price. The algorithm runs iteratively until the conditions in (4.26)-(4.27) are satisfied, indicating that the Stackelberg equilibrium is reached.

Algorithm 1 Optimal Energy-Price (OEP) Equilibrium Algorithm

1: UC initialize $\boldsymbol{p^t_{uc}} = p^{min}_{uc}$, $U^{t*}_{uc} = C^t_{gen}(D^t_{peak}) - C^t_{gen}(D^t_{base})$
2: **for** p^t_{uc} from p^{min}_{uc} to p^{max}_{uc} **do**
3:     Broadcast p^t_{uc} to all schools in the community
4:     **for** school $n \in \mathcal{N}$ in community **do**
5:         Calculate optimal discharge energy from its ESBs (x^t_n) using (4.29)
6:         Send x^t_n back to the UC
7:     **end for**
8:     UC summarizes all the discharged energy from all the schools using (4.6)
9:     UC calculates the value of its utility function using (4.9)
10:     **if** $U^t_{uc} \leq U^{t*}_{uc}$ **then**
11:         UC record new incentive price and cost value
12:         $p^{t*}_{uc} = p^t_{uc}$, $U^{t*}_{uc} = U^t_{uc}$
13:     **end if**
14: **end for**
15: The equilibrium $(\boldsymbol{x^{t*}}, p^{t*}_{uc})$ is reached where the cost of UC is minimized

---

4.4.4 Implementation Process

The process can be divided into two stages: G2V is used for filling valleys and typically occurs on a day-ahead basis. Then, V2G for peak shaving takes place during the day when requests for peak shaving are made.

G2V for valley filling

The UC attempts to fill up the valley periods by managing and allocating the demand charge energy from schools that need to charge their ESBs.

1) First, assume that the UC has accurate forecasting capabilities for the energy profile of a community on a day-ahead basis and announces the valley period that need to be filled by charging at the school.

2) Each school then requests the amount of energy needed to charge its ESBs from the UC.

3) The UC allocates the demand to flatten the valley period and sends the relevant information back to the schools for implementation.

V2G for peak shaving

During the day, the UC will request V2G services from schools that possess a number of ESBs capable of discharging the energy stored in their batteries.

1) The Utility Company (UC) announces the peak periods and sends an incentive signal to schools before the peak period begins.

2) Each school submits the amount of energy they plan to discharge from their Electric School Buses (ESBs) during the peak period.

3) UC calculates its own utility and announces a new price to the schools based on this calculation.

4) The process returns to steps 2 and 3 and repeats until an equilibrium is reached.

4.5 Evaluation Studies

4.5.1 Simulation Setup

In this section, we evaluate the performance of the proposed V2G model, where both entities, UC and schools, seek to find optimal strategies in response to each other's actions. Given that the USA has the world's largest usage of ESBs, we focus on and utilize data from the USA. The electrical load profile is obtained from the U.S. Energy Information Administration [94]. The daily school schedule is from Rochester Community Schools in Michigan, USA, where the ESBs operate by picking up students in the morning from 6 a.m. to 8 a.m. and dropping them back home in the afternoon from 3 p.m. to 5 p.m. [95]. This means h_d is 2 hrs. Hence, during these intervals, the ESBs cannot be used for V2G service. At other times, schools that possess ESBs can participate in the V2G peak shaving program, effectively acting as stationary batteries. In this Rochester community, there are approximately 21,000 people of student age [96], and typically in the US, about 38% of students take school buses [97]. Hence, the number of students taking the school bus is around 8,000, with each bus accommodating 40-60 students comfortably and up to 80 students at maximum capacity [95]. Hence, the number of ESBs in real-world scenarios

in this community should range between 100 and 200 buses The number of schools (N) in a community is 20, including elementary schools, middle schools, and high schools. Each school possesses 10 buses. Therefore, the total number of ESBs used in the simulation is 200 buses. The preference parameter of schools is randomly selected from the range of [1, 1.2]. The parameter θ is set to 0.001 The ESB with a capacity of 200 kWh is used. The minimum SoC is 20%, and the maximum SoC is 90% [?, 98], as this range would prolong the battery life. The ESB travel distance each round is 70 km [67, 99]. The energy consumption rate for traveling is 1 kWh/km [100, 101]. The maximum charging and discharging power is 60 kW [67, 101]. We utilize MATLAB to implement Algorithm (??) in order to find the equilibrium solution.

4.5.2 Energy Profile Results and Discussion

In this subsection, the energy profile results are compared among three scenarios: charge-after-use (CAU) charging, grid-to-vehicle (G2V) charging, and the proposed optimal energy-price (OEP) V2G model.

- Charge-after-use (CAU) [102]: The ESBs are charged immediately until full after their pick-up and delivery service in the morning and afternoon, following typical human behavior.

- Grid-to-Vehicle (G2V) [103]: This charging involves the ESBs being charged only during the valley period, where the electricity price is the lowest, until full. This typically occurs after midnight until early morning before the service starts, and no discharging energy is provided to the grid.

- Centralized approach (CEN) [77]: This scenario employs centralized control from the UC to maximize the reduction of generation costs by fully utilizing all ESBs to discharge energy during peak periods. This approach does not consider the schools' efforts to maximize their own benefits, but the schools still receive monetary compensation for providing the discharged energy.

- The proposed optimal energy-price (OEP): This scenario utilizes both charging during the lowest price period and discharging energy during peak periods to receive monetary benefits from the utility company.

The profiles are studied across three seasons: winter, spring, and fall, when the school is normally open.

The energy profile in winter in Figure 4.2 shows that CAU charging will cause high peaks during the morning and evening due to the ESBs charging aligning with the peak energy demand profile. In contrast, G2V only charges during the valley period in the early morning and can be used for travel services in both the morning and afternoon. On the other hand, the proposed OEP algorithm not only fills the valley period during 0-6 am but also helps shave the peak demand during 8-11 am, where the original peak demand is reduced by 11.15 MWh.

Figure 4.3 and 4.4 show the energy profiles for the spring and fall seasons, where both seasons typically have very similar energy profiles. The results indicate that CAU charging will cause two peak demands after the travel service. G2V charging helps fill the valley in the early morning by charging at the lowest price. On the other hand, the proposed OEP charging and discharging algorithm can help fill the valley during 1-6 am and also reduce the original peak during the evening (6 pm-10 pm) by 9.3 MWh and 9.7 MWh in spring and fall, respectively.

Table 4.1 illustrates the percentage reduction results comparing the G2V, CEN, and proposed OEP algorithms with CAU charging across three seasons. The results indicate that the cost for the utility company is reduced the most with the proposed OEP algorithm compared to both G2V and CAU charging. On the other hand, the cost for the UC is reduced the most with the CEN approach, as this centralized strategy primarily focuses on reducing the UC's costs, rather than the bills of the schools. Conversely, the bills of the schools decrease the most with the proposed OEP algorithm, which considers both the cost to the UC and the bills of the schools. As a result, the combined reductions in the cost to the UC and the bills of the schools for CEN and the proposed OEP are
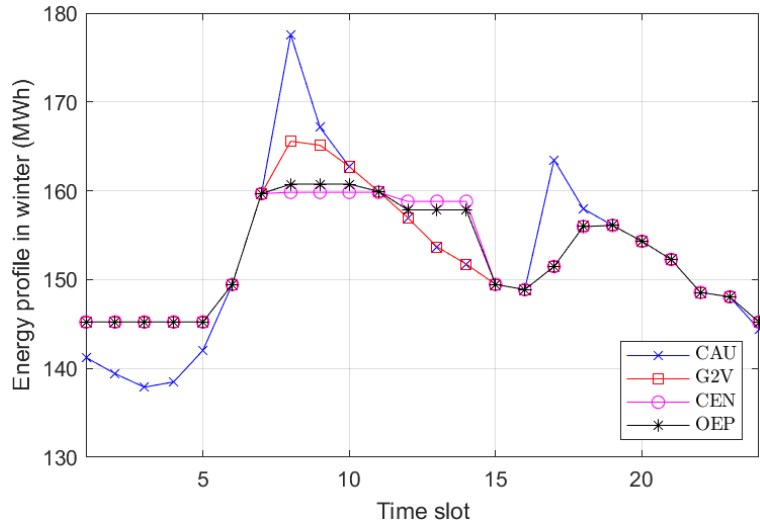
Figure 4.2: Energy profile in winter
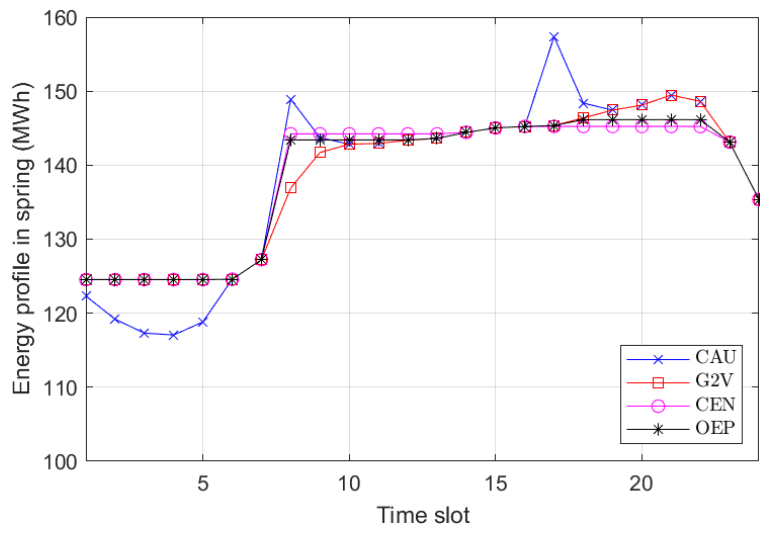
Figure 4.3: Energy profile in spring
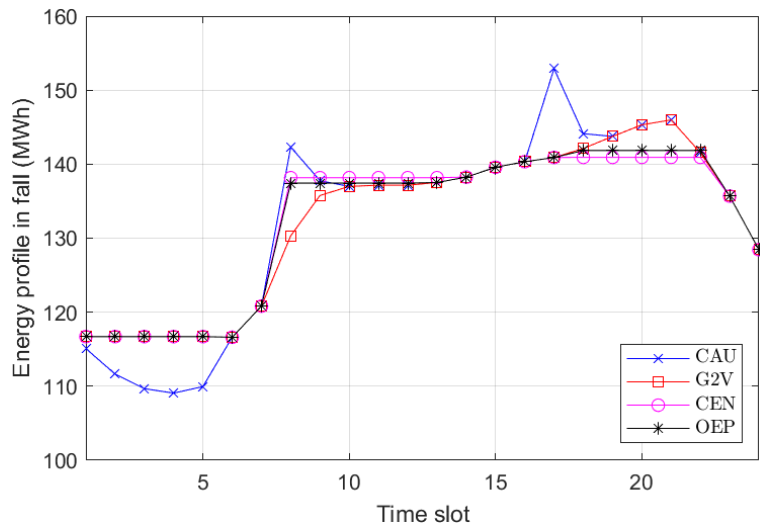
Figure 4.4: Energy profile in fall

89

Table 4.1: Percentage reduction comparing the G2V, CEN, and proposed OEP algorithm with CAU charging over 24 hours

% Reduction	Winter			Spring			Fall		
	G2V	CEN	OEP	G2V	CEN	OEP	G2V	CEN	OEP
Cost of UC	0.11	0.71	0.59	0.15	0.79	0.58	0.17	0.85	0.63
Bill of schools	7.75	19.56	22.57	9.10	20.05	22.10	9.80	20.03	22.61
peak-to-average ratio	6.76	11.11	9.48	5.01	8.34	7.12	4.53	8.51	7.24

20.27% and 23.16% for winter, 20.84% and 22.68% for spring, and 20.89% and 23.24% for fall, respectively. This shows that, although CEN provides the greatest reduction in the cost to the UC and also significantly lowers the bills of the schools, the total reduction is consistently better with the proposed OEP approach across all seasons. This is because the OEP approach accounts for the benefits to both the UC and the schools. Although the percentage reduction in the total 24-hour cost of UC is small due to the typically very high demand compared to the amount the peak can be shaved out, the effective impact of the proposed OEP algorithm is evident in the significantly reduced additional cost during peak periods, which will be shown and discussed later on. This effectiveness extends to the total bills for all the schools, which can be reduced by up to 22.6%. Additionally, the peak-to-average ratio is also reduced in the proposed OEP algorithm compared to both G2V and CAU charging by up to 9.5%.

4.5.3 Sensitivity Analysis Results and Discussion

We study the characteristics of the proposed OEP V2G model by varying important input parameters, such as the number of schools, battery capacity, and travel distance, while fixing D_{base} at 150 MW and changing D_{req} to 1, 2, 3, and 4 and MW. Hence, four different line colors: black, red, blue, and magenta are used to show different results.

Number of schools

Figure 4.5, 4.6, and 4.7 show the normalized incentive price of UC, the total discharged energy from schools in the community, and the percentage reduction in cost of UC when the number of schools varies from 0 to 20.
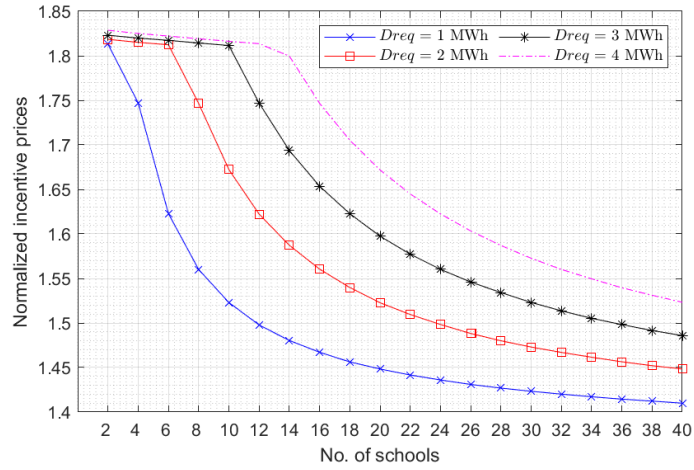
Figure 4.5: Incentive price of UC vs. number of schools.
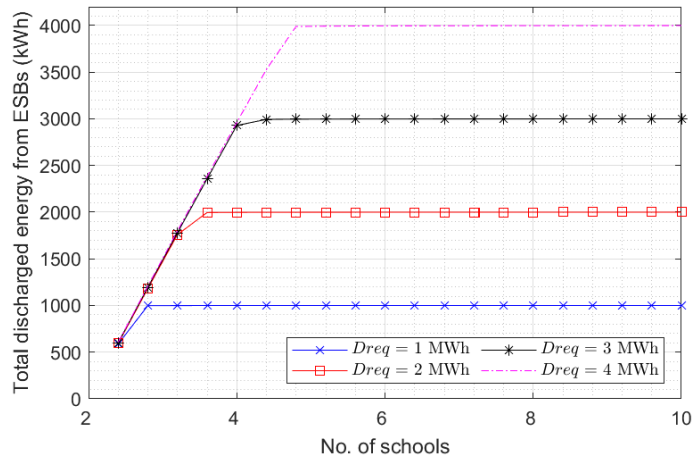
Figure 4.6: Total discharge energy from ESBs vs. number of schools.
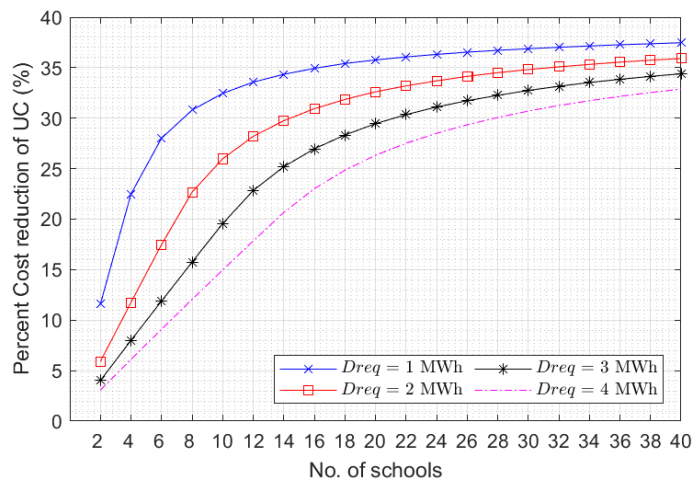
Figure 4.7: Percentage reduction in cost of UC vs. number of schools.
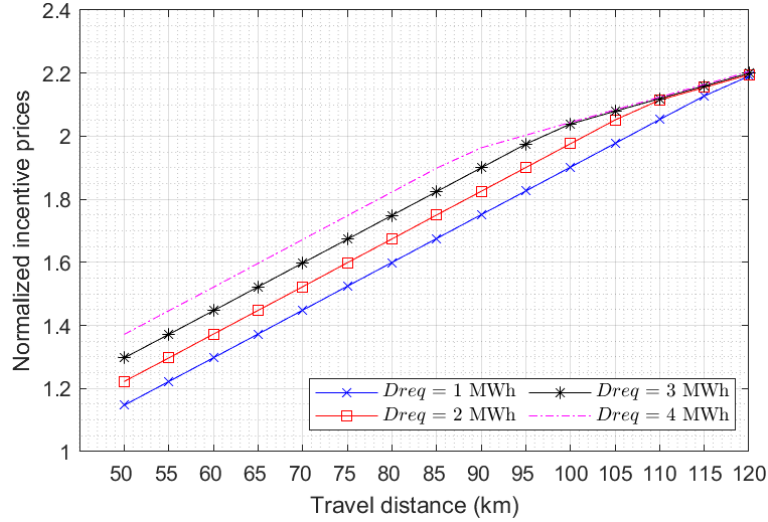
Figure 4.8: Incentive price of UC vs. daily travel distance of each ESB.

The result reveals in figure 4.5 that the greater number of schools in the community, the incentive price paid by UC decreases. This is because there is more energy inside the ESBs to be discharged into the system, hence the competition between schools is higher. Each school is willing to accept the lower incentive price while still discharging the same amount of energy. As we expected, as the number of schools increases, the discharged energy and the percentage reduction in cost of UC will also increase, as shown in figure 4.6 and 4.7.

When the D_{req} is changed by different line colors, figure 4.5 show that when the D_{req} is increased, the incentive price of UC is also increases as we expected. Since the higher the D_{req} will cause higher unit prices for generation cost. So, UC is willing to pay higher incentive prices for the schools to discharge energy from their ESBs to fulfill the D_{req}. Similar to figure 4.6, when the D_{req} increase, total discharge energy also increase. On the other hand, the percentage reduction in the cost of UC decreases when D_{req} is higher, since at higher peak demand, the cost of generating energy is significantly higher and harder to reduce.

Travel distance

Figure 4.8, 4.9, and 4.10 depict the normalized incentive price of UC, the total discharged energy from schools in the community, and the percentage reduction in the cost of UC
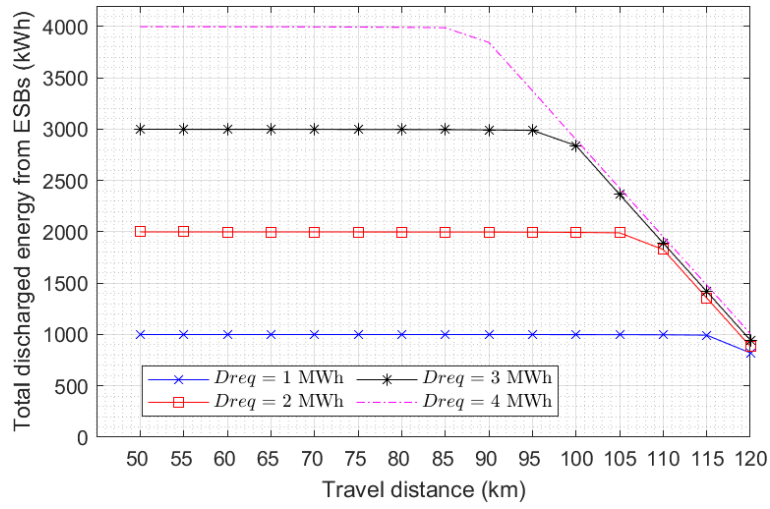
Figure 4.9: Total discharge energy from ESBs vs. daily travel distance of each ESB.
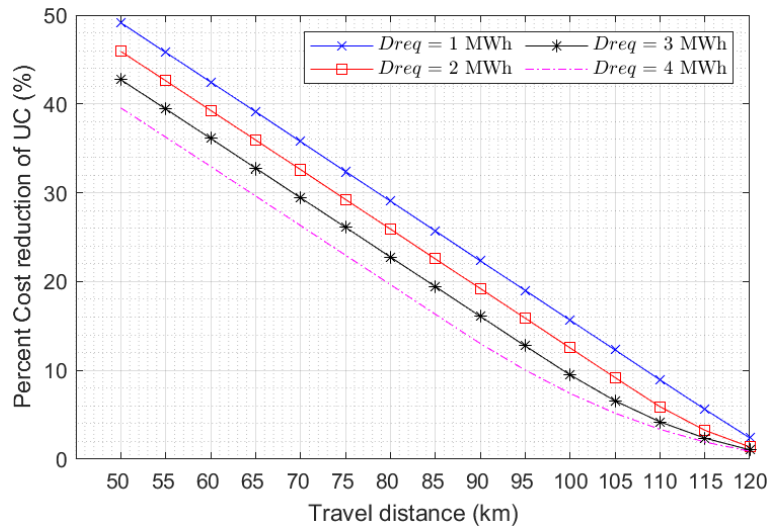
Figure 4.10: Percentage reduction in cost of UC vs. daily travel distance of each ESB.
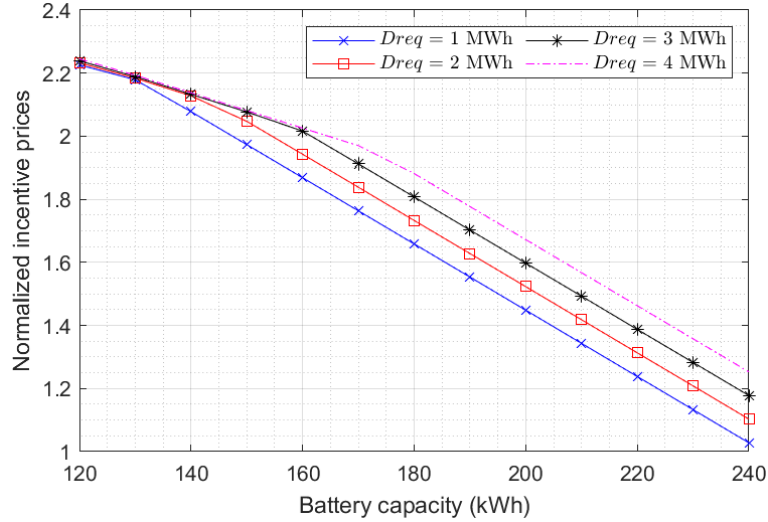
Figure 4.11: Incentive price of UC vs. battery capacity of each ESB.

when the traveling distance varies from 50 km to 120 km.

This shows that when the traveling distance is longer, the incentive price will increase. The reason is that when the traveling distance is longer, there is less energy remaining inside the battery of ESBs to discharge after completing traveling tasks. Therefore, UC is willing to pay a higher incentive for ESBs to discharge to the grid.

And as expected, when daily travel distance is very high the total discharged energy are lower as shown in figure 4.9. For the percentage reduction in the cost of UC, it also decreases with increasing distance, as shown in figure 4.10.

Battery capacity of each ESB

In this subsection, we study the effect of the battery capacity of each ESB by varying the value from 120 kWh to 240 kWh. Figures 4.11, 4.12, and 4.13 illustrate the incentive price from UC, total discharged energy from ESBs, and the percentage reduction in UC costs, respectively.

In Figure 4.11, it is observed that when the battery capacity of each ESB is higher, the incentive price from UC is lower. This is because there will be more energy available to assist UC during peak demand, prompting UC to offer a lower price. Figure 4.12 demonstrates that increasing battery capacity leads to higher total discharged energy, especially when the battery capacity is very low. However, in higher capacity values, the

94
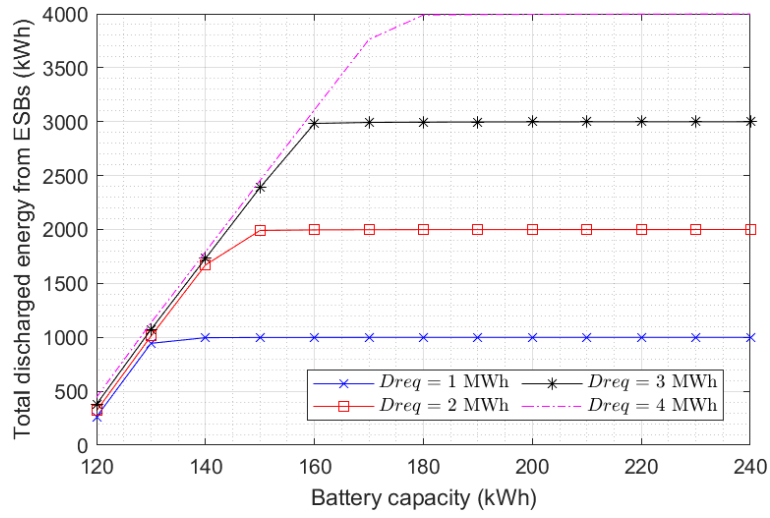
Figure 4.12: Total discharge energy from ESBs vs. battery capacity of each ESB
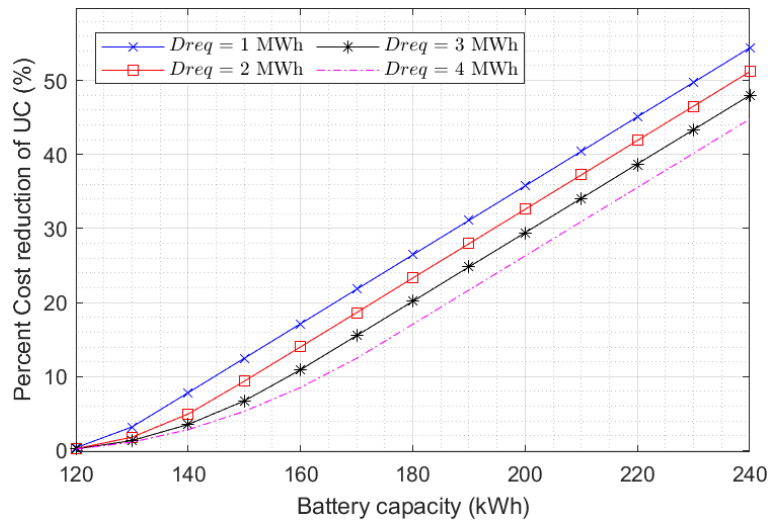
Figure 4.13: Percentage reduction in cost of UC vs. battery capacity of each ESB
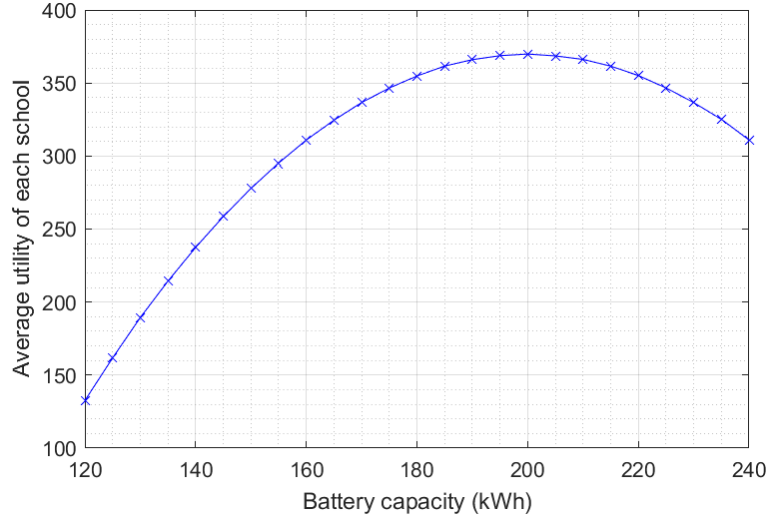
Figure 4.14: Average utility of each school vs. battery capacity of each ESB

total discharged energy remains unchanged as it already covers the D_{req}.

Regarding the percentage reduction in the cost of UC shown in Figure 4.13, it is observed that when the battery capacity increases, the percentage reduction also increases, as expected. This is because there is more stored energy available to assist UC, leading to a greater reduction in cost.

Optimal Battery capacity of ESB

Figures 4.14 illustrate that when the battery capacity for each ESB varies from 120 kWh to 240 kWh, there is an optimal value at which the average utility of each school is maximized, which is 200 kWh, as we have used this value in our simulation. Examples of real ESBs that use this amount of battery capacity include the GreenPower: BEAST [104], Blue Bird: All American Electric [105], and Lion Electric: LionD [106].

When utilizing the optimal battery capacity of 200 kWh, with 20 schools as indicated in the community data, a distance of 70 km, and a mean D_{req} of 1 MWh, the effectiveness of the proposed OEP model is demonstrated by significantly reducing the additional generation cost for UC by around 36% during peak periods.

4.6 Summary

This chapter presents a V2G energy sharing management model for UCs and schools that possess ESBs. Since the ESBs have a predictable usage in terms of time and energy consumption, they are highly suitable for use in peak shaving services, in contrast to personal EVs. The problem is formulated as a Stackelberg game, where a UC is the leader in setting the incentive price for providing the peak shaving service. On the other hand, the followers are the schools, which try to find the optimal discharge energy to help the UC shave the peak. The evaluation is performed in four different scenarios across three different seasons. The sensitivity analysis of the V2G model is also conducted by varying the number of schools, daily travel distance, and battery capacity of each ESB. The effectiveness of the proposed OEP algorithm is demonstrated by a 36% reduction in the additional generation cost for the UC during peak periods and a decrease in electricity bills for schools by up to 22.6%. Furthermore, the peak-to-average ratio is reduced by up to 9.5%.

Chapter 5

Inter-Community Energy Sharing Management for Fully Moving Energy Storage Scheme

5.1 Introduction

The widespread adoption of Electric Vehicles (EVs) in the smart grid is transforming the traditional grid into a more complex system. EVs have the ability to both charge and discharge, acting as loads that draw high power and sources that inject energy back into the grid. Consequently, energy sharing and management within smart grid communities integrated with EVs have become interesting aspects to study in order to efficiently utilize this energy. However, most existing research focuses solely on energy sharing within single communities, utilizing homogeneous energy profiles and neglecting the potential of heterogeneous energy across multiple communities. EVs also possess the capability to travel to different places and communities where they can engage in energy sharing with areas that have varying load profiles and prices. In this chapter, we propose a novel three-level energy sharing management approach for multiple communities integrating with movable energy storage such as EVs. This model involves three main entities: the Utility Company (UC), Community Energy Aggregator (CEA), and EVs, each aiming to
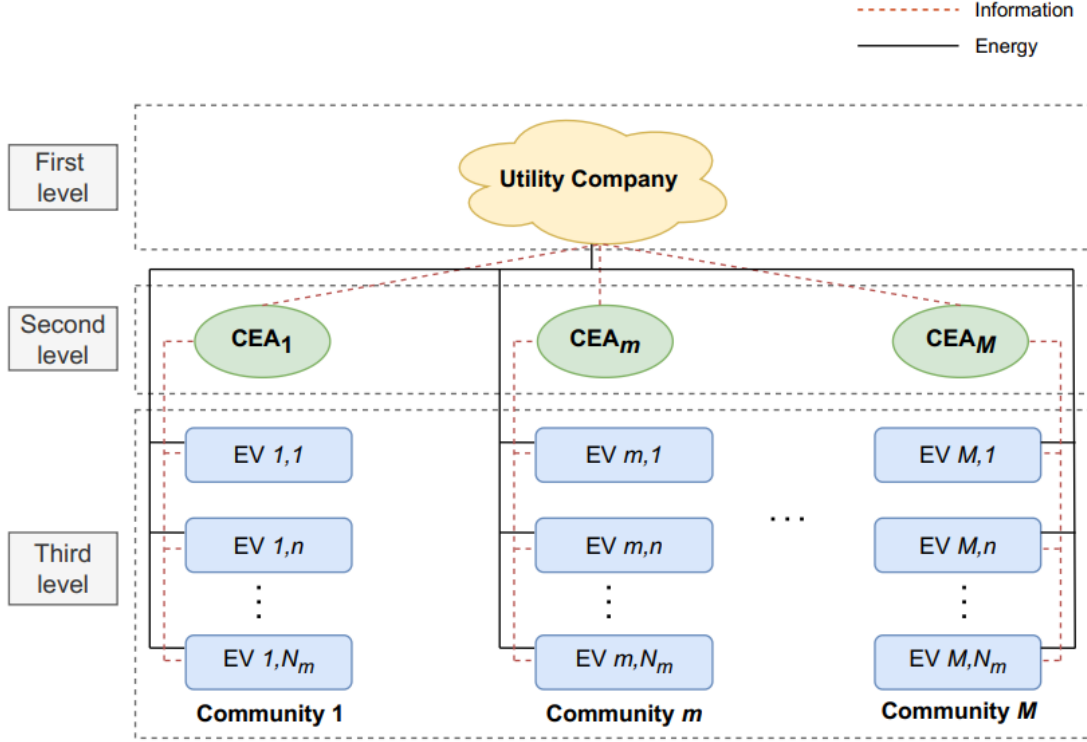
Figure 5.1: Hierarchical multi-communities energy sharing management model

maximize its benefit through optimal strategies, including pricing, energy demand, and supply.

5.2 System Model

5.2.1 Overview Structure

Fig. 5.1 shows the system model of the multi-communities' energy sharing, consisting of one utility company (UC), multiple community energy aggregators (CEA), and multiple EVs within multiple communities. We will briefly explain each entity as follows:

- Electric Vehicles (EVs) : Each electric vehicle is capable of charging and discharging energy through CEA. We assume that all EVs are equipped with a smart energy management system (SEMS), through which they can communicate with CEA via charging facilities. The SEMS sends consumption data and receives shared price information. It is able to perform necessary computational tasks and control charging

and discharging.

- Community Energy Aggregator (CEA) : Each CEA facilitates energy sharing within the community by engaging in two-way communication with EVs within its community. It also communicates with UC for the purpose of energy sharing between communities and determines the energy sharing prices within the community. The CEA ensures payment and energy balance for the community in which it sells or buys energy to or from EVs within the community and the utility company. If there is a net surplus of energy within the community, the CEA is responsible for selling the excess energy to the utility company. Similarly, if the generated energy within the community is insufficient, the CEA is responsible for purchasing the energy from the utility company.

- Utility Company (UC) : The UC sells or buys energy to or from CEAs at real-time pricing according to the net aggregated energy from the multi-communities.

The proposed energy sharing management model consists of three hierarchical levels: UC level, CEA level, and electric vehicle level. Firstly, at the upper level, the UC supplies/buys electricity to/from the multi-communities system. The price between the UC and multiple CEAs is called the "multi-communities sharing price". The UC tries to maximize profit by setting the optimal multi-communities sharing price (p_{uc}^t), which is related to the amount of net energy in the multi-communities system at a given time slot. Secondly, at the middle level, CEAs act as intermediaries who buy/sell energy from/to the UC and also buy/sell energy from/to EVs within their community. The CEAs try to maximize their profit by setting the optimal sharing price within their own community $(p_{CEA,m}^t)$, considering the amount of net energy of the community and the multi-communities sharing price from the upper level. Finally, at the bottom level, each EV within the community determines its optimal charging/discharging energy in response to the energy sharing prices from its CEA to maximize its own utility.

Let $\mathcal{M} = 1, 2, \ldots, M$ denote the set of communities and CEAs, where each community $m \in \mathcal{M}$ has only one CEA, and let $\mathcal{N}_m^t = 1, 2, \ldots, N$ denote the set of EVs in a single

community, with $n \in \mathcal{N}_m^t$. Let $\mathcal{K}$ be the set of EVs in the system, where K is the total number of EVs in the system, given by $K = M \cdot N$. The time operation in one day is divided into T time slots, where $t \in \mathcal{T} = 1, 2, \ldots, T$. For simplicity, we consider each t to represent 1 hour, and thus $T = 24$.

5.2.2 Electric Vehicle (EV) Model

Let $x_{m,n}^t$ denote the charging/discharging energy of the m, n-th EV. When $x_{m,n}^t \geq 0$, the m, n-th EV is charging. However, the EV will discharge when $x_{m,n}^t < 0$. Let $p_{CEA,m}^t$ be the energy sharing price inside community m, which is sent from CEA $m \in \mathcal{M}$. In this model, the utility function of an EV consists of increase of satisfaction function and cost/revenue from energy sharing. The goal of each m, n-th EV is to maximize its own utility as follows:

$$\max_{x_{m,n}^t} U_{m,n}^t = \psi(E_{m,n}^t + x_{m,n}^t) - \psi(E_{m,n}^t) - p_{CEA,m}^t x_{m,n}^t \tag{5.1}$$

$$s.t.\ x_{m,n}^{min,t} \leq x_{m,n}^t \leq x_{m,n}^{max,t} \tag{5.2}$$

where $E_{m,n}^t$ is the remaining energy in the EV that can be further utilized at time t before deciding to charge or discharge, defined as $E_{m,n}^t = ES_{m,n}^t - ES_{min}^t$. The first term, $\psi(E_{m,n}^t)$, represents the satisfaction value of having $E_{m,n}^t + x_{m,n}^t$ stored energy after charging for $x_{m,n}^t$. The second term also represents a satisfaction value, but it original satisfaction before deciding on the amount of energy. The satisfaction cost should be an increasing function with decreasing marginal profit. In this work, we utilize a quadratic satisfaction cost function, which is widely used in the literature.

$$\psi(E_{m,n}^t) = \lambda_{m,n} E_{m,n}^t - \frac{\theta_{m,n}}{2}(E_{m,n}^t)^2 \tag{5.3}$$

where $\lambda_{m,n} > 0$ is the preference parameter of the m, n-th EV, which distinguishes the EV from other EVs, and $\theta_{m,n} > 0$ is a predetermined constant. The EV with a higher

value of $\lambda_{m,n}$ will obtain more satisfaction compared to the EV with a lower value of $\lambda_{m,n}$ for the same amount of $E_{m,n}^t$.

The third term, $-p_{CEA,m}^t x_{m,n}^t$, represents the energy sharing term, which denotes the cost/revenue from buying/selling energy from/to CEA m. If the EV is charging, this term will be negative, indicating the cost of charging. If the EV is discharging, this term will be positive, indicating the revenue from discharging. From Equation (5.1), if $x_{m,n}^t$ is positive and increases, the satisfaction function will increase. However, the cost of charging will also increase. Hence, there is a trade-off between the satisfaction function and the cost/revenue from energy sharing, and thus the EV needs to adjust the charging/discharging energy to maximize utility. When CEA m sends the sharing price $p_{CEA,m}^t$ to EVs, the EVs will adjust their charging/discharging energy $x_{m,n}^t$ in response to $p_{CEA,m}^t$ from CEA m to maximize utility, which results in a change in the net energy of the system. If $p_{CEA,m}^t$ is high, the discharging EVs tend to increase their discharge energy to maximize their utility by selling more energy. In contrast, if $p_{CEA,m}^t$ decreases, the discharging EVs will discharge less or instead charge some energy to increase utility instead of selling the energy at a low price.

Constraint (5.2) provides the lower and upper limits of the m, n-th EV's charging/discharging at time slot t

5.2.3 Community Energy Aggregator (CEA) Model

The CEAs at the middle level of the multi-communities system facilitate energy sharing by connecting with both EVs at the lower level for inside-community energy sharing and the UC at the upper level for multi-communities energy sharing. If there is a net surplus of energy inside community m, CEA m is responsible for selling the surplus energy to the UC. Likewise, if the generated energy inside community m is not sufficient, CEA m is responsible for buying the deficit energy from the UC. The objective of CEA $m \in \mathcal{M}$ is to maximize its utility by determining the optimal energy sharing price $p_{CEA,m}^t$ inside community m, considering the multi-communities energy sharing price p_{uc}^t from the UC

and the aggregated net energy inside community $D_{CEA,m}^t$, which can be written as follows:

$$\max_{p_{CEA,m}^t} U_{CEA,m}^t = (p_{CEA,m}^t - p_{uc}^t)D_{CEA,m}^t \tag{5.4}$$

$$s.t. \ p_{CEA,m}^{min} \le p_{CEA,m}^t \le p_{CEA,m}^{max} \tag{5.5}$$

Constraint (5.5) provides the lower and upper limits of the sharing price within community m at time slot t. The aggregated net energy within a community can be computed as

$$D_{CEA,m}^t = E_{CEA,m}^t + L_m^t \tag{5.6}$$

where L_m^t is the fixed demand of community m at time t, and $E_{CEA,m}^t$ is the net energy from EV charging and discharging in community m at time t, given by:

$$E_{CEA,m}^t = \sum_{n \in \mathcal{N}_m^t} x_{m,n}^t \tag{5.7}$$

Note that, in the model, both charging and discharging EVs receive the same unit price $p_{CEA,m}^t$ for selling and buying energy.

5.2.4 Utility Company (UC) Model

The UC, located at the upper level, buys and sells energy with multiple CEAs in the middle level. The objective of the UC is to maximize the profit of selling energy to the multi-communities system by setting the optimal multi-communities sharing price p_{uc}^t. The objective function is composed of two parts: the revenue from selling the net aggregated energy D_{uc}^t and the cost of generating that amount of energy $(C_{gen}^t(D_{uc}^t))$.

$$\max_{p_{uc}^t} U_{uc}^t = p_{uc}^t D_{uc}^t - C_{gen}^t(D_{uc}^t) \tag{5.8}$$

$$s.t.\ p_{uc}^{min} \le p_{uc}^t \le p_{uc}^{max} \tag{5.9}$$

The generation cost $C_{gen}^t(D_{uc}^t)$ is generally assumed to be a monotonically increasing function of the amount of generated energy D_{uc}^t and is strictly convex. Therefore, the generation cost can be formulated as

$$C_{gen}^t(D_{uc}^t) = a(D_{uc}^t)^2 + bD_{uc}^t + c \tag{5.10}$$

where a, b, and c are the coefficients of the generation cost function.

Constraint (5.9) provides the lower and upper limits of the multi-communities sharing price p_{uc}^t at time slot t. The aggregated net energy of the multi-communities system is the summation of the aggregated net energy of each community $m \in \mathcal{M}$.

$$D_{uc}^t = \sum_{m \in \mathcal{M}} D_{CEA,m}^t = \sum_{m \in \mathcal{M}} (E_{CEA,m}^t + L_m^t) \tag{5.11}$$

5.3 eFMES Scheme

The Stackelberg game is a non-cooperative game that models scenarios involving a hierarchical structure among players. In this game, players are rational, self-interested, and seek to maximize their own utility. Typically, this type of game is applied in a two-level framework with one leader and multiple followers. The leader makes the first move, after which the followers choose their strategies based on the leader's action. Followers employ the *best response strategy* to maximize their own payoff. Anticipating the followers' responses, the leader aims to select a strategy that maximizes their own utility. The solution to this game is known as the *Stackelberg equilibrium*. The hierarchical structure of the Stackelberg game is analogous to the structure of electrical systems, particularly the distribution networks we are focusing on. This similarity makes the game particularly suitable for modeling interactions related to energy sharing and trading.

5.3.1 Game Formulation

In this work, we employ a two-loop Stackelberg game to model the three-level multi-community energy sharing management. This model includes three types of players: UC, CEAs, and EVs. The first loop represents the game between UC and CEAs, while the second loop represents the game between each CEA and its associated EVs within that community.

In the first loop, UC acts as the leader, aiming to maximize its utility (5.8) by setting the optimal multi-communities sharing price for the multi-communities system. This involves a trade-off between revenue from selling the generated energy and the cost of producing the generated energy in the utility model. The followers in this loop are the CEAs of communities $m \in \mathcal{M}$. The CEAs respond to the multi-communities sharing price sent from UC by participating in the second loop game with EVs to determine the amount of net aggregated community energy for each community. Consequently, the multi-communities sharing price set by UC will affect the total aggregated energy in the system that UC needs to accommodate.

In the second loop, after each CEA receives the multi-communities sharing price from UC, each CEA m plays the leader role and determines the optimal sharing price for its community m to maximize its utility (5.4). In the CEA's utility model, there is a trade-off between revenue/cost from selling/buying energy with EVs inside the community and the payment/revenue of buying/selling the net aggregated community energy with UC. The EVs m, n inside community m, who are the followers, respond to the sharing price sent by CEA m by adjusting their energy strategy to maximize their utility (5.1). Once again, there is a trade-off between the satisfaction function and the revenue/cost of selling/buying the energy with CEA m.

Note that, CEAs play two roles in the 3-level Stackelberg game, acting as followers in the upper loop and leaders in the lower loop.

For this hierarchical Stackelberg game, the solution for the game that is the Stackelberg equilibrium is defined as follows:

Definition 2. *For the proposed 3-level Stackelberg game, a set of strategies $(\boldsymbol{x}^{t*}, \boldsymbol{p}^{t*}_{\boldsymbol{CEA}}, p^{t*}_{uc})$ constitutes a Stackelberg equilibrium, if and only if the following set of conditions is satisfied:*

$$U^t_{m,n}(\boldsymbol{x}^{t*}_{\boldsymbol{m}}, p^{t*}_{CEA,m}) \geq U^t_{m,n}(x^t_{m,n}, \boldsymbol{x}^{t*}_{\boldsymbol{-m,n}}, p^{t*}_{CEA,m}) \tag{5.12}$$

$$U^t_{CEA,m}(\boldsymbol{x}^{t*}_{\boldsymbol{m}}, p^{t*}_{CEA,m}, p^{t*}_{uc}) \geq U^t_{CEA,m}(\boldsymbol{x}^{t*}_{\boldsymbol{m}}, p^t_{CEA,m}, p^{t*}_{uc}) \tag{5.13}$$

$$U^t_{uc}(\boldsymbol{x}^{t*}, \boldsymbol{p}^{t*}_{\boldsymbol{CEA}}, p^{t*}_{uc}) \geq U^t_{uc}(\boldsymbol{x}^{t*}, \boldsymbol{p}^{t*}_{\boldsymbol{CEA}}, p^t_{uc}) \tag{5.14}$$

where $\boldsymbol{x}^{t*}_{\boldsymbol{-m,n}} = \{x^{t*}_{m,1}, x^{t*}_{m,2}, ..., x^{t*}_{m,n-1}, x^{t*}_{m,n+1}, ..., x^{t*}_{m,N}\}$ is the optimal strategies of all the EVs in community m in time slot t except the EV m, n. Hence, the optimal strategies of all EVs in community m in time slot t is expressed as $\boldsymbol{x}^{t*}_{\boldsymbol{m}} = \{x^{t*}_{m,n}, \boldsymbol{x}^{t*}_{\boldsymbol{-m,n}}\}$. $\boldsymbol{x}^{t*} = \{\boldsymbol{x}^{t*}_{\boldsymbol{1}}, \boldsymbol{x}^{t*}_{\boldsymbol{2}}, ..., \boldsymbol{x}^{t*}_{\boldsymbol{M}}\}$ denotes the set of the optimal strategies of all EVs in the multi-communities system. Lastly, $\boldsymbol{p}^{t*}_{\boldsymbol{CEA}} = \{p^{t*}_{CEA,1}, p^{t*}_{CEA,2}, ..., p^{t*}_{CEA,M}\}$ is the set of optimal strategies of all CEAs.

The equation (5.12)-(5.14) mean that when all players are at the Stackelberg equilibrium, no EV can increase his utility by deviating from $x^{t*}_{m,n}$, no CEA can improve his utility by choosing different strategy other than $p^{t*}_{CEA,m}$, and UC cannot increase his utility by selecting different strategy other than p^{t*}_{uc}.

5.3.2 Existence and Uniqueness of the Equilibrium

In the Stackelberg game, an equilibrium in pure strategies is not always guaranteed to exist. Hence, we need to validate whether there exists a Stackelberg equilibrium in the proposed Stackelberg game in which we propose a theorem and related proof for clarification in this section.

Theorem 2. *There exists a unique Stackelberg equilibrium in the proposed 3-level Stackelberg game among UC, CEAs, and EVs that satisfies (5.12)-(5.14)*

Proof. Considering that the proposed game model has a hierarchical structure, *backward induction* is an effective approach to derive the equilibrium of the game. The first step of the proof starts at the first level by identifying the best response of each EV which is the optimal energy consumption $(x_{m,n}^{t*})$ responding to the CEA's strategy $(p_{CEA,m}^t)$ in the second level. From the best response information of each EV, then we can trace back to find each CEA's best strategy which is the optimal sharing price inside community m $(p_{CEA,m}^{t*})$. Lastly, at the final step, given the information from all CEAs, the best strategy of UC that is the multi-communities sharing price (p_{uc}^{t*}) will be found. The mathematical proof is shown as follows:

(1) First level: optimal energy consumption of EVs

Given the community sharing price $p_{CEA,m}^t$ sent by CEA m in the second level, the best response strategy for each EV m, n in the first level can be obtained by taking the first-order derivative of $U_{m,n}^t$ in (5.1) with respect to $x_{m,n}^t$:

$$\frac{\partial U_{m,n}^t}{\partial x_{m,n}^t} = \lambda_{m,n} - \theta_{m,n}(E_{m,n}^t + x_{m,n}^t) - p_{CEA,m}^t \tag{5.15}$$

Let (5.15) equal to zero, the optimal energy consumption of EV m, n that maximize his utility function can be obtained as follows:

$$x_{m,n}^t = \frac{\lambda_{m,n} - p_{CEA,m}^t}{\theta_{m,n}} - E_{m,n}^t \tag{5.16}$$

From (5.16), we can see that the optimal energy consumption of m, n-th EV depends on the strategy of CEA m that is the community sharing price $p_{CEA,m}^t$. Then, the second-order derivative of $U_{m,n}^t$ is:

$$\frac{\partial^2 U_{m,n}^t}{\partial x_{m,n}^{t}{}^2} = -\theta_{m,n} < 0 \tag{5.17}$$

Since the second-order derivative of $U_{m,n}^t$ is always negative as in (5.17) due to $\theta_{m,n} > 0$, it means that $U_{m,n}^t$ is strictly concave with respect to $x_{m,n}^t$. Therefore, the best response strategy of EV m, n as in (5.16) is guaranteed to be unique and optimal.

(2) Second level: optimal community sharing price of CEA

Given the best-response strategy of EVs from the first level in (5.16), we can reformulate the utility function of CEA m by substituting optimal energy consumption in (5.16) into (5.4). Therefore, $U^t_{CEA,m}$ can be reformulated as

$$
\begin{aligned}
U^t_{CEA,m} &= (p^t_{CEA,m} - p^t_{uc})\Big(\sum_{n\in\mathcal{N}^t_m}\frac{\lambda_{m,n} - p^t_{CEA,m}}{\theta_{m,n}} - \sum_{n\in\mathcal{N}^t_m} E^t_{m,n} + L^t_m\Big) \\
&= -(p^t_{CEA,m})^2 \sum_{n\in\mathcal{N}^t_m}\frac{1}{\theta_{m,n}} + p^t_{CEA,m}\Big(\sum_{n\in\mathcal{N}^t_m}\frac{\lambda_{m,n}}{\theta_{m,n}} - \sum_{n\in\mathcal{N}^t_m} E^t_{m,n} + p^t_{uc}\sum_{n\in\mathcal{N}^t_m}\frac{1}{\theta_{m,n}} + L^t_m\Big) \\
&\quad + p^t_{uc}\Big(\sum_{n\in\mathcal{N}^t_m} E^t_{m,n} - \sum_{n\in\mathcal{N}^t_m}\frac{\lambda_{m,n}}{\theta_{m,n}} - L^t_m\Big)
\end{aligned}
\tag{5.18}
$$

The best response strategy for each CEA m in the second level can be obtained by taking the first-order derivative of $U^t_{CEA,m}$ in (5.18) with respect to $p^t_{CEA,m}$:

$$
\frac{\partial U^t_{CEA,m}}{\partial p^t_{CEA,m}} = -2p^t_{CEA,m}\sum_{n\in\mathcal{N}^t_m}\frac{1}{\theta_{m,n}} + \sum_{n\in\mathcal{N}^t_m}\frac{\lambda_{m,n}}{\theta_{m,n}} - \sum_{n\in\mathcal{N}^t_m} E^t_{m,n} + p^t_{uc}\sum_{n\in\mathcal{N}^t_m}\frac{1}{\theta_{m,n}} + L^t_m \tag{5.19}
$$

Let (5.19) equal to zero, the optimal community sharing price of CEA m that maximize its utility function can be obtained as follows:

$$
p^{t*}_{CEA,m} = \frac{1}{2}p^t_{uc} + \frac{1}{2}\frac{\sum_{n\in\mathcal{N}^t_m}\frac{\lambda_{m,n}}{\theta_{m,n}}}{\sum_{n\in\mathcal{N}^t_m}\frac{1}{\theta_{m,n}}} - \frac{1}{2}\frac{\sum_{n\in\mathcal{N}^t_m} E^t_{m,n}}{\sum_{n\in\mathcal{N}^t_m}\frac{1}{\theta_{m,n}}} + \frac{1}{2}\frac{L^t_m}{\sum_{n\in\mathcal{N}^t_m}\frac{1}{\theta_{m,n}}} \tag{5.20}
$$

From (5.20), we can make some observations that the optimal community price ($p^{t*}_{CEA,m}$) consists of 4 terms. The first term tells that the community sharing price depends on the multi-communities sharing price from UC (p^t_{uc}). The second term says that the parameter of each EV also affects the community sharing price. And the third term reveal that, if the community has high stored energy in EVs, the community sharing price will be low. And finally, the fourth term indicates that if the fixed load demand is high, the $p^{t*}_{CEA,m}$ will also be high, aligning with reality. Hence, this shows that each CEA m acts as a representative

of community m for participating in the multi-communities energy sharing.

By taking the second-order derivative of $U^t_{CEA,m}$ with respect to $p^{t*}_{CEA,m}$, we obtain

$$\frac{\partial^2 U^t_{CEA,m}}{\partial p^t_{CEA,m}{}^2} = -2 \sum_{n \in \mathcal{N}^t_m} \frac{1}{\theta_{m,n}} < 0 \tag{5.21}$$

Since the value of $\theta_{m,n} > 0$, the second-order derivative of $U^t_{m,n}$ is always negative as in (5.21). This means that $U^t_{CEA,m}$ is strictly concave with respect to $p^t_{CEA,m}$. Hence, the best response strategy of CEA m as in (5.20) is guaranteed to be unique and optimal.

(3) Third level: optimal multi-communities sharing price of UC

Now, we have obtained the best response function of EVs and CEAs in (5.16) and (5.20) which can be used to find the best response strategy of UC. First, From the best-response strategy of CEA m that we derived in the second level, we can substitute (5.20) into EV's best-response function (5.16) in order to find optimal energy consumption $x^{t*}_{m,n}$ of each m, n-th EV given the optimal sharing price of CEA m as

$$
\begin{aligned}
x^{t*}_{m,n} &= \frac{\lambda_{m,n} - \frac{1}{2}p^t_{uc} - \frac{1}{2}\frac{\sum_{n \in \mathcal{N}^t_m}\frac{\lambda_{m,n}}{\theta_{m,n}}}{\sum_{n \in \mathcal{N}^t_m}\frac{1}{\theta_{m,n}}} + \frac{1}{2}\frac{\sum_{n \in \mathcal{N}^t_m}E^t_{m,n}}{\sum_{n \in \mathcal{N}^t_m}\frac{1}{\theta_{m,n}}} + \frac{1}{2}\frac{L^t_m}{\sum_{n \in \mathcal{N}^t_m}\frac{1}{\theta_{m,n}}}}{\theta_{m,n}} - E^t_{m,n} \\
&= -\frac{1}{2}\frac{p^t_{uc}}{\theta_{m,n}} - \frac{1}{2}\frac{\sum_{n \in \mathcal{N}^t_m}\frac{\lambda_{m,n}}{\theta_{m,n}}}{\sum_{n \in \mathcal{N}^t_m}\frac{1}{\theta_{m,n}}}\frac{1}{\theta_{m,n}} + \frac{1}{2}\frac{\sum_{n \in \mathcal{N}^t_m}E^t_{m,n}}{\sum_{n \in \mathcal{N}^t_m}\frac{1}{\theta_{m,n}}}\frac{1}{\theta_{m,n}} - \frac{1}{2}\frac{L^t_m}{\sum_{n \in \mathcal{N}^t_m}\frac{1}{\theta_{m,n}}}\frac{1}{\theta_{m,n}} + \frac{\lambda_{m,n}}{\theta_{m,n}} + E^t_{m,n}
\end{aligned}
\tag{5.22}
$$

Then, the aggregated net energy of EVs in community m can be obtained by substituting (5.22) into (5.7) as

$$E_{CEA,m}^{t*} = \sum_{n \in \mathcal{N}_m^t} x_{m,n}^{t*}$$

$$= -\frac{1}{2}p_{uc}^t \sum_{n \in \mathcal{N}_m^t} \frac{1}{\theta_{m,n}} - \frac{1}{2}\Big[\sum_{n \in \mathcal{N}_m^t}\Big(\sum_{n \in \mathcal{N}_m^t} \frac{\lambda_{m,n}}{\theta_{m,n}} \frac{1}{\sum_{n \in \mathcal{N}_m^t}\frac{1}{\theta_{m,n}}} \frac{1}{\theta_{m,n}}\Big)\Big]$$

$$+ \frac{1}{2}\Big[\sum_{n \in \mathcal{N}_m^t}\Big(\sum_{n \in \mathcal{N}_m^t} E_{m,n}^t \frac{1}{\sum_{n \in \mathcal{N}_m^t}\frac{1}{\theta_{m,n}}} \frac{1}{\theta_{m,n}}\Big)\Big] - \frac{1}{2}\Big[\sum_{n \in \mathcal{N}_m^t} \frac{L_m^t}{\sum_{n \in \mathcal{N}_m^t}\frac{1}{\theta_{m,n}}} \frac{1}{\theta_{m,n}}\Big] + \sum_{n \in \mathcal{N}_m^t} \frac{\lambda_{m,n}}{\theta_{m,n}} - \sum_{n \in \mathcal{N}_m^t} E_{m,n}^t$$

$$= -\frac{1}{2}p_{uc}^t \sum_{n \in \mathcal{N}_m^t} \frac{1}{\theta_{m,n}} + \frac{1}{2}\sum_{n \in \mathcal{N}_m^t} \frac{\lambda_{m,n}}{\theta_{m,n}} - \frac{1}{2}\sum_{n \in \mathcal{N}_m^t} E_{m,n}^t - \frac{1}{2}L_m^t$$

(5.23)

After that, the total aggregated net energy of the entire multi-communities system can be calculated by summarizing all net energy of community $m \in \mathcal{M}$ as

$$D_{uc}^t = \sum_{m \in \mathcal{M}} D_{CEA,m}^{t*}$$

$$= \sum_{m \in \mathcal{M}} (E_{CEA,m}^{t*} + L_m^t)$$

$$= -\frac{1}{2}p_{uc}^t \sum_{m \in \mathcal{M}}\sum_{n \in \mathcal{N}_m^t} \frac{1}{\theta_{m,n}} + \frac{1}{2}\sum_{m \in \mathcal{M}}\sum_{n \in \mathcal{N}_m^t} \frac{\lambda_{m,n}}{\theta_{m,n}} - \frac{1}{2}\sum_{m \in \mathcal{M}}\sum_{n \in \mathcal{N}_m^t} E_{m,n}^t + \frac{1}{2}\sum_{m \in \mathcal{M}} L_m^t$$

(5.24)

where we define new parameters at time slot t for the summation parts in (5.24) as α, β^t, and γ^t

$$\alpha^t = \sum_{m \in \mathcal{M}}\sum_{n \in \mathcal{N}_m^t} \frac{1}{\theta_{m,n}} \tag{5.25}$$

$$\beta^t = \sum_{m \in \mathcal{M}}\sum_{n \in \mathcal{N}_m^t} \frac{\lambda_{m,n}}{\theta_{m,n}} \tag{5.26}$$

$$\gamma^t = \sum_{m \in \mathcal{M}}\sum_{n \in \mathcal{N}_m^t} E_{m,n}^t \tag{5.27}$$

$$\delta^t = \sum_{m \in \mathcal{M}} L_m^t \tag{5.28}$$

Hence, (5.24) can be rewritten as

$$D_{uc}^t = -\frac{1}{2}p_{uc}^t \alpha^t + \frac{1}{2}\beta^t - \frac{1}{2}\gamma^t + \frac{1}{2}\delta^t \tag{5.29}$$

By substituting (5.29) and (5.10) into (5.8), the original utility function of UC can be reformulated as

$$\begin{aligned}
U_{uc}^t &= p_{uc}^t\left(-\frac{p_{uc}^t}{2}\alpha + \frac{1}{2}\beta^t - \frac{1}{2}\gamma^t + \frac{1}{2}\delta^t\right) - a\left(-\frac{p_{uc}^t}{2}\alpha + \frac{1}{2}\beta^t - \frac{1}{2}\gamma^t + \frac{1}{2}\delta^t\right)^2 \\
&\quad - b\left(-\frac{p_{uc}^t}{2}\alpha + \frac{1}{2}\beta^t - \frac{1}{2}\gamma^t + \frac{1}{2}\delta^t\right) - c \\
&= -a\left(-\frac{p_{uc}^t}{2}\alpha + \frac{1}{2}\beta^t - \frac{1}{2}\gamma^t + \frac{1}{2}\delta^t\right)^2 - b\left(-\frac{p_{uc}^t}{2}\alpha + \frac{1}{2}\beta^t - \frac{1}{2}\gamma^t + \frac{1}{2}\delta^t\right) \\
&\quad - \frac{(p_{uc}^t)^2}{2}\alpha + \frac{p_{uc}^t}{2}\beta^t - \frac{p_{uc}^t}{2}\gamma^t + \frac{p_{uc}^t}{2}\delta^t - c
\end{aligned} \tag{5.30}$$

The best-response strategy for UC in the third level can be obtained by taking the first-order derivative of U_{uc}^t in (5.30) with respect to p_{uc}^t as:

$$\begin{aligned}
\frac{\partial U_{uc}^t}{\partial p_{uc}^t} &= -2a\left(-\frac{\alpha p_{uc}^t}{2} + \frac{\beta^t}{2} - \frac{\gamma^t}{2} + \frac{1}{2}\delta^t\right)\left(-\frac{\alpha}{2}\right) + \frac{b\alpha}{2} - \alpha p_{uc}^t + \frac{\beta^t}{2} - \frac{\gamma^t}{2} + \frac{1}{2}\delta^t \\
&= a\alpha\left(\frac{\beta^t}{2} - \frac{\gamma^t}{2} + \frac{1}{2}\delta^t\right) - \frac{a\alpha^2}{2}p_{uc}^t - \alpha p_{uc}^t + \frac{b\alpha}{2} + \frac{\beta^t}{2} - \frac{\gamma^t}{2} + \frac{1}{2}\delta^t \\
&= p_{uc}^t\left(-\frac{a\alpha^2}{2} - \alpha\right) + a\alpha\left(\frac{\beta^t}{2} - \frac{\gamma^t}{2} + \frac{1}{2}\delta^t\right) + \frac{b\alpha}{2} + \frac{\beta^t}{2} - \frac{\gamma^t}{2} + \frac{1}{2}\delta^t
\end{aligned} \tag{5.31}$$

Let (5.31) equal to zero, the optimal multi-communities sharing price of UC that maximize its utility function can be obtained as follows:

$$p_{uc}^{t*} = \frac{a\alpha(\beta^t - \gamma^t + \delta^t) + b\alpha + \beta^t - \gamma^t + \delta^t}{\alpha(a\alpha + 2)} \tag{5.32}$$

By taking the second-order derivative of U_{uc}^t with respect to p_{uc}^{t*}, we obtain

$$\frac{\partial^2 U_{uc}^t}{\partial {p_{uc}^t}^2} = -\frac{a\alpha^2}{2} - \alpha < 0 \tag{5.33}$$

Since the value of a and α is positive, the second-order derivative of U_{uc}^t is always negative as in (5.33). This means that U_{uc}^t is strictly concave with respect to p_{uc}^t. Thus, the best-response strategy of UC as in (5.32) is guaranteed to be unique and optimal.

From the above proof, we can see that once the unique and optimal strategy of UC (p_{uc}^{t*}) is determined, the unique and optimal strategy of all CEA $m \in \mathcal{M}$ will also be determined, and then the unique and optimal strategy of each and every EV m, n can be calculated and adjusted. Hence, the unique Stackelberg equilibrium in the form of $(\boldsymbol{x}^{t*}, \boldsymbol{p}_{CEA}^{t*}, p_{uc}^{t*})$ exists for the proposed 3-level Stackelberg energy sharing management game. $\qquad\square$

5.3.3 Three-Level Optimal Energy-Price (3OEP) Equilibrium Algorithm

In the previous subsection, the analytical solution is obtained in a centralized way in order to prove that the proposed 3-level Stackelberg game always has a unique and optimal solution in which we assume that the UC has the private parameters of all the EVs. However, such an approach is not desirable in which all EVs have to reveal their private preferences to UC. Therefore, we design an algorithm in a distributed manner to obtain the approximate solution.

We can see from the previous subsection that the objective function of UC is strictly convex with respect to p_{uc}^t. From the nature of the leader-follower game, therefore, in order to find the Stackelberg equilibrium, we have to find the optimal solution for the leader. To do that, we can enumerate the leader strategy p_{uc}^t from $p_{uc,min}^t$ to $p_{uc,max}^t$ and the optimal solution is the one that maximizes the utility of UC. When the optimal multi-communities sharing price p_{uc}^{t*} is found, the optimal sharing price $p_{CEA,m}^{t*}$ for $m \in \mathcal{M}$ are found, and the optimal energy consumption of m, n-th EV $x_{m,n}^{t*}$ are found also. Hence, the strategy profile $(\boldsymbol{x}^{t*}, \boldsymbol{p}_{CEA}^{t*}, p_{uc}^{t*})$ for stackelberg equilibrium is found.

In the Algorithm 2, we try to find the Stackelberg equilibrium at each time slot t. First, the algorithm is iteratively update p_{uc}^t from $p_{uc,min}^t$ to $p_{uc,max}^t$. At each p_{uc}^t, after CEA m recieved broadcasted p_{uc}^t from UC, the CEA m will calculate the optimal sharing price ($p_{CEA,m}^t$) responding to p_{uc}^t by (5.20) and then announce it to EVs inside its community m. Each EV m, n further calculates the optimal energy consumption ($x_{m,n}^t$) that maximizes his utility given the $p_{CEA,m}^t$ by (5.16) and send this information back to CEA m. Then, CEA will gather the optimal energy consumption from EVs inside its community m and fix load demand L_m^t of its community m and calculate the aggregated net energy in the community ($D_{CEA,m}^t$) using (5.6) then further send it back to UC. UC summarizes all aggregated net energy from all communities $m \in \mathcal{M}$ using (5.11) and use it to calculate the value of UC's utility function using (5.8). Finally, the UC compare the value of newly calculated utility with the recorded utility, if the new one is higher, UC update recorded utility value U_{uc}^{t*} and p_{uc}^{t*} of that utility value. If not, UC just ignore that new calculated utility value and price. The algorithm will run iteratively until the conditions in (5.12)-(5.14) are satisfied, which means the Stackelberg equilibrium is reached.

Algorithm 2 Optimal 3-Level Energy-Price (3OEP) Equilibrium Algorithm

---

1: UC initialize $\boldsymbol{U}_{uc}^* = 0, \boldsymbol{p}_{uc}^* = 0$
2: **for** $t = 1$ to $\mathcal{T}$ **do**
3:     **for** p_{uc}^t from $p_{uc}^{min,t}$ to $p_{uc}^{max,t}$ **do**
4:         Broadcast p_{uc}^t to all CEAs in multi-communities system
5:         **for** each CEA $m \in \mathcal{M}$ **do**
6:             Calculates the optimal community sharing price ($p_{CEA,m}^t$) using (5.20)
7:             Announce $p_{CEA,m}^t$ to EVs in community m
8:             **for** each EV $n \in \mathcal{N}_m^t$ in community m **do**
9:                 Calculate optimal energy consumption ($x_{m,n}^t$) using (5.16)
10:                 Send $x_{m,n}^t$ back to CEA m
11:             **end for**
12:             Calculates aggregated net energy in community m ($D_{CEA,m}^t$) using (5.6)
13:             Then send $D_{CEA,m}^t$ back to UC
14:         **end for**
15:         UC summarizes all aggregated net energy from all communities using (5.11)
16:         UC calculates the value of utility function using (5.8)
17:         **if** $U_{uc}^t \geq U_{uc}^{t*}$ **then**
18:             UC record new multi-communities sharing price and utility value
19:             $p_{uc}^{t*} = p_{uc}^t, U_{uc}^{t*} = U_{uc}^t$
20:         **end if**
21:     **end for**
22:     The equilibrium ($\boldsymbol{D}^{t*}, \boldsymbol{p}_{CEA,m}^{t*}, p_{uc}^{t*}$) is reached where utlity of UC is maximized
23: **end for**

5.4   Evaluation Studies

5.4.1   Simulation Setup

In this section, the performance of the proposed model is studied, where all players aim to maximize their utility functions. The data from three communities is utilized, where Community 1 is a residential community consisting of 1000 households, Community 2 comprises two shopping malls, and Community 3 is an office area with three office buildings. The load profile data is obtained from IEEE open data [107]. A total of 2000 EVs are assumed to move around these three communities. For simulation purposes, we employ the Nissan Leaf with a 40 kWh battery capacity and an energy consumption rate of 0.16 kWh/km [108]. The EV trip data is obtained from a source [109, 110] that synthesizes this data from the actual US National Household Travel Survey [111]. The preference

parameter is randomly selected from the range of [50-70], and θ is set to 2. The State of Charge (SoC) at the beginning of the day is 50%. The minimum and maximum SoC are set to 20% and 90% [98], respectively, to prolong battery life. The maximum charging and discharging rate is 7 kW, as this is the typical wall charging rate widely used in residential areas and office buildings. The simulation is implemented in MATLAB.

Table 5.1 shows the trips of 10 EVs, where individuals typically depart from their households between 7-9 am and reach their workplace to start working between 8-10 am. Those working in shopping malls depart later than those working in offices. About half of the office workers will have lunch near their office and won't use their cars during lunchtime. However, the other half of the office workers choose to go to the shopping mall to have lunch with their colleagues during lunchtime. People working in the office area usually leave work between 4-6 pm. On the other hand, people working in the mall will return home between 7-8 pm. If the cell is blank, it means the EV stays in the same community. However, if there is information in the cell, it means the EV moves from one community to another. For example, "30 C1,C3" in slot 7 for EV1 means that EV1 moves from community 1 to community 3 by driving for 30 km during 7 am - 8 am. So, during that time, EVs will not be able to charge or discharge energy.

Table 5.1: EV trip data

Period	EV1	EV2	EV3	EV4	EV5	EV6	EV7	EV8	EV9	EV10
1										
2										
3										
4										
5										
6										
7	30 C1,3	40 C1,3	50 C1,3							
8				30 C1,3	40 C1,3	20 C1,3	30 C1,2	60 C1,2		
9									40 C1,2	60 C1,2
10										
11										
12		10 C3,2,3	10 C3,2,3			5 C3,2				
13				10 C3,2,3	10 C3,2,3	5 C2,3				
14										
15										
16	30 C3,1									
17		40 C3,1								
18			50 C3,1	30 C3,1	40 C3,1	5 C3,2				
19							30 C2,1	60 C2,1		
20						20 C2,1			40 C2,1	50 C2,1
21										
22										
23										
24										
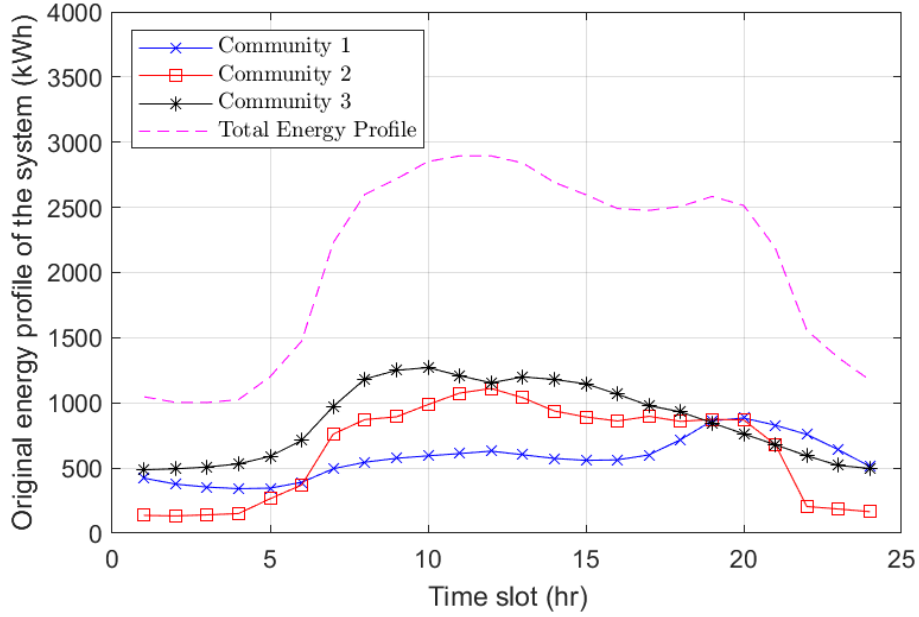
Figure 5.2: Original energy profile without EVs

Figures 5.2 show the original energy profile, which includes the energy profiles of communities 1, 2, and 3, as well as the total energy profile of the entire system.

5.4.2 Results and Discussion

In this subsection, the results are compared between two scenarios: typical charging and the proposed three-level optimal energy-price (3OEP).

- Typical charging [102]: Individuals charge their EVs upon returning home in the evening, following typical human behavior.

- The two-level Stackelberg game (2LV) [24]: The two-level Stackelberg game is widely utilized in the literature, as discussed in Chapter 2, where it typically considers the interaction between an aggregator or a coordinator and end-users such as prosumers and EVs. However, the literature often overlooks the benefit model of the UC and frequently assumes pricing based on time-of-use (ToU), where the on-peak period is from 9 am to 10 pm, and the rest of the time is considered off-peak.

- Proposed three-level optimal energy-price (3OEP): EVs will charge and discharge continuously across different communities, such as residential areas, offices, and
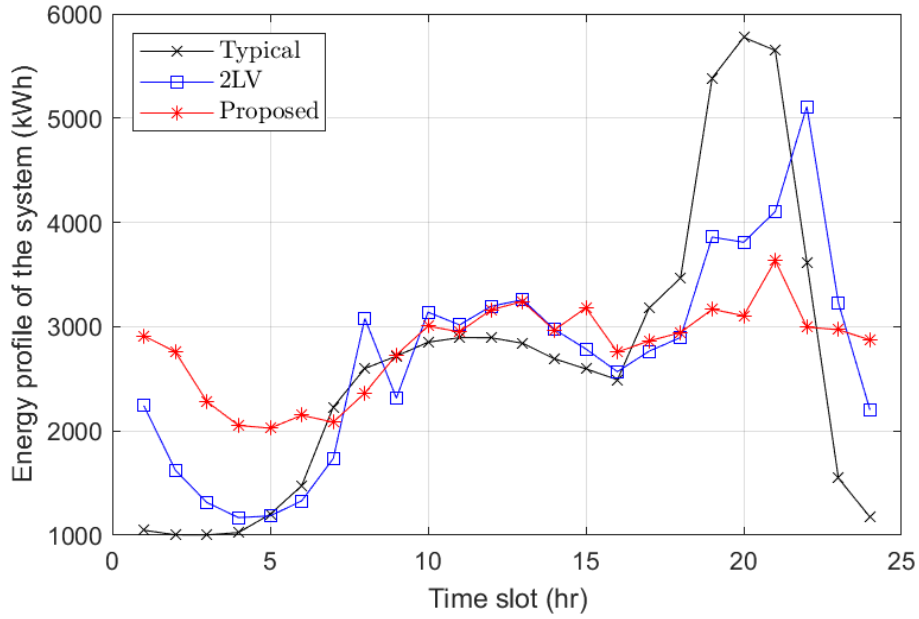
Figure 5.3: Total energy profile with EVs

shopping malls. The electricity price varies across these locations, and the amount of charging and discharging is determined by the proposed algorithm.

Figures 5.3 show the total energy profile, including the energy used by EVs during charging and discharging. The typical charging scenario results in a significant peak in the evening as all EV owners plug in their vehicles after returning from work. On the other hand, the two-level approach utilizing ToU pricing shows that during off-peak periods, there is very low demand, with some charging occurring during on-peak times. However, there is a high demand during the night after the on-peak period has passed. The proposed scheme appears to be the most effective at maintaining a flatter total load profile compared to both approaches. It even results in a flatter profile than the original energy profile without EVs by utilizing charging energy during low-demand periods in the early morning and evening.

Figures 5.4 show the total energy profile of each CEA and the total hourly charging and discharging power, respectively. The proposed scheme indicates that EVs primarily charge at home from the evening until early morning (blue line). However, the demand is more evenly distributed over time, preventing the high peaks seen in typical charging scenarios. During the daytime, the demand for EV charging in the residential community (C1) is
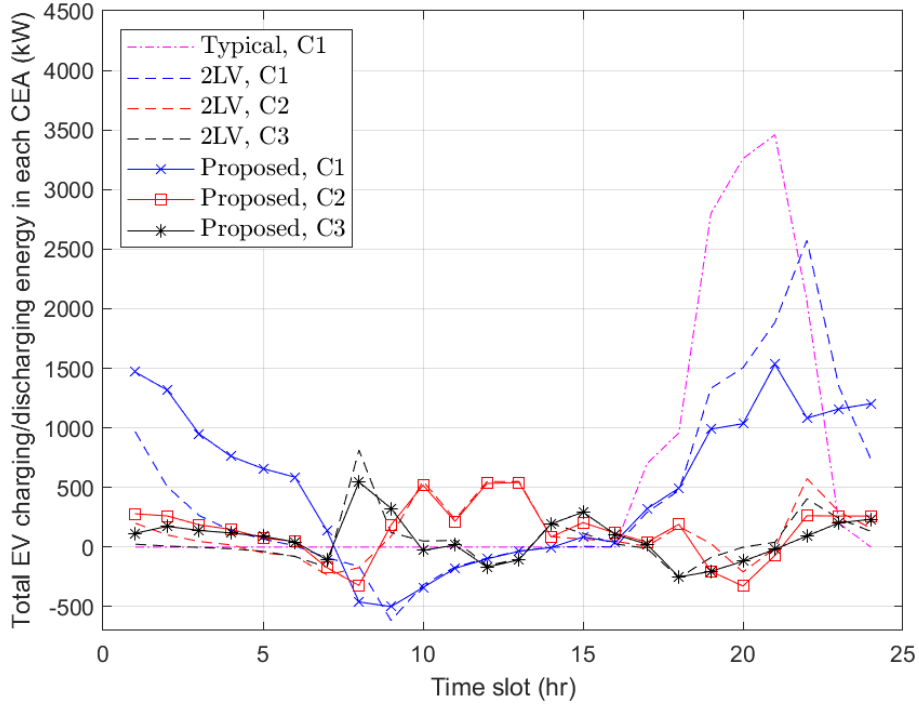
Figure 5.4: Charging and discharging power

very low, as most EVs are at work or shopping malls. During this period, EVs engage in charging and discharging activities within communities 2 and 3, based on the energy sharing prices and the participation of stakeholders in the community energy management system. In contrast, with the two-level approach, EV owners often charge their cars in the evening after the on-peak period has passed, which results in a peak in the evening.

Figures 5.5 shows that the retail price for typical charging scenarios is significantly higher than the energy sharing price of the proposed scheme during the evening, reflecting the higher demand during that time when people typically charge their personal EVs. It also shows the community energy sharing price $p_{CEA,m}$ and the multi-community energy sharing price p_{uc}. The results indicate that the prices in all communities will be similar due to the sharing mechanism between multiple communities. However, the price for community 1 is generally the lowest since its original energy demand is the lowest among all communities. For the two-level approach, the pricing aligns with ToU rates, so the price during off-peak periods is very low and increases during on-peak periods.

From Figure 5.6, the bar graph shows that the proposed charge/discharge scheme is effective in reducing the peak-to-average ratio by 40.7% compared to the scenario where
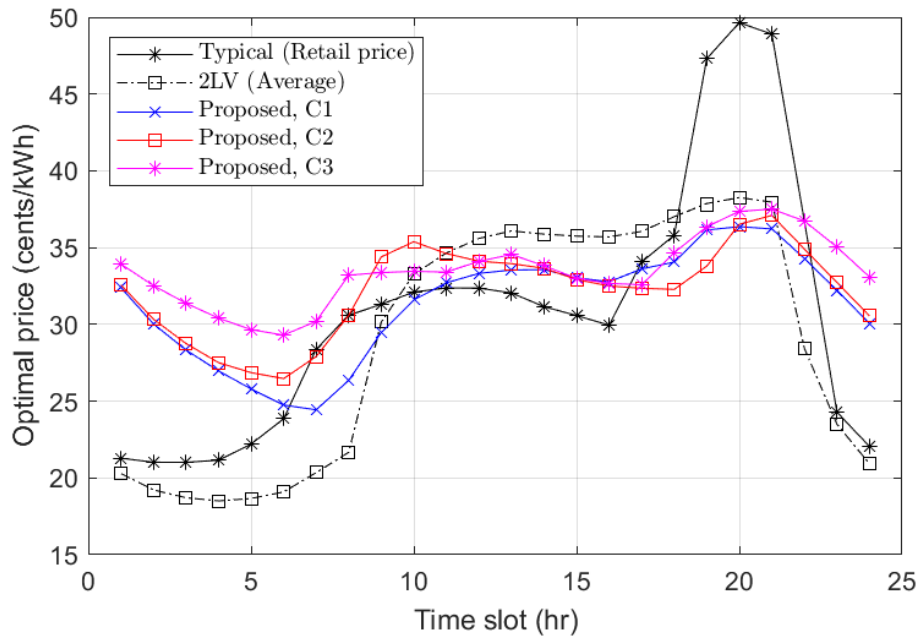
Figure 5.5: Energy sharing price comparison
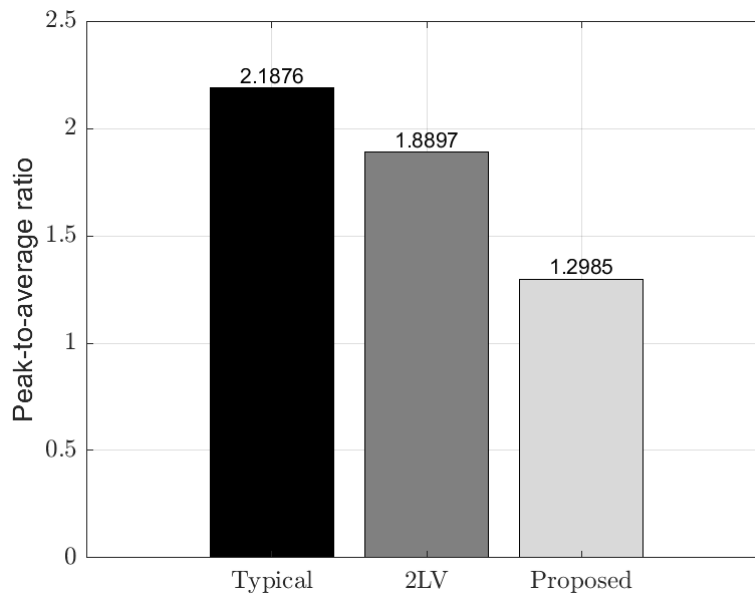
Figure 5.6: Peak-to-average ratio comparison
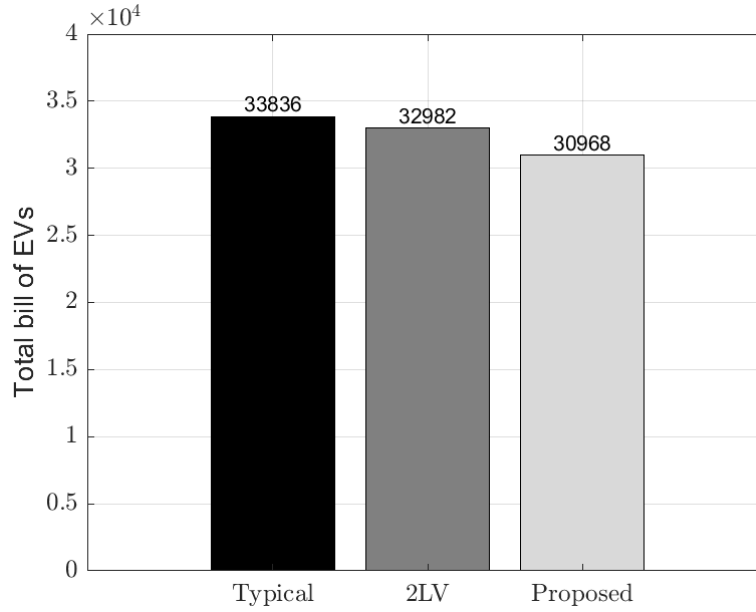
Figure 5.7: Total bill of EVs comparison

humans use typical charging habits and by 31.3% compared to the two-level approach. It also demonstrates that the two-level approach is more effective than typical charging behavior, with a PAR reduction of 13.6%.

The total bill for all EVs is depicted in Figure 5.7. The figure illustrates that the proposed three-level scheme can reduce the total bill by 8.3% compared to typical charging methods and by 6.1% compared to the two-level approach. It also further shows that the two-level approach has reduced the total bills by 21.5% compared to typical charging.

5.5 Summary

This chapter presents a novel multi-communities energy sharing management scheme integrated with electric vehicles capable of traversing multiple areas across diverse communities characterized by different energy profiles and prices. The model is formulated as a three-level Stackelberg game to capture the interaction among three entities at three levels: the Utility Company (UC), Community Energy Aggregators (CEAs), and Electric Vehicles (EVs). The UC and CEAs aim to find optimal energy sharing prices to maximize their respective benefits, while EVs seek to determine optimal charging/discharging

strategies to maximize their utility. The scheme presents the optimal three-level energy-price (3OEP) equilibrium algorithm to obtain an equilibrium that is proven to be unique and always existent. The results demonstrate that the proposed scheme outperforms typical human charging behavior, significantly reducing the peak-to-average ratio by 40.7% compared to typical charging and by 31.3% compared to the two-level approach, while also flattening the total energy profile.

Chapter 6

Conclusions and Future Works

6.1 Conclusion

This dissertation introduces the hierarchical multi-communities energy sharing management Framework (hMESH), which integrates various energy storage solutions into the future smart grid. The proposed framework addresses three key problems at different levels: managing non-moving energy storage in smart homes, critical hour energy management for partially moving energy storage within a single community, and inter-community energy sharing for fully moving energy storage across multiple communities. By incorporating renewable energy resources and the increasing prevalence of electric vehicles, hMESH aims to transform the current grid structure and enhance energy sharing management within the electrical grid.

The energy sharing management for non-moving energy storage (eNMES) scheme is proposed to optimize energy storage capacity and minimize energy loss in smart home environments. This is achieved through a newly introduced distributed power flow assignment (DPFA), which assigns power flow paths from energy sources, such as renewable energy (RE), to household loads. Furthermore, eNMES integrates DPFA with a load-shifting algorithm to further reduce energy loss and the required battery storage capacity.

The critical hour energy management for partially moving energy storage (ePMES) scheme is proposed to optimize energy use during peak periods using partially moving

energy storage, such as electric school buses (ESBs). This scheme introduces a vehicle-to-grid model between utility companies (UC) and schools with ESBs, leveraging their idle periods for peak shaving services. During peak hours, the UC sends incentive price signals to schools, encouraging them to discharge stored energy from ESBs, thus reducing peak demand and generation costs while providing monetary benefits to the schools. The model employs a non-cooperative game to determine optimal incentive pricing and discharge energy amounts. Additionally, during low demand periods, ESBs can charge, helping to flatten the energy profile curve and ultimately reducing the system's peak-to-average ratio.

The proposed inter-community energy sharing management for fully moving energy storage (eFMES) scheme addresses the optimization of energy pricing in hierarchical multi-communities integrated with electric vehicles (EVs). With a projected increase in EVs on the road, they become significant power consumers and sources, capable of moving across different smart grid communities, each with its energy profile and pricing. By utilizing energy sharing prices from utility companies, EVs can contribute to grid stabilization by adjusting their charging or discharging activities, thus smoothing the grid profile. To mitigate peak demands caused by typical human behavior, the scheme employs a three-level Stackelberg game involving utility companies, community energy aggregators, and EVs. Through strategic decision-making, all entities can maximize their benefits, receiving monetary rewards while reducing the peak-to-average ratio, ultimately enhancing grid efficiency.

6.2 Contributions

The main contribution of the dissertation can be concluded as follows:

- The eNMES Scheme is proposed: This scheme introduces DPFA that helps reduce energy loss in DPFS and proposes a load-shifting algorithm to further reduce energy loss and energy storage capacity. The findings and results indicate that the MPFA significantly outperforms the SPFA, reducing energy loss by up to 55.2%.

Additionally, with the implementation of a load-shifting algorithm, energy loss is further reduced to 72.9%, and the required energy storage capacity is decreased by up to 57%.

- The ePMES Scheme is proposed: This scheme introduces a critical hour energy sharing management model using ESBs that are highly suitable to provide any ancillary services and presents an OEP algorithm to achieve the equilibrium that is unique and always exists. The findings and results demonstrate that the electricity bills for schools are reduced by up to 22.6%. The peak-to-average ratio is decreased by up to 9.5%, and the additional generation cost during peak periods is reduced by 36%.

- The ePMES Scheme is proposed: This scheme proposes a novel inter-communities energy sharing management model for movable energy storage and presents a 3OEP algorithm to obtain the equilibrium that is unique and always exists.The findings and results demonstrate that the scheme effectively helps prevent peak load and flatten the energy profile, reducing the peak-to-average ratio by 40.7%. Additionally, the total electricity bills for EVs are reduced by 8.3%.

The main findings and results are also presented in Figure 6.1.

6.3   Future Works

Although this dissertation has fulfilled the objective of introducing a novel hierarchical multi-community energy sharing management framework (hMESH), there remain certain gaps that could be further studied in the future.

For the smart home environment level, future research directions could explore the proposed MPFA/SG and MPFA/MG algorithms in scenarios with a large number of power loads (PLs). Additionally, investigating the impacts of charging and discharging efficiencies, as well as storage capacity, on distributed power-flow assignment warrants attention. Furthermore, examining power priority assignments to PLs while considering

124

Framework:	Hierarchical Multi-Communities Energy Sharing Management Framework (hMESH)		
	Chapter 3	**Chapter 4**	**Chapter 5**
Contributions:	Energy Sharing Management for NMES (eNMES)	Critical Hour Energy Sharing Management for PMES (ePMES)	Inter-community Energy Sharing Management for FMES (eFMES)
Findings and Results:	❑ MPFA compare with SPFA ▪ Energy loss: reduced up to **55.2%** ❑ With Load shifting ▪ Energy loss: reduced up to 2.1% ▪ Storage Capacity: reduced up to **29.6%**	❑ Bill of school: reduced up to **24.9%** ❑ PAR: reduced up to 9.5% ❑ Additional cost of UC at peak period: reduced **36%**	❑ Help prevent peak load, and flatten the energy profile ❑ PAR: Compare with typical charging: reduced **40.7%** ❑ Bill of EVs: Compare with typical charging: reduced 8.3%
Problems:	Optimal Energy Storage Capacity Design with Minimum Energy Loss	Optimal Critical Hour Energy Sharing using Electric School Buses	Optimal Energy-Price Management for Electric Vehicles

Figure 6.1: Main finding of the dissertation.

constraints on total energy supply is crucial. Finally, addressing fluctuations in power supply and variations in demand within the Distributed Power Flow System (DPFS), taking into account the irregular daily activities of residents, presents a significant avenue for further investigation.

At the single community level, exploring the integration of electric buses with other community loads and generation sources would provide valuable insights into their mutual impacts and interactions within the system dynamics. Secondly, investigating the direct sharing of stored energy within large batteries such as ESB with other institutions, such as schools or buildings, within the community offers a promising avenue for study.

At the multi-community level, future research could focus on several directions. One approach is to consider a greater variety of loads and building types in detail to understand their effects on the overall energy profile. Expanding the study to encompass larger areas would provide a broader perspective on how the total energy profile changes. Additionally, incorporating other types of electric vehicles (EVs) beyond personal cars, such as electric taxis, electric trucks, and electric vans, would be valuable. However, this requires the

accurate prediction of EV trips to be introduced for effective analysis.

Bibliography

[1] A Muir and J Lopatto. Final report on the august 14, 2003 blackout in the united states and canada: causes and recommendations. 2004.

[2] Stephan Singer et al. *The energy report: 100% renewable energy by 2050.* Ecofys bv, 2010.

[3] Avi Gopstein, Cuong Nguyen, Cheyney O'Fallon, Nelson Hastings, David Wollman, et al. *NIST framework and roadmap for smart grid interoperability standards, release 4.0.* Department of Commerce. National Institute of Standards and Technology . . . , 2021.

[4] Tiago Sousa, Tiago Soares, Pierre Pinson, Fabio Moret, Thomas Baroche, and Etienne Sorin. Peer-to-peer and community-based markets: A comprehensive review. *Renewable and Sustainable Energy Reviews*, 104:367–378, 2019.

[5] Shuocheng Wang, Bo Hu, Kaigui Xie, Jiahao Yan, Yanlin Li, Huawei Chao, and Yi Zeng. Optimal configuration of energy storage capacity in multi-energy system with temperature control equipment based on discrete fourier transform. In *2019 IEEE Innovative Smart Grid Technologies-Asia (ISGT Asia)*, pages 2677–2681. IEEE, 2019.

[6] IRENA. Electricity storage and renewables: Costs and markets to 2030. *International Renewable Energy Agency*, 164, 2017.

[7] Duong Quoc Hung and Nadarajah Mithulananthan. Multiple distributed generator placement in primary distribution networks for loss reduction. *IEEE Transactions on industrial electronics*, 60(4):1700–1708, 2011.

[8] Tianmeng Yang. The optimal capacity determination method of energy storage system with different applications in wind farm. In *2016 IEEE PES Asia-Pacific Power and Energy Engineering Conference (APPEEC)*, pages 2081–2085. IEEE, 2016.

[9] Md Rokonuzzaman, Muhaiminul Islam Akash, Mahmuda Khatun Mishu, Wen-Shan Tan, Mahammad A Hannan, and Nowshad Amin. Iot-based distribution and control system for smart home applications. In *2022 IEEE 12th Symposium on Computer Applications & Industrial Electronics (ISCAIE)*, pages 95–98. IEEE, 2022.

[10] Tolga Ercan, Mehdi Noori, Yang Zhao, and Omer Tatari. On the front lines of a sustainable transportation fleet: applications of vehicle-to-grid technology for transit and school buses. *Energies*, 9(4):230, 2016.

[11] Irina N Krivoshto, John R Richards, Timothy E Albertson, and Robert W Derlet. The toxicity of diesel exhaust: implications for primary care. *The Journal of the American Board of Family Medicine*, 21(1):55–62, 2008.

[12] Zoya Pourmirza. *An ICT architecture for the neighbourhood area network in the Smart Grid*. The University of Manchester (United Kingdom), 2015.

[13] Richard Harper. Inside the smart home: Ideas, possibilities and methods. In *Inside the smart home*, pages 1–13. Springer, 2003.

[14] Annette Werth, Nobuyuki Kitamura, and Kenji Tanaka. Conceptual study for open energy systems: Distributed energy network using interconnected dc nanogrids. *IEEE Transactions on Smart Grid*, 6(4):1621–1630, 2015.

[15] Vagelis Vossos, Daniel L Gerber, Melanie Gaillet-Tournier, Bruce Nordman, Richard Brown, Willy Bernal Heredia, Omkar Ghatpande, Avijit Saha, Gabe Arnold, and

Stephen M Frank. Adoption pathways for dc power distribution in buildings. *Energies*, 15(3):786, 2022.

[16] Nian Liu, Xinghuo Yu, Cheng Wang, Chaojie Li, Li Ma, and Jinyong Lei. Energy-sharing model with price-based demand response for microgrids of peer-to-peer prosumers. *IEEE Transactions on Power Systems*, 32(5):3569–3583, Sep. 2017.

[17] Nian Liu, Xinghuo Yu, Cheng Wang, and Jinjian Wang. Energy sharing management for microgrids with pv prosumers: A stackelberg game approach. *IEEE Transactions on Industrial Informatics*, 13(3):1088–1098, June 2017.

[18] Amrit Paudel, Kalpesh Chaudhari, Chao Long, and Hoay Beng Gooi. Peer-to-peer energy trading in a prosumer-based community microgrid: A game-theoretic model. *IEEE Transactions on Industrial electronics*, 66(8):6087–6097, 2018.

[19] Min Zhang, Frank Eliassen, Amir Taherkordi, Hans-Arno Jacobsen, Hwei-Ming Chung, and Yan Zhang. Demand–response games for peer-to-peer energy trading with the hyperledger blockchain. *IEEE Transactions on Systems, Man, and Cybernetics: Systems*, 52(1):19–31, 2021.

[20] Jiawen Kang, Rong Yu, Xumin Huang, Sabita Maharjan, Yan Zhang, and Ekram Hossain. Enabling localized peer-to-peer electricity trading among plug-in hybrid electric vehicles using consortium blockchains. *IEEE transactions on industrial informatics*, 13(6):3154–3164, 2017.

[21] Jangkyum Kim, Joohyung Lee, and Jun Kyun Choi. Joint demand response and energy trading for electric vehicles in off-grid system. *Ieee Access*, 8:130576–130587, 2020.

[22] Sima Aznavi, Poria Fajri, Mohammad B Shadmand, and Arash Khoshkbar-Sadigh. Peer-to-peer operation strategy of pv equipped office buildings and charging stations considering electric vehicle energy pricing. *IEEE Transactions on Industry Applications*, 56(5):5848–5857, 2020.

[23] Baochuan Fu, Mengkai Chen, Zhaoan Fei, Jianhan Wu, Xiaoshu Xu, Zhen Gao, Zhengtian Wu, and Yalong Yang. Research on the stackelberg game method of building micro-grid with electric vehicles. *Journal of Electrical Engineering & Technology*, 16:1637–1649, 2021.

[24] Jangkyum Kim, Joohyung Lee, Sangdon Park, and Jun Kyun Choi. Power scheduling scheme for a charging facility considering the satisfaction of electric vehicle users. *IEEE Access*, 10:25153–25164, 2022.

[25] Fabio Moret and Pierre Pinson. Energy collectives: A community and fairness based approach to future electricity markets. *IEEE Transactions on Power Systems*, 34(5):3994–4004, 2018.

[26] Liudong Chen, Nian Liu, and Jianhui Wang. Peer-to-peer energy sharing in distribution networks with multiple sharing regions. *IEEE Transactions on Industrial Informatics*, 16(11):6760–6771, Nov 2020.

[27] Yuntao Wang, Zhou Su, Qichao Xu, Tingting Yang, and Ning Zhang. A novel charging scheme for electric vehicles with smart communities in vehicular networks. *IEEE Transactions on Vehicular Technology*, 68(9):8487–8501, 2019.

[28] Ehsan Shokouhmand and Ahmad Ghasemi. Stochastic optimal scheduling of electric vehicles charge/discharge modes of operation with the aim of microgrid flexibility and efficiency enhancement. *Sustainable Energy, Grids and Networks*, 32:100929, 2022.

[29] Ping Chen, Lu Han, Guoyu Xin, Aiwei Zhang, Hui Ren, and Fei Wang. Game theory based optimal pricing strategy for v2g participating in demand response. *IEEE Transactions on Industry Applications*, 2023.

[30] IEA. Global energy & co2 status report. *International Energy Agency*, 2018.

[31] Benedikt Reick, Anja Konzept, André Kaufmann, Ralf Stetter, and Danilo Engelmann. Influence of charging losses on energy consumption and co2 emissions of battery-electric vehicles. *Vehicles*, 3(4):736–748, 2021.

[32] Saher Javaid, Mineo Kaneko, and Yasuo Tan. Safe operation conditions of electrical power system considering power balanceability among power generators, loads, and storage devices. *Energies*, 14(15):4460, 2021.

[33] Saher Javaid, Mineo Kaneko, and Yasuo Tan. System condition for power balancing between fluctuating and controllable devices and optimizing storage sizes. *Energies*, 15(3):1055, 2022.

[34] Philipp Fortenbacher, Johanna L Mathieu, and Göran Andersson. Modeling and optimal operation of distributed battery storage in low voltage grids. *IEEE Transactions on Power Systems*, 32(6):4340–4350, 2017.

[35] Meisam Farrokhifar, Samuele Grillo, and Enrico Tironi. Loss minimization in medium voltage distribution grids by optimal management of energy storage devices. In *2013 IEEE Grenoble Conference*, pages 1–5. IEEE, 2013.

[36] Junainah Sardi, Nadarajah Mithulananthan, Duong Quoc Hung, and Krischonme Bhumkittipich. Load levelling and loss reduction by es in a primary distribution system with pv units. In *2015 IEEE Innovative Smart Grid Technologies-Asia (ISGT ASIA)*, pages 1–6. IEEE, 2015.

[37] Mohammad Rasol Jannesar, Alireza Sedighi, Mehdi Savaghebi, and Josep M Guerrero. Optimal placement, sizing, and daily charge/discharge of battery energy storage in low voltage distribution network with high photovoltaic penetration. *Applied energy*, 226:957–966, 2018.

[38] Jun Xiao, Zequn Zhang, Linquan Bai, and Haishen Liang. Determination of the optimal installation site and capacity of battery energy storage system in distribution

network integrated with distributed generation. *IET Generation, Transmission & Distribution*, 10(3):601–607, 2016.

[39] Mostafa Nick, Marc Hohmann, Rachid Cherkaoui, and Mario Paolone. Optimal location and sizing of distributed storage systems in active distribution networks. In *2013 IEEE grenoble conference*, pages 1–6. IEEE, 2013.

[40] Andrey V Savkin, Muhammad Khalid, and Vassilios G Agelidis. A constrained monotonic charging/discharging strategy for optimal capacity of battery energy storage supporting wind farms. *IEEE Transactions on Sustainable Energy*, 7(3):1224–1231, 2016.

[41] Haoran Li, Bo Sun, and Chenghui Zhang. Capacity design of a distributed energy system based on integrated optimization and operation strategy of exergy loss reduction. *Energy Conversion and Management*, 231:113648, 2021.

[42] Zheng Chen, Bing Xia, Chunting Chris Mi, and Rui Xiong. Loss-minimization-based charging strategy for lithium-ion battery. *IEEE Transactions on Industry Applications*, 51(5):4121–4129, 2015.

[43] Zheng Chen, Xing Shu, Mengmeng Sun, Jiangwei Shen, and Renxin Xiao. Charging strategy design of lithium-ion batteries for energy loss minimization based on minimum principle. In *2017 IEEE Transportation Electrification Conference and Expo, Asia-Pacific (ITEC Asia-Pacific)*, pages 1–6. IEEE, 2017.

[44] Kailong Liu, Xiaosong Hu, Zhile Yang, Yi Xie, and Shengzhong Feng. Lithium-ion battery charging management considering economic costs of electrical energy loss and battery degradation. *Energy conversion and management*, 195:167–179, 2019.

[45] Michael Schimpe, Christian Piesch, Holger C Hesse, Julian Paß, Stefan Ritter, and Andreas Jossen. Power flow distribution strategy for improved power electronics energy efficiency in battery storage systems: development and implementation in a utility-scale system. *Energies*, 11(3):533, 2018.

[46] Jin-Young Choi, In-Sun Choi, Geon-Ho Ahn, and Dong-Jun Won. Advanced power sharing method to improve the energy efficiency of multiple battery energy storages system. *IEEE Transactions on Smart Grid*, 9(2):1292–1300, 2016.

[47] Sung-Min Cho and Sang-Yun Yun. Optimal power assignment of energy storage systems to improve the energy storage efficiency for frequency regulation. *Energies*, 10(12):2092, 2017.

[48] Peng Wang, Kenli Li, Bin Xiao, and Keqin Li. Multiobjective optimization for joint task offloading, power assignment, and resource allocation in mobile edge computing. *IEEE internet of things journal*, 9(14):11737–11748, 2021.

[49] Ali Salam Al-Khayyat, Mustafa Jameel Hameed, and Amel Ahmed Ridha. Optimized power flow control for pv with hybrid energy storage system hess in low voltage dc microgrid. *e-Prime-Advances in Electrical Engineering, Electronics and Energy*, 6:100388, 2023.

[50] Rita Shaw, Mike Attree, Tim Jackson, and Mike Kay. The value of reducing distribution losses by domestic load-shifting: a network perspective. *Energy Policy*, 37(8):3159–3167, 2009.

[51] Shuvangkar Das, Partha Protim Saha, Md Forkan Uddin, and Eklas Hossain. Reducing generation cost by optimum load scheduling in smart grid considering system loss. In *2018 IEEE Energy Conversion Congress and Exposition (ECCE)*, pages 2663–2669. IEEE, 2018.

[52] Nor Erniza Mohammad Rozali, Wai Shin Ho, Sharifah Rafidah Wan Alwi, Zainuddin Abdul Manan, Jiří Jaromír Klemeš, Mohamad Nur Salam Mohd Yunus, and Syed Amarul Adli Syed Mohd Zaki. Peak-off-peak load shifting for optimal storage sizing in hybrid power systems using power pinch analysis considering energy losses. *Energy*, 156:299–310, 2018.

[53] Zhe Yan, Yongming Zhang, Runqi Liang, and Wenrui Jin. An allocative method of hybrid electrical and thermal energy storage capacity for load shifting based on seasonal difference in district energy planning. *Energy*, 207:118139, 2020.

[54] Qibin Duan, Jinran Wu, and You-Gan Wang. Optimal battery capacity in electrical load scheduling. *Journal of Energy Storage*, 50:104190, 2022.

[55] Annu Ahlawat and Debapriya Das. Optimal sizing and scheduling of battery energy storage system with solar and wind dg under seasonal load variations considering uncertainties. *Journal of Energy Storage*, 74:109377, 2023.

[56] Ruengwit Khwanrit, Yuto Lim, Saher Javaid, Somsak Kittipiyakul, and Yasuo Tan. Study of energy loss for distributed power-flow assignment in a smart home environment. *Designs*, 6(6):99, 2022.

[57] Yuto Lim, Saher Javaid, Ruengwit Khwanrit, and Yasuo Tan. Seasonal storage capacity design for distributed power flow system with safe operation conditions. In *2022 IEEE International Conference on Consumer Electronics-Taiwan*, pages 577–578. IEEE, 2022.

[58] JP Tewari. *Basic electrical engineering*. New Age International, 2003.

[59] Xiangjun Li, Dong Hui, and Xiaokang Lai. Battery energy storage station (bess)-based smoothing control of photovoltaic (pv) and wind power generation fluctuations. *IEEE transactions on sustainable energy*, 4(2):464–473, 2013.

[60] Nihal Kularatna and Kosala Gunawardane. *Energy storage devices for renewable energy-based systems: Rechargeable batteries and supercapacitors*. Academic Press, 2021.

[61] Kai Peter Birke. *Modern battery engineering: A comprehensive introduction*. World Scientific, 2019.

[62] Yuto Lim, Nyiak Tien Tang, Yoshiki Makino, Tze Kin Teo, and Yasuo Tan. Simulation of solar photovoltaic and fuel cell energy system for smart community simulator. In *IEICE Technical Committee on Information Networks (IN)*, volume 117, pages 1–6, 2017.

[63] Toshiba. Toshiba household fuel cell system: Ecofarm. `https://www.toshiba.co.jp/product/fc/products/pdf/TENA-chofu16-7.pdf` (accessed on 12 December 2023).

[64] NHK Broadcasting Culture Research Institute. Time habits of japanese in 2005: A nhk survey regarding the use of time in the daily life of japanese citizens. *Japan Broadcasting Publishers Association*, 2006.

[65] Ruengwit Khwanrit, Yuto Lim, Chalie Charoenlarpnopparut, Somsak Kittipiyakul, Saher Javaid, and Yasuo Tan. Optimal vehicle-to-grid strategies for electric school bus using game-theoretic approach. In *2023 International Conference on Consumer Electronics-Taiwan (ICCE-Taiwan)*, pages 191–192. IEEE, 2023.

[66] Yuan Liu and Hao Liang. A three-layer stochastic energy management approach for electric bus transit centers with pv and energy storage systems. *IEEE Transactions on Smart Grid*, 12(2):1346–1357, 2020.

[67] Melanie Elliott and Noah Kittner. Operational grid and environmental impacts for a v2g-enabled electric school bus fleet using dc fast chargers. *Sustainable Production and Consumption*, 30:316–330, 2022.

[68] Lance Noel and Regina McCormack. A cost benefit analysis of a v2g-capable electric school bus compared to a traditional diesel school bus. *Applied Energy*, 126:246–255, 2014.

[69] Timothy KM Beatty and Jay P Shimshack. School buses, diesel emissions, and respiratory health. *Journal of health economics*, 30(5):987–999, 2011.

[70] John Neff and Matthew Dickens. *Public transportation fact book.* American Public Transportation Association, 2015.

[71] Wayes Tushar, Walid Saad, H Vincent Poor, and David B Smith. Economics of electric vehicle charging: A game theoretic approach. *IEEE Transactions on Smart Grid*, 3(4):1767–1778, 2012.

[72] Yue Yu, Chunxia Su, Xiao Tang, BaekGyu Kim, Tiecheng Song, and Zhu Han. Hierarchical game for networked electric vehicle public charging under time-based billing model. *IEEE Transactions on Intelligent Transportation Systems*, 22(1):518–530, 2020.

[73] Aurobinda Laha, Bo Yin, Yu Cheng, Lin X Cai, and Yu Wang. Game theory based charging solution for networked electric vehicles: A location-aware approach. *IEEE Transactions on Vehicular Technology*, 68(7):6352–6364, 2019.

[74] Tao Rui, Cungang Hu, Guoli Li, Jisheng Tao, and Weixiang Shen. A distributed charging strategy based on day ahead price model for pv-powered electric vehicle charging station. *Applied Soft Computing*, 76:638–648, 2019.

[75] Dalong Guo and Chi Zhou. Utility optimization using game-based sg-dr algorithm in v2g. In *2018 IEEE Vehicle Power and Propulsion Conference (VPPC)*, pages 1–6. IEEE, 2018.

[76] Hui Ren, Aiwei Zhang, and Wei Li. Study on optimal v2g pricing strategy under multi-aggregator competition based on game theory. In *2019 IEEE Sustainable Power and Energy Conference (iSPEC)*, pages 1027–1032. IEEE, 2019.

[77] Donovan Aguilar Dominguez. *The Influence of Electric Vehicle Availability on Vehicle-to-Grid Provision within a Microgrid.* PhD thesis, University of Sheffield, 2023.

[78] Hongbin Zhou, Chensheng Liu, Bo Yang, and Xinping Guan. Optimal dispatch of electric taxis and price making of charging stations using stackelberg game. In

IECON 2015-41st Annual Conference of the IEEE Industrial Electronics Society, pages 004929–004934. IEEE, 2015.

[79] Kai Ma, Xiaoyan Hu, Jie Yang, Zhiyuan Yue, Bo Yang, Zhixin Liu, and Xinping Guan. Electric taxi charging strategy based on stackelberg game considering hotspot information. *IEEE Transactions on Vehicular Technology*, 71(3):2427–2436, 2022.

[80] Yuqing Yang, Weige Zhang, Liyong Niu, and Jiuchun Jiang. Coordinated charging strategy for electric taxis in temporal and spatial scale. *Energies*, 8(2):1256–1272, 2015.

[81] Zaiyue Yang, Tianci Guo, Pengcheng You, Yunhe Hou, and S Joe Qin. Distributed approach for temporal–spatial charging coordination of plug-in electric taxi fleet. *IEEE Transactions on Industrial Informatics*, 15(6):3185–3195, 2018.

[82] Fan Fei, Wenzhe Sun, Riccardo Iacobucci, and Jan-Dirk Schmöcker. Exploring the profitability of using electric bus fleets for transport and power grid services. *Transportation Research Part C: Emerging Technologies*, 149:104060, 2023.

[83] Shu-Xia Yang, Xiong-Fei Wang, Wen-Qin Ning, and Xue-feng Jia. An optimization model for charging and discharging battery-exchange buses: Consider carbon emission quota and peak-shaving auxiliary service market. *Sustainable Cities and Society*, 68:102780, 2021.

[84] Z Wu, F Guo, J Polak, and G Strbac. Evaluating grid-interactive electric bus operation and demand response with load management tariff. *Applied energy*, 255:113798, 2019.

[85] Jônatas Augusto Manzolli, João Pedro F Trovão, and Carlos Henggeler Antunes. Electric bus coordinated charging strategy considering v2g and battery degradation. *Energy*, 254:124252, 2022.

[86] Nader A El-Taweel, Abdelrahman Ayad, Hany EZ Farag, and Moataz Mohamed. Optimal energy management for battery swapping based electric bus fleets with

consideration of grid ancillary services provision. *IEEE Transactions on Sustainable Energy*, 14(2):1024–1036, 2022.

[87] Francisco Haces-Fernandez. Framework to develop electric school bus vehicle-to-grid (esb v2g) systems supplied with solar energy in the united states. *Energies*, 17(12):2834, 2024.

[88] Pedram Samadi, Amir-Hamed Mohsenian-Rad, Robert Schober, Vincent W. S. Wong, and Juri Jatskevich. Optimal real-time pricing algorithm based on utility maximization for smart grid. In *2010 First IEEE International Conference on Smart Grid Communications*, pages 415–420, Oct 2010.

[89] Amir-Hamed Mohsenian-Rad, Vincent W. S. Wong, Juri Jatskevich, Robert Schober, and Alberto Leon-Garcia. Autonomous demand-side management based on game-theoretic energy consumption scheduling for the future smart grid. *IEEE Transactions on Smart Grid*, 1(3):320–331, Dec 2010.

[90] Stephen P Boyd and Lieven Vandenberghe. *Convex optimization*. Cambridge university press, 2004.

[91] Prasertsak Charoen, Marios Sioutis, Saher Javaid, Chalie Charoenlarpnopparut, Yuto Lim, and Yasuo Tan. User-centric consumption scheduling and fair billing mechanism in demand-side management. *Energies*, 12(1):156, 2019.

[92] Bo Chai, Jiming Chen, Zaiyue Yang, and Yan Zhang. Demand response management with multiple utility companies: A two-level game approach. *IEEE Transactions on Smart Grid*, 5(2):722–731, March 2014.

[93] Heinrich Von Stackelberg. *Market structure and equilibrium*. Springer Science & Business Media, 2010.

[94] U.S. Energy Information Administration. Hourly electric grid monitor. `https://www.eia.gov/electricity/gridmonitor` (accessed on 12 December 2023).

[95] Rochest Community Schools. School buses - general information. `https://www.rochester.k12.mi.us/about-us/departments/transportation/test-page-photos-content` (accessed on 12 December 2023).

[96] US Census Bureau. American community survey 5-year data estimates. `http://censusreporter.org/profiles/97000US2629940-rochester-community-school-district-mi/` (accessed on 12 December 2023).

[97] Adella Santos, Nancy McGuckin, Hikari Yukiko Nakamoto, Danielle Gray, Susan Liss, et al. Summary of travel trends: 2009 national household travel survey. Technical report, United States. Federal Highway Administration, 2011.

[98] Chao Long, Jianzhong Wu, Yue Zhou, and Nick Jenkins. Peer-to-peer energy sharing through a two-stage aggregated battery control in a community microgrid. *Applied energy*, 226:261–276, 2018.

[99] Sadia Sadiq, Ewan Pritchard, Ken Dulaney, and Ali Emadi. Plug-in hybrid market transformation by leveraging a niche market: School buses. In *2007 IEEE Vehicle Power and Propulsion Conference*, pages 483–492. IEEE, 2007.

[100] Ali Saadon Al-Ogaili, Ali Q Al-Shetwi, Hussein MK Al-Masri, Thanikanti Sudhakar Babu, Yap Hoon, Khaled Alzaareer, and NV Phanendra Babu. Review of the estimation methods of energy consumption for battery electric buses. *Energies*, 14(22):7578, 2021.

[101] Andy Moore and Steve Crolius. Vehicle-to-grid electric school bus commercialization project. Technical report, Blue Bird Corporation, Fort Valley, GA (United States), 2022.

[102] Dong Sik Kim, Young Mo Chung, and Beom Jin Chung. Statistical analysis of electric vehicle charging based on ac slow chargers. *Energies*, 16(6):2735, 2023.

[103] Tze Wood Ching. Design of electric vehicle charging station in macau. *Journal of Asian Electric Vehicles*, 9(1):1453–1458, 2011.

[104] Green Power Motor Company. Beast school bus. `https://greenpowermotor.com/gp-products/beast-school-bus` (accessed on 12 January 2024).

[105] BLUE BIRD. All american electric. `https://www.blue-bird.com/all-american-electric` (accessed on 12 January 2024).

[106] LION Electric. Lion d. `https://pages.thelionelectric.com/liond-the-all-electric-type-d-school-bus-usa` (accessed on 12 January 2024).

[107] PES. Ieee open data sets. `https://site.ieee.org/pes-iss/data-sets` (accessed on 12 January 2024).

[108] Bruno Canizes, João Soares, Zita Vale, and Juan M Corchado. Optimal distribution grid operation using dlmp-based pricing for electric vehicle charging infrastructure in a smart city. *Energies*, 12(4):686, 2019.

[109] Tiago Sousa, Hugo Morais, Zita Vale, Pedro Faria, and João Soares. Intelligent energy resource management considering vehicle-to-grid: A simulated annealing approach. *IEEE Transactions on Smart Grid*, 3(1):535–542, 2011.

[110] João Soares, Tiago Sousa, Hugo Morais, Zita Vale, and Pedro Faria. An optimal scheduling problem in distribution networks considering v2g. In *2011 IEEE Symposium on Computational Intelligence Applications In Smart Grid (CIASG)*, pages 1–8. IEEE, 2011.

[111] J Bose, L Giesbrecht, and J Sharp. Highlights of the 2001 national household travel survey. us, 2001.

Publications

Journals

[1] **R. Khwanrit**, Y. Lim, S. Javaid, S. Kittipiyakul, and Y. Tan, "Study of Energy Loss for Distributed Power-flow Assignment in a Smart Home Environment," *Designs*, vol.6, no.6, pp. 99, 2022.

[2] **R. Khwanrit**, Y. Lim, S. Javaid, C. Charoenlarpnopparut, and Y. Tan, "Incorporating a Load-Shifting Algorithm for Optimal Energy Storage Capacity Design in Smart Homes," *Designs*, vol.8, no.1, pp. 11, 2024.

[3] **R. Khwanrit**, S. Javaid, Y. Lim, C. Charoenlarpnopparut, and Y. Tan, "Optimal Vehicle-to-Grid Strategies for Energy Sharing Management using Electric School Buses," *Energies*, vol.17, no.16, pp. 4182, 2024.

[4] **R. Khwanrit**, Y. Lim, C. Charoenlarpnopparut, S. Javaid, and Y. Tan, "Hierarchical Multi-Communities Energy Sharing Model with Electric Vehicles Integration," *Energies*, 2024. (Under Revision)

International Conferences

[5] **R. Khwanrit**, Y. Lim, S. Kittipiyakul, S. Javaid, and Y. Tan. "Multi-Communities Energy Sharing Management in Residential Prosumers : A Game-theoretic Approach", *9th IEEE International Conference on Consumer Electronics – Taiwan (ICCE-TW)*, Taipei, Taiwan, 6–8 July 2022.

[6] **R. Khwanrit**, Y. Lim, C. Charoenlarpnopparut, S. Kittipiyakul, S. Javaid, and Y. Tan. "Optimal Vehicle-to-Grid Strategies for Electric School Bus using Game-Theoretic Approach", *10th IEEE International Conference on Consumer Electronics – Taiwan (ICCE-TW)*, Pingtung, Taiwan, 17–19 July 2023.

[7] **R. Khwanrit**, S. Javaid, Y. Lim, C. Charoenlarpnopparut, and Y. Tan. "Three-Level Energy Sharing Management in Residential Prosumer Multi-Communities", *11th IEEE International Conference on Consumer Electronics – Taiwan (ICCE-TW)*, Taichung, Taiwan, 9–11 July 2024.

[8] Y. Lim, S. Javaid , **R. Khwanrit**, and Y. Tan. "Seasonsal Storage Capacity Design for Distributed Power Flow System with Safe Operation Conditions", *9th IEEE International Conference on Consumer Electronics – Taiwan (ICCE-TW)*, Taipei, Taiwan, 6–8 July 2022.

[9] Y. Lim, S. Javaid , Y. Tan, and **R. Khwanrit**. "Minimizing Energy Loss for Multiple Load Power Flow Assignment in Smart Homes", *IEEE Int. Conf. on Energy, Power, Environment, Control, and Computing (ICEPECC)*, Gujrat, Pakistan, 8-9 March 2023.

[10] Y. Lim, S. Javaid , Y. Tan, and **R. Khwanrit**. "Minimizing Energy Loss for Optimal Storage Capacity Design in Distributed Power Flow System", *10th IEEE International Conference on Consumer Electronics – Taiwan, Pingtung, Taiwan (ICCE-TW)*, 17–19 July 2023.

Domestic Conferences

[11] **R. Khwanrit**, Y. Lim, S. Kittipiyakul, and Y. Tan. "Study of Local Energy Sharing Model with Modified Billing Mechanism for Microgrid," *In Proc. of IEICE Technical Committee on Information Networks (IN)*, vol. 119, no. 461, IN2019-83, pp.43–47, 5-6 March 2020.

[12] **R. Khwanrit**, Y. Lim, S. Javaid, S. Kittipiyakul, and Y. Tan. "Study of Storage Energy Loss in a Distributed Power Flow System for Smart Home Environment," *In Proc. of IEICE Technical Committee on Information Networks (IN)*, vol. 122, no. 233, pp.47-52, 27-28 October 2022.